

# Post-Buckling and Nonlinear Free Vibration Response of Elastically Supported Laminated Composite Plates with Uncertain System Properties in Thermal Environment

Stochastic Finite Element Macro-mechanical Model Investigation

Rajesh Kumar<sup>\*1</sup>, Desta Goytom<sup>1</sup>

<sup>1</sup>School of Mechanical Engineering, Jimma Institute of Technology, Jimma University, ETHIOPIA

<sup>\*</sup>rajeshtripathi63@gmail.com; <sup>2</sup>desta.goytom@ju.edu.et

## Abstract

In the present study, post buckling and nonlinear free vibration response of laminated composite plate resting on a two parameters Pasternak foundation with Winkler cubic nonlinearity having uncertain system properties in thermal environments using macro mechanical stochastic finite element model is investigated. The system properties are modeled as basic random variables using macro mechanical model. A C0 nonlinear finite element formulation of the random problem based on higher order shear deformation theory in the von-Karman sense is presented. A direct iterative method conjunction with a stochastic nonlinear finite element method is extended to analyze the effects of uncertainties in the system properties on the post buckling and nonlinear free vibration of the composite plate having Winkler type of geometric nonlinearity. Mean and standard deviation of the response have been obtained for various combinations material properties, geometric parameters, boundary conditions, elastic foundation parameters, aspect ratio, lamina layup compared with those available in the literature and with Monte Carlo Simulation.

## Keywords

*Stochastic Finite Element Method; Random System Properties; Macromechanical Model; Thermal Post Buckling; Nonlinear Thermal Free Vibration; Elastic Foundations.*

## Introduction

There are numerous investigations available which dealt with the post buckling response of laminated composite plates using deterministic and other methods. All the methods used in available literature found the mean response and neglected the coefficients of variations due to randomness in material properties, geometric imperfections, coefficients of thermal expansion and foundation parameters. To enhance the accuracy in the response evaluation a probabilistic analysis favors for composite laminated for the accountability of randomness by modeling their system properties as random variables.

Considerable literature is available on the buckling or post buckling of laminated composite plates in thermal environments based on deterministic analysis and using either classical theory of plates, first order shear deformation theory or higher order shear deformation theory subjected to uniform or non uniform temperature distribution with temperature dependent and independent material properties. Chen & Chen [1989], Huang et al.[1988], Chen & Chen [1991], Shen [2001], Sita et al.[2003], Shariyat [2007], Pandey et al. [2009], Nigam and Narayana [1994], Handa and Anderson [1981], Nakagiri [1990]. Lin and Kam [1992], Englested and Reddy [1994], Zhang and Ellingwood [1995], Graham and Siragy [2001], Singh et al. [2001]. The post buckling analysis of laminated composite plates resting on elastic foundation with random system properties using C0 FEM in conjunction with FOPT based on HSDT has been studied by Singh et al. [2002]. Generalized buckling analysis of laminated plates with random material properties using Stochastic Finite Elements have been investigated by

Ankara et al.[2006]. The random field finite elements have been studied by Liu.[1986]. The post buckling response of laminated composite plate resting on elastic foundation with random system properties, stochastic perturbation finite elements have been investigated by Yamin et al. [1996].

Considerable literature is also available on the prediction of the nonlinear free vibration analysis of conventional structures and composite structures in thermal environment based on deterministic analysis Liu and Liu [1996]. Bailey [1981]. Tauchert [1991]. Chang and Jen Lee and Lee [1986].

However, the literature related to the stochastic analysis of laminated composite plates is limited. Thomsion [1969], Leissa and Martin [1990], Zhang and Chen [1990], Zhang and Ellingwood [1993], Zhang et al. [1996] have investigated the stochastic perturbation method to vector-valued and matrix-valued function for response and reliability of uncertain structures, Manohar and Ibrahim [1999], Salim et al.[1998], Venini and Mariani [2002], Yadav and Verma [2001], Singh et al.[2001, 2003] have analyzed the composite cross-ply laminated composite plate/panel with random material properties for free vibration employing higher order deformation theory (HSDT) with FOPT. Onkar and Yadav [2004], Kitiponarchai [2006], Tripathi [2007] investigated the free vibration response of laminated composite conical shells with random material properties using FEM in conjunction with FOPT based on HSDT. Singh et al. [2010] investigated the Stochastic analysis of laminated composite plates on elastic foundations: The cases of postbuckling behavior and nonlinear free vibration.

It is evident from the existing literatures that very little efforts have been made for the studies on post buckling response of laminated composite plates with temperature independent (TID) and temperature dependent (TD) thermoelastic material properties, thermal expansion coefficients, foundation parameters and nonlinear free vibration response of laminated composite plates with random system properties in thermal environments to the best of authors' knowledge.

In present paper post buckling and nonlinear free vibration response of laminated composite plate resting on a two parameters Pasternak foundation with Winkler cubic nonlinearity having uncertain system properties in thermal environments using macro and micromechanical stochastic finite element model is investigated.

## Mathematical Formulations

Consider a rectangular laminated composite plate of length  $a$ , width  $b$  and total thickness  $h$ , defined in  $(X, Y, Z)$  system with  $x$ - and  $-y$  axes located in the middle plane and its origin placed at the corner of the plate. Let  $(\bar{u}, \bar{v}, \bar{w})$  be the displacement parallel to the  $(X, Y, \text{ and } Z)$  respectively as shown in Fig 1. The thickness coordinate  $Z$  of the top and bottom surfaces of any  $k^{\text{th}}$  layer are denoted by  $Z^{(k-1)}$  and  $Z^{(k)}$  respectively. The fiber of the  $k^{\text{th}}$  layer is oriented with angle  $\theta_k$  to the  $X$ - axes. The plate is supported by the foundation excluding any separation during the process of deformation as shown in Fig. 1. The load displacement relation between the plate and the supporting foundation follows the two- parameters model (Pasternak-type) as

$$P = K_1 w - K_2 \nabla^2 w$$

$$\text{with } \nabla^2 = \partial_{,x^2} + \partial_{,y^2} \quad (1)$$

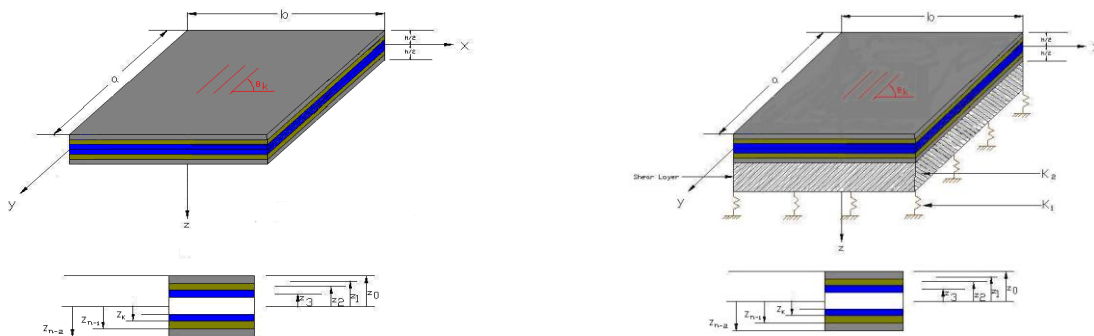


FIGURE 1. GEOMETRY OF LAMINATED COMPOSITE PLATE WITHOUT FOUNDATION AND RESTING ON ELASTIC FOUNDATION

where  $P$  is the foundation reaction per unit area, comma (,) denotes partial differential. and  $\nabla$  is Laplace differential operator;  $K_1$  and  $K_2$  are normal and shear stiffness of the foundation, respectively. This model is simply known as Winkler type when  $K_2 = 0$ . Yamin [1996].

### Displacement Field Model

In the present study the Reddy's higher order shear deformation theory has been employed [1984], Shankara et al.[1996]. The modified displacement field along the  $x$ ,  $y$ , and  $z$  directions for an arbitrary composite laminated plate is now written as

### Strain Displacement Relations

The strain-displacements relations with von Karman type geometric nonlinear elasticity are expressed as Chia[1980].

### Stress-Strain Relation

The constitutive relationship between stress resultants and corresponding strains of laminated composite plate accounting for thermal effect can be written as Reddy[1996], Franklin[1968], and Jones [1975].

$$\{\sigma\}_k = [\bar{Q}]_k \{\varepsilon\}_k \text{ or } \begin{Bmatrix} \sigma_x \\ \sigma_y \\ \sigma_{xy} \\ \sigma_x \\ \sigma_y \\ \sigma_{xz} \\ \sigma_{yz} \end{Bmatrix} = \begin{bmatrix} \bar{Q}_{11} & \bar{Q}_{12} & \bar{Q}_{16} & 0 & 0 \\ \bar{Q}_{12} & \bar{Q}_{22} & \bar{Q}_{26} & 0 & 0 \\ \bar{Q}_{16} & \bar{Q}_{26} & \bar{Q}_{66} & 0 & 0 \\ 0 & 0 & 0 & \bar{Q}_{44} & \bar{Q}_{45} \\ 0 & 0 & 0 & \bar{Q}_{45} & \bar{Q}_{55} \end{bmatrix} \begin{Bmatrix} \varepsilon_x \\ \varepsilon_y \\ \varepsilon_{xy} \\ \varepsilon_{xz} \\ \varepsilon_{yz} \end{Bmatrix} - \begin{Bmatrix} \lambda_1 \\ \lambda_2 \\ \lambda_3 \\ 0 \\ 0 \end{Bmatrix} T(X, Y, Z) \quad (2)$$

where  $\{\bar{Q}\}_k$ ,  $\{\sigma\}_k$  and  $\{\varepsilon\}_k$  are transformed stiffness matrix, stress and strain vectors of the  $k$ th lamina, respectively and  $\alpha_x$ ,  $\alpha_y$ ,  $\alpha_{xy}$  are the thermal expansion coefficients along  $x$ ,  $y$ ,  $z$ , direction, respectively which can be obtained from the thermal coefficients in the longitudinal ( $\alpha_l$ ) and transverse ( $\alpha_t$ ) directions of the fibers using transformation matrix.  $T(X, Y, Z)$  is the uniform temperature field distribution.

Relationship between stress resultants and mid-plane strain are

$$\begin{Bmatrix} N_i \\ M_i \\ P_i \end{Bmatrix} = \begin{bmatrix} A_{ij} & B_{ij} & E_{ij} \\ B_{ij} & D_{ij} & F_{ij} \\ E_{ij} & F_{ij} & H_{ij} \end{bmatrix} \begin{Bmatrix} \varepsilon_j^0 \\ k_j^0 \\ k_j^2 \end{Bmatrix} - \begin{Bmatrix} N_i^T \\ M_i^T \\ P_i^T \end{Bmatrix} \quad (i, j=1, 2, 6) \quad (3a)$$

$$\begin{Bmatrix} Q_2 \\ Q_1 \end{Bmatrix} = \begin{bmatrix} A_{4j} & D_{4j} \\ A_{5j} & D_{5j} \end{bmatrix} \begin{Bmatrix} \varepsilon_j^0 \\ k_j^2 \end{Bmatrix}; \begin{Bmatrix} R_2 \\ R_1 \end{Bmatrix} = \begin{bmatrix} D_{4j} & F_{4j} \\ D_{5j} & F_{5j} \end{bmatrix} \begin{Bmatrix} \varepsilon_j^0 \\ k_j^2 \end{Bmatrix} \quad (j=4, 5) \quad (3b)$$

where the stress resultants per unit length  $\{N_i\} = [N_{ix} \ N_{iy} \ N_{ixy}]^T$ ,  $\{M_i\} = [M_{ix} \ M_{iy} \ M_{ixy}]^T$  and  $\{P_i\} = [P_{ix} \ P_{iy} \ P_{ixy}]^T$  are expressed in terms of mid plane strains and curvatures

The thermal stress resultants and moments per unit length  $N_i^T = [N_{ix}^T \ N_{iy}^T \ N_{ixy}^T]^T$ ,  $M_i^T = [M_{ix}^T \ M_{iy}^T \ M_{ixy}^T]^T$  and  $P_i^T = [P_{ix}^T \ P_{iy}^T \ P_{ixy}^T]^T$  due to temperature change are calculated by

$$[N_i^T, M_i^T, P_i^T] = \sum_{m=1}^N \int_{-h/2}^{h/2} \begin{Bmatrix} (Q_{11} + Q_{12})\alpha_1 \\ (Q_{12} + Q_{22})\alpha_2 \\ 0 \end{Bmatrix} (1, z, z^3) T(X, Y, Z) dz \quad (4)$$

For the post buckling problem it is assumed that the temperature field exhibit the linear variation through the plate thickness ( $T, T$ )

$$T(X, Y, Z) = T0 \left[ 1 + \frac{z}{h} \right] \quad (5)$$

For the plate subjected with uniform temperature rise (U.T)

$$T(X, Y, Z) = T0 \quad (6)$$

### Strain Energy of the Plate

The strain energy of the plate is given by  $U = \frac{1}{2} \int_V \{\varepsilon\}^T [\sigma] dV$ ,

Strain energy U can be rewritten as

$$U = U_l + U_{nl} \quad (7)$$

Where  $U_l$  and  $U_{nl}$  are the linear and nonlinear part of the strain energy, respectively which can be expressed as

$$U_l = \frac{1}{2} \int_A \{\varepsilon_l\}^T [\bar{Q}] \{\varepsilon_l\} dA, U_{nl} = \frac{1}{2} \int_A \{\varepsilon_l\}^T \{\bar{Q}\} \{\varepsilon_{nl}\} dA + \frac{1}{2} \int_A \{\varepsilon_{nl}\}^T \{\bar{Q}\} \{\varepsilon_l\} dA + \frac{1}{2} \int_A \{\varepsilon_{nl}\}^T \{\bar{Q}\} \{\varepsilon_{nl}\} dA, \quad (8)$$

### Nonlinear Part of the Strain Energy of the Plate

Using nonlinear strain-displacement relations in the von Karman sense Liu et al.[1986] the nonlinear part of energy as given above can be expressed as

$$U_{nl} = \frac{1}{2} \int_A [\bar{\varepsilon}_l]^T [D_3] \{A\} \{\phi\} dA + \frac{1}{2} \int_A \{A\}^T \{\phi\}^T [D_4] \{\bar{\varepsilon}_l\} dA + \frac{1}{2} \int_A \{A\}^T \{\phi\}^T [D_5] \{A\} \{\phi\} dA,$$

Where  $[D_3]$ ,  $[D_4]$  and  $[D_5]$  are the laminate stiffness matrices and  $[A]$  and  $\{\phi\}$  of the plate defined as

$$A = \frac{1}{2} \begin{bmatrix} w_{,x} & 0 \\ 0 & w_{,y} \\ w_{,x} & w_{,y} \\ 0 & 0 \\ 0 & 0 \end{bmatrix}, \text{ and } \{\phi\} = \begin{Bmatrix} w_{,x} \\ w_{,y} \end{Bmatrix} \quad (9)$$

and

$$\{\bar{\varepsilon}_l\} = (\varepsilon_1^0 \quad \varepsilon_2^0 \quad \varepsilon_6^0 \quad k_1^0 \quad k_2^0 \quad k_6^0 \quad k_1^2 \quad k_2^2 \quad k_6^2 \quad \varepsilon_4^0 \quad \varepsilon_5^0 \quad k_4^2 \quad k_5^2)^T,$$

### Strain Energy Due to Elastic Foundation

The potential energy ( $\Pi_2$ ) for nonlinear elastic foundation having shear deformable layers can be written as

$$\Pi_2 = \frac{1}{2} \int_A \left\{ K_1 w^2 + \frac{1}{2} K_3 W^4 + K_2 \left[ (w_{,x})^2 + (w_{,y})^2 \right] \right\} dA, \Pi_2 = \frac{1}{2} \int_A \begin{Bmatrix} w \\ w_{,x} \\ w_{,y} \end{Bmatrix}^T \begin{bmatrix} K_1 & 0 & 0 \\ 0 & K_2 & 0 \\ 0 & 0 & K_2 \end{bmatrix} \begin{Bmatrix} w \\ w_{,x} \\ w_{,y} \end{Bmatrix} dA \quad (10)$$

### Potential Energy Due to Thermal Stresses

The potential energy ( $\Pi_3$ ) due to applied in-plane thermal forces in producing is written a

$$\Pi_3 = \frac{1}{2} \int_A \left[ N_x (w_{,x})^2 + N_y (w_{,y})^2 + 2N_{xy} (w_{,x})(w_{,y}) \right] dA = \frac{1}{2} \int_A \begin{Bmatrix} w_{,x} \\ w_{,y} \end{Bmatrix}^T \begin{bmatrix} N_x & N_{xy} \\ N_{xy} & N_y \end{bmatrix} \begin{Bmatrix} w_{,x} \\ w_{,y} \end{Bmatrix} dA \quad (11)$$

where,  $N_x$ ,  $N_y$  and  $N_{xy}$  are in plane applied thermal loads along x, y and z axis.

### Kinetic Energy of the Laminate.

The kinetic energy (T) of the vibrating laminated plate can be expressed as

$$T = \frac{1}{2} \int_V \rho^{(k)} \left\{ \dot{\mathbf{u}} \right\}^T \left\{ \dot{\mathbf{u}} \right\} dV, \quad (12)$$

where  $\rho$  and  $\left\{ \dot{\mathbf{u}} \right\} = \left\{ \dot{u} \quad \dot{v} \quad \dot{w} \right\}^T$  are the density and velocity vector of the plate respectively.

### Finite Element Model

In the finite element method the domain is discretized into a set of finite elements. Over each of the elements, the displacement vector and element geometry are represented as

$$\left\{ \Lambda \right\} = \sum_{i=1}^{NN} \varphi_i \left\{ \Lambda \right\}_i; \quad x = \sum_{i=1}^{NN} \varphi_i x_i; \quad \text{and} \quad y = \sum_{i=1}^{NN} \varphi_i y_i \quad (13)$$

where  $\varphi_i$  is the interpolation (shape function) function for the  $i$ th node,  $\left\{ \Lambda \right\}_i$  is the vector of unknown displacements for the  $i$ th node, NN is the number of nodes per element and  $x_i$  and  $y_i$  are Cartesian Coordinate of the  $i$ th node.

### Strain Energy of the Laminated Plate

The linear and the nonlinear functional are computed for each element and then summed over all the elements in the domain to get the total functional. Following this

$$\Pi = \sum_{e=1}^{NE} (\Pi_l^{(e)} + \Pi_{nl}^{(e)}) \quad (14)$$

where, NE is the number of elements and where

$$\Pi_{nl}^{(e)} = \frac{1}{2} \int_A \left\{ \Lambda^{(e)} \right\} \left[ K_{1nl} \right]^{(e)} \left\{ \Lambda^{(e)} \right\} dA + \frac{1}{2} \int_A \left\{ \Lambda^{(e)} \right\}^T \left[ K_{2nl} \right]^{(e)} \left\{ \Lambda^{(e)} \right\} dA$$

$$\Pi_l^{(e)} = \frac{1}{2} \int_A \left\{ \Lambda^{(e)} \right\} \left[ K_l \right]^{(e)} \left\{ \Lambda^{(e)} \right\} dA$$

Here  $\left[ K_{1nl} \right]^{(e)}$  and  $\left[ K_{2nl} \right]^{(e)}$  are the elemental nonlinear stiffness matrices,  $\left[ K_l \right]^{(e)}$  is the elemental linear stiffness matrix and  $\left\{ \Lambda^{(e)} \right\}$  is the elemental nodal displacement vector.

$$\begin{aligned} \Pi_{nl}^{(e)} &= \sum_{e=1}^{NE} \left[ \frac{1}{2} \left\{ \Lambda^{(e)} \right\}^T \left[ K_l^{s(e)} + K_{nl}^{(e)} \right] \left\{ \Lambda^{(e)} \right\} - \left\{ \Lambda^{(e)} \right\}^T \left[ F_l^{(e)} \right] \right] \\ &= \frac{1}{2} \left\{ q \right\}^T \left[ K_l + K_{nl} \right] \left\{ q \right\} - \left\{ q \right\}^T \left[ F^T \right] \end{aligned} \quad (15)$$

with  $\left[ K_l \right] = \left[ K_b \right] + \left[ K_s \right]$

where global bending stiffness matrix  $\left[ K_b \right]$ , shear stiffness matrix  $\left[ K_s \right]$ , global nonlinear stiffness matrix  $\left[ K_{nl} \right]$ , global displacement vector  $\left\{ q \right\}$  and thermal load vector  $\left[ F \right]$  are defined in appendix.

### Strain Energy Due to Elastic Foundation

Using finite element notation after summed over all the element can be written as:

$$\Pi_2 = \left( \sum_{e=1}^{NE} \Pi_{fl}^{(e)} + \sum_{e=1}^{NE} \Pi_{fnl}^{(e)} \right), \Pi_{fl}^{(e)} = \frac{1}{2} \int_A \left\{ \Lambda^{(e)} \right\}^T \left[ K_{fl} \right]^{(e)} \left\{ \Lambda^{(e)} \right\} dA, \Pi_{fnl}^{(e)} = \frac{1}{2} \int_A \left\{ \Lambda^{(e)} \right\}^T \left[ K_{fnl} \right]^{(e)} \left\{ \Lambda^{(e)} \right\} dA \quad (16)$$

here,  $[K_f]^{(e)}$  and  $[K_{fnl}]^{(e)}$  are the elemental linear and nonlinear foundation stiffness matrices respectively.

### Thermal Post Buckling Analysis

Using finite element model Equation can also be written as

$$\Pi_3 = \sum_{e=1}^{NE} \Pi_3^{(e)} = \sum_{e=1}^{NE} \{\Lambda\}^{T(e)} \lambda [K_g]^{(e)} \{\Lambda\}^{(e)} = \frac{1}{2} \sum_{e=1}^{NE} \{\Lambda\}^{T(e)} \lambda [K_g]^{(e)} \{\Lambda\}^{(e)} dA \quad (17)$$

Where,  $\lambda$  and  $[K_g]^{(e)}$  represent the thermal buckling load parameter and the elemental geometric stiffness matrix, for the  $e^{\text{th}}$  element respectively.

### Kinetic Energy of Laminate Plate

Using Eq. (16) and Eq. (15) can also be written as

$$T = \sum_{e=1}^{NE} T^{(e)}, \quad T^{(e)} = \frac{1}{2} \sum_{e=1}^{NE} \{\dot{\Lambda}\}^{T(e)} [M]^{(e)} \{\dot{\Lambda}\}^{(e)} \quad (18)$$

where  $[M]^{(e)}$  is consistent inertia matrix of  $e^{\text{th}}$  element.

Adopting Gauss quadrature integration numerical rule, the elemental linear, non-linear, foundation stiffness matrices and geometric stiffness matrix respectively can be obtained by transforming expression in Cartesian  $x, y$  coordinate system to natural coordinate system  $\xi, \eta$ .

### Governing Equations

The governing equation for thermal buckling and thermal nonlinear free vibration plate analysis can be derived using the Lagrange's equation of motion Reddy [1984] in terms of global matrices. This gives

$$[M]\{\Lambda\} + [K_s + K_g]\{\Lambda\} = 0 \quad (19)$$

The above equation can be expressed in the form of nonlinear generalized eigen value problem for both thermal post buckling and thermal nonlinear free vibration as

$$[K]\{q\} = \lambda_1 [K_g]\{q\} + \lambda_2 [M]\{q\} \quad (20)$$

Where

$$[K] = [K_l] + [K_f] + [K_{nl}\{q\}] + [K_{fnl}\{q\}] \text{ and } \{q\} = \sum_{e=1}^{NE} \{\Lambda\}^{(e)} \quad (21)$$

here  $\{q\}, [K_l], [K_g], [K_{nl}], [K_f], [K_{fnl}], [M], \lambda_1$  and  $\lambda_2 = \omega^2$  are defined as the global displacement vector, the global linear stiffness matrix, the global geometric stiffness matrix, global nonlinear stiffness matrix, global foundation stiffness matrix, the global nonlinear foundation stiffness matrix, the global mass matrix, the thermal post buckling parameter and thermal nonlinear natural frequency parameter respectively. Since the matrix  $[K]$  is random in nature involving the uncertain material properties and foundation stiffness parameters, the thermal post buckling load parameters, nonlinear natural frequency parameter and their displacement vector also become random.

Therefore the eigen values and eigenvectors also become random. The Eq. (20) can be solved with the help probabilistic DISFEM combined in conjunction with perturbation technique or Monte Carlo simulation (MCS) to compute the mean and variance of the thermal post buckling temperature.

### Solution Approach- a DISFEM for Thermal Post-buckling and Thermal Nonlinear Free Vibration Problem

A DISFEM approach has been adopted for obtaining the second order statistics of dimensionless thermal nonlinear fundamental frequency and thermal post-buckling response of laminated composite plate resting on elastic

foundation with randomness in material properties and foundation parameters. The material properties and foundation parameters are assumed to be basic input random variables. Without any loss of generality, the random variable can be split up as the sum of a mean and a zero random part Singh et al.[2002]. In general a random variable can be represented as the sum of its mean and zero mean random variable, denoted by superscripts 'd' and 'r', respectively.

$$K = K^d + K^r; \lambda_{1i} = \lambda_{1i}^d + \lambda_{1i}^r, \lambda_{2i} = \lambda_{2i}^d + \lambda_{2i}^r \quad (22)$$

and

$$q_i = q_i^d + q_i^r \quad (23)$$

where  $\lambda_{2i}^d = \omega_i^{d^2}$ ,  $\lambda_{2i}^r = 2\omega_i^d \omega_i^r + \omega_i^{r^2}$ ,  $i = 1, 2, \dots, p$ . The parameter  $p$  indicates the size of eigen problem.

Consider a class of problems where the random variation is very small as compared to the mean part of material properties. Further it is quite logical to assume that the coefficient of variation in the derived quantities like  $\lambda, \omega, q, r$  and  $K, r$  are also small as compared to mean values.

By substituting Eq. (22) in Eq. (20) and expanding the random parts in Taylor's series keeping the first order terms and neglecting the second and higher order terms, same order of the magnitude term, one obtains as

For thermal nonlinear free vibration and thermal post buckling analysis Klieber et al.[1992]

Zeroth order:

$$[K^d] \{q_i^d\} = \lambda_{2i}^d M \{q_i^d\} + \lambda_{1i}^d K_g \{q_i^d\} \quad (24)$$

First order:

$$[(K^d - \lambda_{2i}^d M - \lambda_{1i}^d K_g)] \{q_i^r\} = -(K^r - \lambda_{2i}^r M - \lambda_{1i}^r K_g) \{q_i^d\} \quad (25)$$

Eq. (23) is the deterministic equations relating to the mean eigen values and corresponding mean eigenvectors, which can be determined by conventional eigen solution procedures. Eq. (24) the first order perturbation approach is employed in the present study Singh et al.[2001,2002].

Using this Eq. (24) can be decoupled and the expression for  $\lambda_{1i}^r$  and  $\lambda_{2i}^r$  separately for thermal post buckling and thermal nonlinear free vibration are obtained.

The FEM in conjunction with first order perturbation has been found to be accurate and efficient Klieber et al.[1992]. According to this method, the random variables are expressed by Taylor's series. Keeping the first order terms and neglecting the second and higher-order terms Eq. (22) can be expressed as because, the first order is sufficient to yield results with desired accuracy for problems with low variability.

$$\lambda_i^r = \sum_{j=1}^q \lambda_{i,j}^d b_j^r; \{q_i^r\} = \sum_{j=1}^p q_{i,j}^d b_j^r; [K^r] = \sum_{j=1}^q [K_{,j}^d] b_j^r; \quad (26)$$

Using the above and decoupled equations, the expressions for  $\lambda_{1i,j}^d$  and  $\lambda_{2i,j}^d$  are obtained. Using Eq. (25) the variances of the eigen values can now be expressed as :

$$Var(\lambda_{1i}) = \sum_{j=1}^p \sum_{k=1}^p \lambda_{1i,j}^d \lambda_{1i,k}^d Cov(b_j^r, b_k^r) \quad (27)$$

$$Var(\lambda_{2i}) = \sum_{j=1}^p \sum_{k=1}^p \lambda_{2i,j}^d \lambda_{2i,k}^d Cov(b_j^r, b_k^r) \quad (28)$$

where  $Cov(b_j^r, b_k^r)$  is the cross variance between  $b_j^r$  and  $b_k^r$ . The standard deviation (SD) is obtained by the square root of the variance Zhang et al.[1991].

## Results and Discussions

In present work a program in mat lab has been developed to find out Second-order statistics of the thermal post buckling temperature for laminated composite plates subjected to uniform temperature distribution with temperature independent thermo-elastic properties. Amplitude ratios, boundary conditions, plate thickness ratios and aspect ratios are varied for detailed analysis. A nine noded Lagrange isoparametric element with 63 DOFs per element for the present HSDT model has been used for discretizing the laminate and  $(4 \times 4)$  mesh has been used throughout the study. Unless otherwise mentioned all the results reported in this paper have been obtained employing the full integration  $(3 \times 3)$  rule. The coding has been done in MATLAB. The mean and standard deviation of the thermal post buckling temperature are obtained considering the random material input variables, thermal expansion coefficients and lamina plate thickness taking combined as well as separately as basic random variables (RVs) as stated earlier. However, the results are only presented taking SD/mean of the system property equal to 0.10 Liu et al. [1986] as the nature of the SD (Standard deviation) variation is linear and passing through the origin. Hence, the presented results would be sufficient to extrapolate the results for other SD/mean value keeping in mind the limitation of FOPT Liu et al. [1986]. The basic random variables such as  $E_1, E_2, G_{12}, G_{13}, G_{23}, \nu_{12}, \alpha_1, \alpha_2$  and  $k_1, k_2$  are sequenced and defined as

$$b_1 = E_{11}, \quad b_2 = E_{22}, \quad b_3 = G_{12}, \quad b_4 = G_{13}, \quad b_5 = G_{23}, \quad b_6 = \nu_{12}, \quad b_7 = \alpha_1, \quad b_8 = \alpha_2, \quad b_9 = k_1, \quad b_{10} = k_{10}$$

The following dimensionless thermal post buckling load, foundation parameters has been used in this study.  $T_{cr} = \lambda_{cr} T \alpha_o * 1000$ ;  $k_1 = K_1 D_{11} / a^4$ ;  $k_2 = K_2 D_{11} / a^2$ ; Where  $\lambda_{cr}, \alpha_o, T, k_1$  and  $k_2$  are the dimensional mean thermal buckling load, the initial thermal expansion coefficient and the initial guessed temperature, Dimensionless Winkler and Pasternak foundation parameters, respectively.

The dimensionless nonlinear thermal free vibration  $\varpi = (\omega a^2 \sqrt{\rho / E_{22}^d}) / h$ ,  $\lambda_T = \lambda_{cr} T \alpha_o (b/h)^2$ , Frequency ratio =  $\varpi_{nl} / \varpi_1$ . has been use for analysis. The following material properties are used for computation for thermal nonlinear free vibration.

$$E_{11}^d = 40E_{22}^d, \quad G_{12}^d = G_{13}^d = 0.6E_{22}^d, \quad G_{23}^d = 0.5E_{22}^d, \quad \nu_{12}^d = 0.25, \quad \rho = 1. \\ \alpha_1^d = 1.14 * 10^{-6} \text{ } ^\circ\text{C}^{-1}, \quad \alpha_2^d = 11.4 * 10^{-6} \text{ } ^\circ\text{C}^{-1}, \quad \alpha_0^d = 1 * 10^{-6} \text{ } ^\circ\text{C}^{-1}, \quad E_{22}^d = 6.92 * 10^9 \text{ Pa.}$$

The plate geometry used is characterized by aspect ratios  $(a/b) = 1$  and  $1.5$ , side to thickness ratios  $(a/h) = 10, 20$

In the present study various combination of edge support conditions namely clamped (C) and simply supported (S) have been used for the investigation. For example, CSCS means clamped edges at  $x = 0, a$  while simply supported at edges at  $y = 0$  and  $b$ . The boundary conditions for the plate are Fig. [2].

All edges simply supported (S1):

$$u = w = \theta_y = \psi_y = 0, \text{ at } x = 0, a; \quad v = w = \theta_x = \psi_x = 0 \text{ at } y = 0, b;$$

All edges simply supported (S2):

$$v = w = \theta_y = \psi_y = 0, \text{ at } x = 0, a; \quad u = w = \theta_x = \psi_x = 0 \text{ at } y = 0, b;$$

All edges clamped (CCCC):

$$u = v = w = \psi_x = \psi_y = \theta_x = \theta_y = 0, \text{ at } x = 0, a \quad \text{and } y = 0, b;$$

Two opposite edges clamped and other two simply supported (CSCS):

$$u = v = w = \psi_x = \psi_y = \theta_x = \theta_y = 0, \quad v = w = \theta_y = \psi_y = 0, \text{ at } x = a \\ \text{at } x = 0 \quad \text{and } y = 0; \quad u = w = \theta_x = \psi_x = 0, \text{ at } y = b;$$

For thermal post buckling with foundation parameters the plate geometry used is characterized by aspect ratios  $(a/b) = 1$  and  $2$ , side to thickness ratios  $(a/h) = 20, 30, 40, 50$  and  $100$ . The following mean values of the material

constants and thermal expansion coefficients are used for computation. We consider now a second steps as the elastic constants and thermal expansion coefficients of each layers are assumed to be linear function of temperature. The only exception is the Poisson's ratio, which can reasonably be assumed as constant due to weakly dependency on temperature change Shen [2001].

$$E_{11}(T) = E_{10}(1 + E_{11}^1 T), \quad E_{22}(T) = E_{20}(1 + E_{21}^1 T), \quad G_{12}(T) = G_{120}(1 + G_{121}^1 T), \quad G_{13}(T) = G_{130}(1 + G_{131}^1 T)$$

$$G_{23}(T) = G_{230}(1 + G_{231}^1 T), \quad \alpha_1(T) = \alpha_{10}(1 + \alpha_{11}^1 T), \quad \alpha_2(T) = \alpha_{20}(1 + \alpha_{21}^1 T)$$

and

$$E_{10}/E_{20} = 40, \quad G_{120}/E_{20} = G_{130}/E_{20} = 0.5 G_{230}/E_{20} = 0.2, \quad \nu_{12} = 0.25, \quad \alpha_{10}/\alpha_1 = 1, \alpha_{20}/\alpha_1 = 10, \quad E_{11}^1 = -0.5 \times 10^{-3}$$

$$E_{21}^1 = G_{121}^1 = G_{131}^1 = G_{231}^1 = -0.2 \times 10^{-3}, \alpha_{11}^1 = \alpha_{21}^1 = 0.5 \times 10^{-3}$$

All layers are of equal thickness. For the temperature independent material properties (TID)  $E_{11}^1, E_{21}^1, G_{121}^1, G_{131}^1, G_{231}^1, \alpha_{11}^1$  and  $\alpha_{21}^1$  quantities are equal to zero.

The material properties of the laminated composite plate for Table (3) are given in Pandey et al.[2009].  $E_1/E_2 = 25; G_{12} = 0.5E_2; G_{23} = 0.2E_2; E_{20} = 1 \times 10^5; \nu_{12} = 0.25; E_{10} = m_1 \times E_{20}; G_{120} = m_2 \times E_{20}; G_{130} = G_{120}; G_{230} = m_3 \times E_{20}; \nu_{21} = \nu_{12} \times E_{20}/E_{10}; \alpha_{110} = 1 \times 10^{-6}; \alpha_{210} = 10.0 \times 10^{-6}; \alpha_{12} = 0; \alpha_0 = 1 \times 10^{-6}$ ; The non dimensionalised foundation parameters are as;  $K_1 = k_1 \times D_{11} / a^4, K_2 = k_2 \times D_{11} / a^2, K_3 = k_3 \times D_{11} / a^4 \times h^2$ .

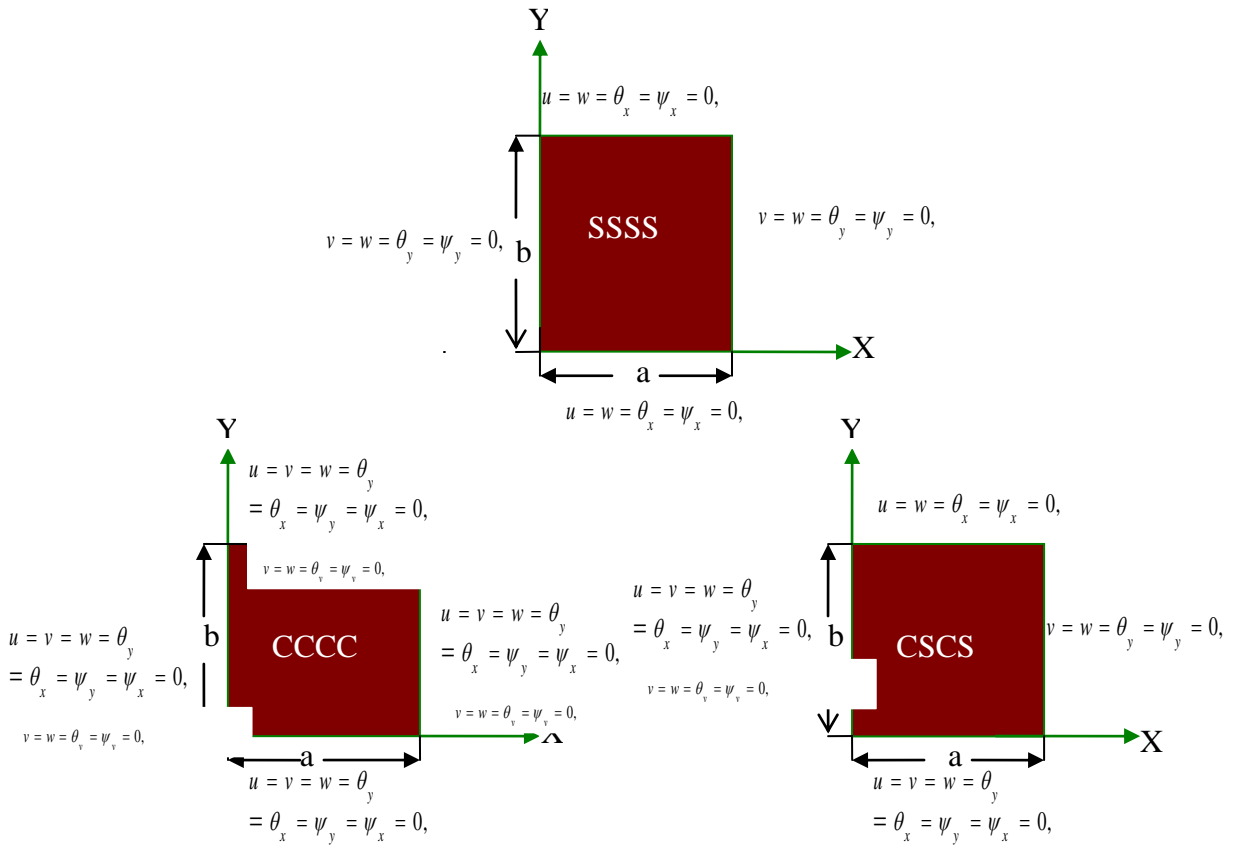


FIGURE 1. VARIOUS BOUNDARY CONDITIONS FOR A RECTANGULAR PLATE

### Validation Results for Mean Dimensionless Thermal Post Buckling Load

The present deterministic FEM results are compared and validated with the results available in the literature. The dimensionless critical buckling temperature of simply supported (S2) angle-ply ( $\pm 45$ ) $_2$ T square laminated composite plate resting on Winkler and Pasternak elastic foundations with various amplitude ratios, subjected to uniform constant temperature (U.T) is presented in Table (1) and compared with that of Shen [2001]. It can be seen that the present results are in good agreement. The difference from present results is due to semi analytical

approach used in Shen [2001].

TABLE 1 COMPARISON OF THERMAL POST BUCKLING LOADS OF ANGLE-PLY ( $\pm 45^\circ$ ) 2T SQUARE LAMINATED COMPOSITE PLATE RESTING ON WINKLER ( $k_1=2, k_2=0$ ) AND PASTERNAK ( $k_1=2, k_2=0.5$ ) ELASTIC FOUNDATIONS FOR DIFFERENT AMPLITUDE RATIOS ( $W_{max}/h$ ) SUBJECTED TO UNIFORM CONSTANT TEMPERATURE (U.T) DISTRIBUTION AND IN-PLANE BI-AXIAL COMPRESSION. PLATE THICKNESS RATIO  $A/H=30$  WITH SIMPLY SUPPORTED S2 BOUNDARY CONDITIONS. (TID) AND (TD) ARE TEMPERATURE INDEPENDENT & TEMPERATURE DEPENDENT MATERIAL PROPERTIES RESPECTIVELY.

$W_{max}/h$	$k_1=2, k_2=0$				$k_1=2, k_2=0.5$			
	(TID)		(TD)		(TID)		(TD)	
	Present [HSDT]	Shen [2001]	Present [HSDT]	Shen [2001]	Present [HSDT]	Shen [2001]	Present [HSDT]	Shen [2001]
0.0	1.4141	1.3675	0.9206	0.8880	1.5547	1.5200	1.0073	0.9570
0.1	1.4255	1.3846	0.9280	0.8970	1.5661	1.5384	1.0147	0.9740
0.2	1.4578	1.4188	0.9490	0.9230	1.5984	1.5726	1.0358	0.9910
0.3	1.5057	1.4700	0.9811	0.9570	1.6463	1.6230	1.0679	1.0250
0.4	1.5672	1.5720	1.0229	0.9910	1.7078	1.7260	1.1096	1.0427
0.5	1.6294	1.6580	1.0705	1.0250	1.7700	1.8110	1.1573	1.0760

In the first sets of example, the dimensionless critical buckling temperature of simply supported isotropic plate with various aspect ratios subjected to uniform temperature distribution is presented in Table (2) and compared with the result available in Sita [2003], Chen et al. [1991] and Boley [1960]. It can be seen that the present results are in good agreement.

TABLE 2 COMPARISON OF CRITICAL BUCKLING TEMPERATURE PARAMETERS ( $T_{cr} = \lambda_{cr} T \alpha_o * (a/h)^2$ ) FOR THE SIMPLY SUPPORTED (S1) THIN LAMINATED COMPOSITE ISOTROPIC PLATE. PLATE THICKNESS RATIO ( $A/H=100$ ), ASPECT RATIOS ( $A/B$ ) AND MATERIAL PROPERTIES ( $\nu=0.30, E_{11}/E_{22}=1.00, A=1.0 \times 10^{-6}$ ).

$a/b$	$T_{cr} = \lambda_{cr} T \alpha_o * (a/h)^2$			
	Chen[1991]	Sita et al.[2003]	Boley[1960]	Present [HSDT]
0.25	0.691	0.672	0.686	0.690
0.50	0.814	0.791	0.808	0.805
1.00	1.319	1.265	1.283	1.306

The parametric studies results for aspect ratio  $a/b=1$ , thickness ratios  $b/h=10$ , simply supported SSSS S2, angle ply ( $\pm 45^\circ$ ) 2T laminated composite plate with foundation parameters  $k_1=50, k_2=10$  and  $k_3=100$ , rise in temperature ( $T_1$ ) =100, (dimensionless critical temperature  $T_{cr} = T_1 * \alpha_0 * 1000$ ) with biaxial compression is presented in Table (3) and compared with the analytical results of Pandey et al. [2009].

TABLE 3 COMPARISON OF PARAMETRIC STUDIES RESULTS FOR ASPECT RATIO ( $A/B=1$ ), PLATE THICKNESS RATIO ( $A/H=10$ ), AMPLITUDE RATIOS ( $W_{max}/h$ ), SIMPLE SUPPORT SSSS S2, ANGLE PLY ( $\pm 45^\circ$ ) 2T LAMINATED COMPOSITE PLATE RESTING ON NONLINEAR ELASTIC FOUNDATIONS ( $k_1=50, k_2=10$  AND  $k_3=100$ ). TEMPERATURE ( $T_1=100K$ ), DIMENSIONLESS CRITICAL TEMPERATURE ( $T_{cr} = T_1 * \alpha_0 * 1000$ ) WITH BIAXIAL COMPRESSION.

$W_{max}/h$	Pandey et al.[2009]	Present [HSDT]
0.0	9.850	9.9812
0.2	10.076	10.1572
0.4	10.998	11.550
0.6	12.282	11.8981

**Validation Results for Mean Thermal Frequency**

The present finite element formulation for dimensionless nonlinear vibration analysis of cross-ply [00/90]S laminated composite square plate with various amplitude ratios, uniform thermal loading condition and all edges simply supported is shown in Table (4). The result is compared with the results of Liu and Huang [1996]. Clearly, it is seen that the present results obtained by HSDT are in good agreement with Liu and Huang results based on first-order shear deformation plate theory. The maximum difference is about 2%.

**Validation Result for Random Material Properties for Thermal Post Buckling Load**

Results for normalized standard deviation for the nonlinear thermal post buckling problems are not available in reported literature therefore present direct iterative method in conjunction with first order perturbation technique [DISFEM] results are compared and validated with an independent MCS approach. Fig. 4 (a)-(b) plots the normalized standard deviation, SD (i.e. the ratio of the standard deviation (SD) to the mean value), of thermal post buckling load versus the SD to the mean value of the random material constants for an all simply supported (S2) square [00/900] laminated composite plate of temperature independent and dependent thermo-elastic material properties. The plate is resting on Pasternak elastic foundation ( $k_1=100, k_2=10$ ),  $b/h=20$ , biaxial compression, amplitude ratio ( $W_{max}/h=0.2$ ) and subjected to uniform temperature distribution changing from 0 to 20%. It is assumed that one of the material property (i.e.,  $E_{11}$ ) change at a time keeping other as a deterministic with their mean values of the material properties. The dashed line is the present DISFEM result and the solid line is independent MCS approach. For the MCS approach, the samples are generated using Mat Lab to fit the desired mean and SD. These samples are used in response equation Eq. (21) which is solved repeatedly, adopting conventional Eigen value procedure, to generate a sample of the thermal post buckling load.

TABLE 4 COMPARISON OF DIMENSIONLESS NONLINEAR FUNDAMENTAL FREQUENCY ( $\omega_{NL}$ ) FOR PLATE THICKNESS RATIO ( $a/h=10$ ), RISE IN TEMPERATURE ( $\delta T$ ) AND AMPLITUDE RATIOS ( $W_{max}/h$ ) OF (0/900)S CROSS PLY LAMINATED COMPOSITE PLATES SUBJECTED TO TWO SETS OF THERMAL LOADING CONDITIONS.  $\omega_L$  – LINEAR FUNDAMENTAL FREQUENCY.

a/h	$\delta T$	$W_{max}/h$	$\omega_{NL}$	
			Liu et al. [1996]	Present [HSDF]
10	0	0.1	15.160	15.0985
		0.2	15.195	15.1543
		0.3	15.272	15.2424
		0.5	15.351	15.4907
		( $\omega_L$ )	15.150	15.0794
	50	0.1	15.062	15.0531
		0.2	15.098	15.0872
		0.3	15.176	15.1435
		0.5	15.254	15.3185
		( $\omega_L$ )	15.052	15.0417

The number of samples used for MCS approach is 12,000 based on satisfactory convergence of the results. The normal distribution has been assumed for random number generations in MCS. However, the present DISFEM used in the study does not put any limitation as regard to probability distribution of the system property. This is an advantage over the MCS. From the Fig. 3 (a)-(b) it is clear that, close correlation is achieved between two results subjected to TID and TD thermo-elastic material properties. It can also be observed that the DISFEM for present analysis is sufficient to give accurate results for the level of variations considered in the basic random variables. The mean response values in the two methods are almost same.

**Validation Result for Random Geometric Property for Thermal Frequency**

Validation of the present DIFOPT results with MCS for a square angle ply[450/-450/450] simply supported (SSSS) laminated composite plate, amplitude ratios subjected to temperature change  $\delta T=100$  with only one geometric property, h random, other deterministic is presented in Table (5).The results are in good agreement.

Fig. 3(c) plots the normalized standard deviation, ratio of the SD/Mean of the nonlinear dimensional fundamental frequency versus the SD/Mean of the random material constant for all simply supported square cross ply [00/900]S laminated composite plate subjected to in-plane thermal loading  $\delta T =100$  changing from 0 to 20%. It is assumed that one of the material property (i.e.,  $E_{11}$ ) change at a time keeping other as a deterministic, with their mean values of the material properties. The dashed line is the present DISFEM result and the solid line is independent MCS results. The results are in good agreement.

TABLE 5 VALIDATION OF PRESENT DIFOPT RESULTS WITH MCS FOR DIMENSIONLESS NONLINEAR MEAN ( $\bar{\omega}_{NL}$ ) AND COEFFICIENT OF VARIATIONS ( $\omega_{NL2}$ ) OF FUNDAMENTAL FREQUENCY FOR SQUARE ANGLE PLY [450/-450/450] SIMPLY SUPPORTED SSSS LAMINATED COMPOSITE PLATE . PLATE THICKNESS RATIO (A/H), ASPECT RATIO (A/B) WITH AMPLITUDE RATIOS ( $W_{max}/h$ ) SUBJECTED TO RISE IN TEMPERATURE ( $\Delta T=100$ ) AND ONLY ONE GEOMETRIC PROPERTY, H RANDOM, OTHER DETERMINISTIC.  $\bar{\omega}_L$  IS LINEAR FUNDAMENTAL FREQUENCY.

a/h	a/b	$W_{max}/h$	$\delta T=100$		
			Mean $\bar{\omega}_{nl}$	COV, $\omega_{nl}^2$	
				DIFOPT, $b_i, i=9$	MCS, $b_i, i=9$
20	1	0.3	17.7283 18.0347 18.4962 (17.6204)	0.0666 0.0651 0.0630	0.0700 0.0661 0.0645
		0.6			
		0.9			
		$\bar{\omega}_L$			

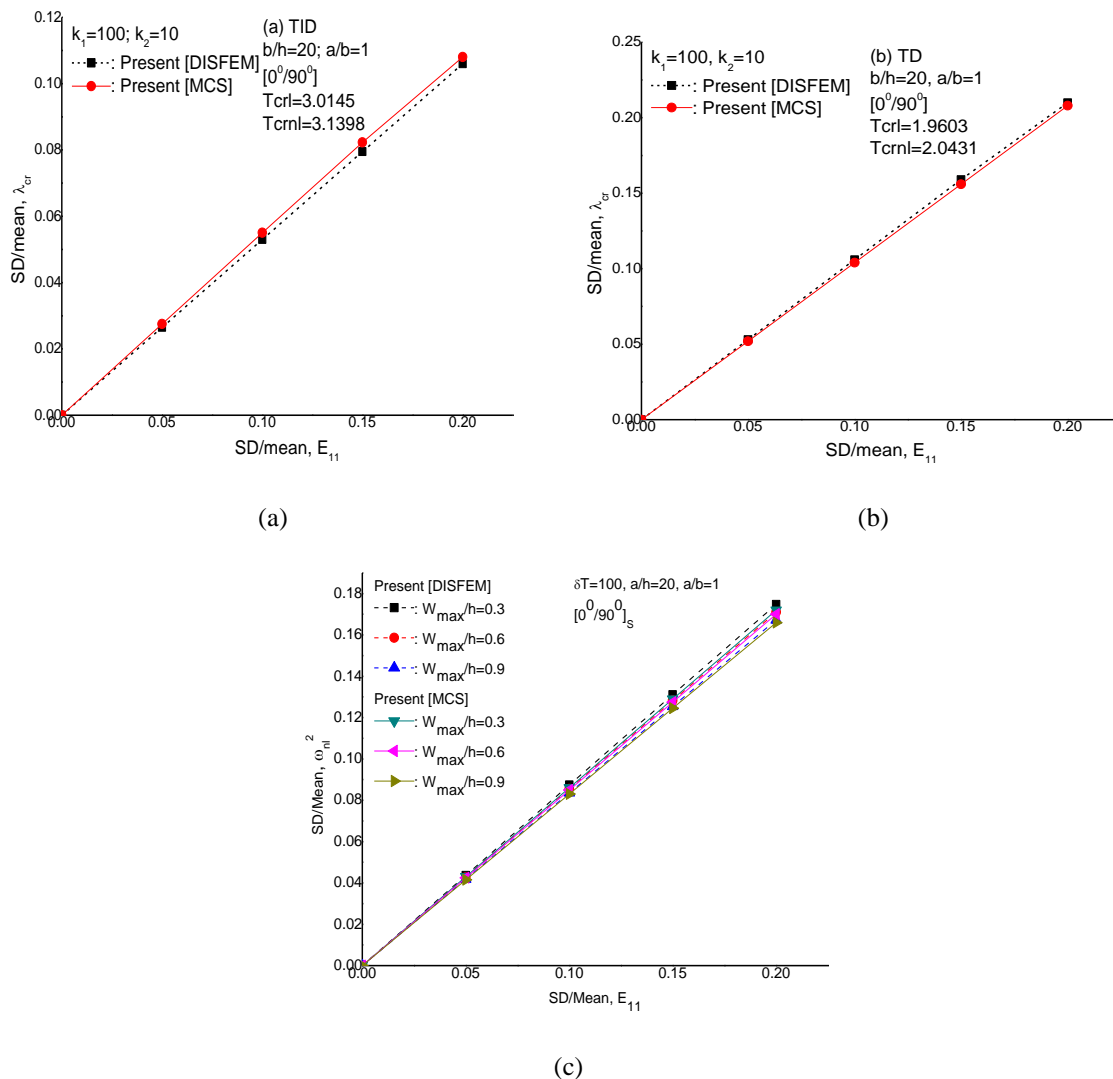


FIGURE 3. VILIDATION OF PRESENT DIFEM RESULTS FOR THERMAL POST BUCKLING AND NONLINEAR FREE VIBRATION WITH INDEPENDENT MCS RESULTS FOR ONLY ONE MATERIAL E11 VARYING SUBJECTED TO BIAXIAL COMPRESSION HAVING SSSS (S2)SUPPORT CONDITION WITH (a) TID (b)TD.(c)VALIDATION OF THE PRESENT DIFEM RESULTS FROM MCS

**Parametric Analysis of Second Order Statistics for Thermal Post Buckling and Non-linear Thermal Frequency**

Table (6)&(7) shows the effects of variation of individual random system properties with amplitude ratios  $W_{max}/h = (0.2, 0.4, 0.6)$  for  $SD/mean, b_i, (i=1 \text{ to } 10) = 0.10$  keeping other as deterministic on the dimensionless mean and coefficient of variation of thermal post buckling temperature of 6-layers anti-symmetric angle-ply ( $\pm 45$ ) $3T$  square

laminated composite plates resting on Winkler ( $k_1=100, k_2=0$ ), & Pasternak ( $k_1=100, k_2=10$ ) elastic foundations with simply supported SSSS (S2) condition,  $b/h=30$ . The dimensionless mean values of thermal post buckling load are given in brackets. It is observed that amplitude ratio increases the mean thermal post buckling load and decreases the coefficient of variations of the plate resting on Winkler and Pasternak elastic foundations. However the values are significant for Pasternak foundation. Among the all system properties considered, the random change in  $E_{11}$ ,  $V_{12}$  are more sensitive with Winkler Foundation TD case, and less for  $G_{12}$  and  $\alpha_{22}$  with Winkler Foundation TID case. There is significant effect of all random input parameters on the laminated composite plate with TD compared to TID.

TABLE 6 EFFECTS OF VARIATION OF INDIVIDUAL RANDOM SYSTEM PROPERTY FOR BI, [(i=1 TO 10) = 0.10] WITH AMPLITUDE RATIOS ( $W_{max}/h$ ) ON THE DIMENSIONLESS EXPECTED MEAN ( $T_{crnl}$ ) AND COEFFICIENT OF VARIATIONS ( $\lambda_{crnl}$ ) OF THERMAL POST BUCKLING LOAD OF ANGLE PLY [ $\pm 45$ ] $^3$ T SQUARE LAMINATED COMPOSITE PLATES RESTING ON WINKLER ( $k_1=100, k_2=0$ ) ELASTIC FOUNDATION, SUBJECTED TO UNIFORM CONSTANT TEMPERATURE (U.T) AND IN-PLANE BI-AXIAL COMPRESSION. PLATE THICKNESS RATIO ( $b/h=30$ ) WITH SIMPLE SUPPORT S2 BOUNDARY CONDITIONS. THE DIMENSIONLESS MEAN THERMAL POST BUCKLING TEMPERATURES ARE GIVEN IN BRACKETS. TCRL - LINEAR SOLUTION

$b_i$	$W_{max}/h$	Winkler foundation ( $k_1=100, k_2=0$ )	
		(TID)	(TD)
		(Mean, $T_{crnl}$ ), $COV, \lambda_{crnl}$	(Mean, $T_{crnl}$ ), $COV, \lambda_{crnl}$
$E_{11}$ ( $i=1$ )	0.2	0.0351 (1.4345)	0.0173(0.9405)
	0.4	0.0338 (1.5461)	0.0173(1.0156)
	0.6	0.0326 (1.6778)	0.0174 (1.1090)
	$T_{cr1}$	1.3898	0.9115
$E_{22}$ ( $i=2$ )	0.2	0.0111	0.0113
	0.4	0.0102	0.0097
	0.6	0.0090	0.0072
$G_{12}$ ( $i=3$ )	0.2	1.0051e-04	1.2991e-04
	0.4	1.4754e-04	1.2991e-04
	0.6	2.0204e-04	2.8278e-04
$G_{13}$ ( $i=4$ )	0.2	0.0071	0.0051
	0.4	0.0069	0.0050
	0.6	0.0071	0.0051
$G_{23}$ ( $i=5$ )	0.2	0.0028	0.0021
	0.4	0.0028	0.0020
	0.6	0.0029	0.0021
$V_{12}$ ( $i=6$ )	0.2	0.0268	0.0974
	0.4	0.0249	0.0905
	0.6	0.0230	0.0832
$\alpha_{11}$ ( $i=7$ )	0.2	0.0494	0.0685
	0.4	0.0458	0.0635
	0.6	0.0422	0.0581
$\alpha_{22}$ ( $i=8$ )	0.2	7.6651e-04	0.0015
	0.4	7.1114e-04	0.0014
	0.6	6.5529e-04	0.0013
$k_1$ ( $i=9$ )	0.2	0.0135	0.0132
	0.4	0.0125	0.0122
	0.6	0.0114	0.0111
$k_2$ ( $i=10$ )	0.2	0	0
	0.4	0	0
	0.6	0	0

Table (8) presents the variation of dimensionless mean and coefficient of variations of nonlinear fundamental frequency with amplitude ratios ( $W_{max}/h = 0.3, 0.6$  and  $0.9$ ) for symmetric 4-layers cross-ply  $[00/900]_2S$  laminated composite square plate, simply supported boundary conditions,  $a/h = 20$  with thermal loadings  $\delta T = 100, 200$ . The individual change in random system properties ( $b_i$ ) such as material properties and thermal expansion coefficients has been considered in the analysis with coefficient of variations  $b_i = 0.10$ , keeping all other random input as deterministic at their mean values. The nonlinear fundamental frequency is most affected by the random change in the coefficient of variations  $E_{11}$  and least affected by Poisson ratio  $\nu_{12}$ . From the table it can be seen that the effect of temperature rise, lowers the fundamental frequency at same amplitude ratio because it brings in a compressive

in-plane prestress state that leads to degradation in plate stiffness. At the same thermal loading the nonlinear mean frequency increases with increase the amplitude ratio. From the table it is clear that temperature increments make the nonlinear frequency more sensitive to the random change in thermal expansion coefficients.

TABLE 7 EFFECTS OF VARIATION OF INDIVIDUAL RANDOM SYSTEM PROPERTY FOR BI, [(i=1 TO 10) = 0.10] WITH AMPLITUDE RATIOS (W<sub>max</sub>/h) ON THE DIMENSIONLESS EXPECTED MEAN (T<sub>CRNL</sub>) AND COEFFICIENT OF VARIATIONS (λ<sub>CRNL</sub>) OF THERMAL POST BUCKLING LOAD OF ANGLE PLY [±45]3T SQUARE LAMINATED COMPOSITE PLATES RESTING ON PASTERNAK (κ<sub>1</sub>=100, κ<sub>2</sub>=10) ELASTIC FOUNDATION, SUBJECTED TO UNIFORM CONSTANT TEMPERATURE (U.T) AND IN-PLANE BI-AXIAL COMPRESSION. PLATE THICKNESS RATIO (B/H=30) WITH SIMPLE SUPPORT S2 BOUNDARY CONDITIONS. THE DIMENSIONLESS MEAN THERMAL POST BUCKLING TEMPERATURES ARE GIVEN IN BRACKETS. TCRL - LINEAR SOLUTION.

b <sub>i</sub>	W <sub>max</sub> /h	Pasternak Foundation (k <sub>1</sub> = 100, k <sub>2</sub> = 10)	
		(TID)	(TD)
		(Mean, T <sub>crnl</sub> ) , COV, λ <sub>crnl</sub>	(Mean, T <sub>crnl</sub> ) , COV, λ <sub>crnl</sub>
E <sub>11</sub> (i=1)	0.2	0.0470 (1.8163)	0.0321(1.1864)
	0.4	0.0453 (1.9279)	0.0312(1.2615)
	0.6	0.0435 (2.0595)	0.0302(1.3548)
	T <sub>cr1</sub>	1.7716	1.1574
E <sub>22</sub> (i=2)	0.2	0.0083	0.0822
	0.4	0.0077	0.0071
	0.6	0.0069	0.0053
G <sub>12</sub> (i=3)	0.2	7.9388e-05	1.0299e-04
	0.4	1.1832e-04	1.6112e-04
	0.6	1.6459e-04	2.3146e-04
G <sub>13</sub> (i=4)	0.2	0.0056	0.0041
	0.4	0.0055	0.0040
	0.6	0.0058	0.0042
G <sub>23</sub> (i=5)	0.2	0.0022	0.0016
	0.4	0.0022	0.0016
	0.6	0.0023	0.0017
V <sub>12</sub> (i=6)	0.2	0.0329	0.1190
	0.4	0.0311	0.1122
	0.6	0.0292	0.1047
α <sub>11</sub> (i=7)	0.2	0.0390	0.0543
	0.4	0.0367	0.0511
	0.6	0.0344	0.0476
α <sub>22</sub> (i=8)	0.2	6.0540e-04	0.0012
	0.4	5.7032e-04	0.0011
	0.6	5.3382e-04	0.0010
k <sub>1</sub> (i=9)	0.2	0.0106	0.0105
	0.4	0.0100	0.0098
	0.6	0.0093	0.0091
k <sub>2</sub> (i=10)	0.2	0.0210	0.0207
	0.4	0.0198	0.0195
	0.6	0.0185	0.0181

Table (9)&(10) show the effects of thickness ratios with amplitude ratios for SD/mean b<sub>i</sub>, [(i = 1 to 8), (7, 8) and (9, 10)] = 0.10] on the dimensionless mean and coefficient of variations of thermal post buckling temperature of cross ply [00/900]2T square laminated composite plate resting on Winkler and Pasternak elastic foundations subjected to uniform constant temperature (U.T) and in-plane bi-axial compression with simple support S2 boundary conditions. The effect of amplitude ratios increases the dimensionless mean and decreases the coefficient of variations of thermal post buckling temperature in both of the TID and TD case. The effect of dimensionless mean and coefficient of variations of thermal post buckling temperature is more prominent in TD case. As the thickness ratio increases the dimensionless mean thermal post buckling temperature decreases in the both of the TID and TD case whereas coefficient of variations increases and is more pronounced for TD case. The effect of random thermal expansion coefficients on the coefficient of variations of thermal buckling load is significant in TD condition and foundation parameters show fewer effects in both TID and TD cases of plate with Winkler elastic foundation. The random foundation parameters have significant effects in case of plate with Pasternak foundation. The results are

more prominent for the plate with Winkler elastic foundation.

TABLE 8 EFFECT OF INDIVIDUAL RANDOM MATERIAL PROPERTIES FOR  $b_i$  ( $i=1$  TO  $8$ ) = 0.10] WITH AMPLITUDE RATIOS ( $W_{max}/h$ ) ON THE DIMENSIONLESS EXPECTED MEAN ( $T_{crnl}$ ) AND COEFFICIENT OF VARIATIONS ( $\lambda_{crnl}$ ) OF NONLINEAR FUNDAMENTAL FREQUENCY OF SYMMETRIC CROSS-PLY [00/900]S LAMINATED COMPOSITE SQUARE PLATE, RISE IN TEMPERATURE ( $\Delta T$ ) AND SIMPLE SUPPORT SSSS BOUNDARY CONDITIONS. PLATE THICKNESS RATIO ( $A/H=20$ ),  $\omega_L$ - LINEAR FUNDAMENTAL FREQUENCY.

$b_i$	$W_{max}/h$	$\delta T=100$	$\delta T=200$
		Mean ( $T_{crnl}$ ) COV, $\omega_{nl}^2$	Mean ( $T_{crnl}$ ) COV, $\omega_{nl}^2$
$E_{11}$ ( $i=1$ )	0.3	0.0874 (17.4131)	0.0973 (17.0465)
	0.6	0.0859 (17.6820)	0.0956 (17.3098)
	0.9	0.0836 (18.1120)	0.0929 (17.7307)
	$\omega_1$	17.3214	16.9567
$E_{22}$ ( $i=2$ )	0.3	0.0042	0.0064
	0.6	0.0041	0.0062
	0.9	0.0040	0.0060
$G_{12}$ ( $i=3$ )	0.3	0.0059	0.0062
	0.6	0.0077	0.0081
	0.9	0.0104	0.0109
$G_{13}$ ( $i=4$ )	0.3	0.0111	0.0116
	0.6	0.0108	0.0113
	0.9	0.0103	0.0107
$G_{23}$ ( $i=5$ )	0.3	0.0033	0.0035
	0.6	0.0032	0.0034
	0.9	0.0031	0.0032
$V_{12}$ ( $i=6$ )	0.3	2.8939e-04	3.0242e-04
	0.6	2.8336e-04	2.9613e-04
	0.9	2.7462e-04	2.8702e-04
$\alpha_1$ ( $i=7$ )	0.3	0.0060	0.0124
	0.6	0.0058	0.0121
	0.9	0.0055	0.0115
$\alpha_2$ ( $i=8$ )	0.3	9.2634e-04	0.0020
	0.6	8.9796e-04	0.0019
	0.9	8.5522e-04	0.0018

TABLE 9 EFFECTS OF PLATE THICKNESS RATIOS ( $b/h$ ) WITH AMPLITUDE RATIOS ( $W_{max}/h$ ) FOR  $b_i$  [( $i=1$  TO  $8$ ), ( $7, 8$ ) AND ( $9, 10$ )] = 0.10] ON THE DIMENSIONLESS EXPECTED MEAN ( $T_{crnl}$ ) AND COEFFICIENT OF VARIATIONS ( $\lambda_{crnl}$ ) OF THERMAL POST BUCKLING TEMPERATURE OF CROSS PLY [00/900] 2T SQUARE LAMINATED COMPOSITE PLATE RESTING ON WINKLER ( $k_1=100, k_2=0$ ) ELASTIC FOUNDATIONS, SUBJECTED TO UNIFORM CONSTANT TEMPERATURE ( $U.T$ ), IN-PLANE BI-AXIAL COMPRESSION WITH SIMPLE SUPPORT S2 BOUNDARY CONDITIONS.  $T_{crL}$  - LINEAR SOLUTION.

$b/h$	$W_{max}/h$	(TID)				(TD)			
		Mean $T_{crnl}$	COV, $\lambda_{crnl}$			Mean $T_{crnl}$	COV, $\lambda_{crnl}$		
			$b_i$				$b_i$		
			( $i=1, \dots, 8$ )	$i=(7,8)$	( $i=9,10$ )		( $i=1, \dots, 8$ )	$i=(7, 8)$	( $i=9,10$ )
40	0.2	0.5890				0.3825			
	0.4	0.6771	0.1359	0.1202	0.0348	0.4402	0.2451	0.1686	0.0337
	0.6	0.7835	0.1176	0.1046	0.0301	0.5064	0.2125	0.1465	0.0292
	$T_{crL}$	(0.5530)	0.1011	0.0904	0.0256	(0.3594)	0.1843	0.1273	0.0252
50	0.2	0.3809	0.2215			0.2469			
	0.4	0.4393	0.1908	0.1859	0.0344	0.2820	0.3627	0.2612	0.0334
	0.6	0.5064	0.1643	0.1612	0.0297	0.3284	0.3164	0.2286	0.0292
	$T_{crL}$	(0.3575)		0.1399	0.0256	(0.2320)	0.2705	0.1963	0.0249

Table (11) & (12). shows the effect of support edge conditions (CCCC, SSSS and CSCS) with amplitude ratio on the mean and coefficient of variations of the dimensionless nonlinear fundamental frequency for cross-ply [00/900] S and angle-ply ( $\pm 45$ )S square laminate with all random input such as combination of material properties and

thermal expansion coefficients as well as thermal expansion coefficients separately, changing simultaneously for  $a/h = 10$ . All the inputs RVs ( $b_i, i = 1, 2, \dots, 8$ ) and thermal expansion coefficient inputs RVs ( $b_i, i = 7, 8$ ) are assumed to have coefficient of variation. From the table it can be seen that the coefficient of variation in the nonlinear fundamental frequency is highest in case of plate with simple support SSSS, while it is lowest for clamped supported CCCC. In contrast the mean values of SSSS plate and CCCC plate show the opposite effect, i.e., vice versa to sensitivity. As the amplitude ratio increases the coefficient of variations of nonlinear frequency of the plate decreases in SSSS and CSCS support conditions, however no definite change is observed in CCCC support condition in the case of cross-ply plate. In the case of angle-ply plate with SSSS and CSCS support conditions coefficient of variations of nonlinear frequency increases with increase the amplitude ratio, however no definite trend is also observed with CCCC support condition. In general, the presented results reveal that the effect of randomness in thermal expansion coefficients on the coefficient of variations of the nonlinear frequency is significant. Finally, we consider the effect of plate geometry on the mean and coefficient of variations of the nonlinear fundamental frequency.

TABLE 10 EFFECTS OF PLATE THICKNESS RATIOS ( $b/h$ ) WITH AMPLITUDE RATIOS ( $W_{max}/h$ ) FOR  $b_i, [(i=1 \text{ to } 8), (7, 8) \text{ AND } (9, 10)] = 0.10$  ON THE DIMENSIONLESS EXPECTED MEAN ( $T_{crl}$ ) AND COEFFICIENT OF VARIATIONS ( $\lambda_{crl}$ ) OF THERMAL POST BUCKLING TEMPERATURE OF CROSS PLY  $[00/900]$  2T SQUARE LAMINATED COMPOSITE PLATE RESTING ON PASTERNAK ( $\kappa_1=100, \kappa_2=10$ ) ELASTIC FOUNDATIONS, SUBJECTED TO UNIFORM CONSTANT TEMPERATURE ( $U.T$ ), IN-PLANE BI-AXIAL COMPRESSION WITH SIMPLE SUPPORT S2 BOUNDARY CONDITIONS.  $T_{crl}$  - LINEAR SOLUTION.

b/h	$W_{max}/h$	(TID)				(TD)			
		Mean $T_{crl}$	$COV, \lambda_{crl}$			Mean $T_{crl}$	$COV, \lambda_{crl}$		
			$b_i$				$b_i$		
			(i=1,...,8)	i=(7, 8)	(i=9,10)		(i=1,...,8)	i=(7, 8)	(i=9,10)
40	0.2	0.9938	0.0873	0.0713	0.0457	0.6374	0.1840	0.1012	0.0448
	0.4	1.0819	0.0807	0.0655	0.0419	0.6951	0.1692	0.0928	0.0411
	0.6	1.1883	0.0742	0.0596	0.0380	0.7614	0.1550	0.0847	0.0374
	$T_{crl}$	(0.9578)				(0.6143)			
50	0.2	0.6400	0.1242	0.1107	0.0454	0.4100	0.2356	0.1573	0.0446
	0.4	0.6984	0.1136	0.1014	0.0415	0.4452	0.2168	0.1448	0.0410
	0.6	0.7654	0.1034	0.0925	0.0378	0.4916	0.1963	0.1312	0.0371
	$T_{crl}$	(0.6166)				(0.3951)			

TABLE 11 EFFECT OF BOUNDARY SUPPORT CONDITIONS (BCs) FOR  $b_i, [(i=1, \dots, 8 \text{ \& } 7, 8) = 0.10]$  WITH AMPLITUDE RATIOS ( $W_{max}/h$ ) ON THE DIMENSIONLESS EXPECTED MEAN ( $\omega_{nl}$ ) AND COEFFICIENT OF VARIATIONS ( $\omega_{nl}^2$ ) OF NONLINEAR FUNDAMENTAL FREQUENCY OF SYMMETRIC CROSS-PLY  $[00/900]$ S LAMINATED COMPOSITE SQUARE PLATE WITH RISE IN TEMPERATURE ( $\Delta T$ ). PLATE THICKNESS RATIO ( $A/h=10$ ).  $\omega_L$  IS LINEAR FUNDAMENTAL FREQUENCY.

BCs	$W_{max}/h$	$\delta T=100$			$\delta T=200$		
		Mean $\omega_{nl}$	$COV, \omega_{nl}^2$		Mean $\omega_{nl}$	$COV, \omega_{nl}^2$	
			$b_i, i=1, \dots, 8$	$b_i, i=7, 8$		$b_i, i=1, \dots, 8$	$b_i, i=7, 8$
SSSS	0.3	15.1052	0.0673	0.0020	15.0288	0.0698	0.0040
	0.6	15.3964	0.0661	0.0019	15.3185	0.0686	0.0039
	0.9	15.8467	0.0645	0.0018	15.7666	0.0669	0.0036
	$\omega_L$	(15.0039)			(14.9279)		
CCCC	0.3	23.9000	0.0614	8.4767e-004	23.8072	0.0625	0.0017
	0.6	27.7153	0.0618	8.0441 e-004	27.8279	0.0645	0.0012
	0.9	27.3002	0.0610	7.7003e-004	27.1658	0.0620	0.0016
	$\omega_L$	(22.4167)			(22.3189)		
CSCS	0.3	18.7673	0.0613	0.0014	18.6807	0.0629	0.0028
	0.6	19.2235	0.0596	0.0013	19.1352	0.0612	0.0026
	0.9	19.8736	0.0577	0.0012	19.7876	0.0591	0.0024
	$\omega_L$	(18.6011)			(18.5146)		

TABLE 12 EFFECT OF BOUNDARY SUPPORT CONDITIONS (BCs) FOR  $b_i, [(i=1, \dots, 8 \& 7, 8) = 0.10]$  WITH AMPLITUDE RATIOS ( $W_{max}/h$ ) ON THE DIMENSIONLESS EXPECTED MEAN ( $\omega_{nl}$ ) AND COEFFICIENT OF VARIATIONS ( $\omega_{nl}^2$ ) OF NONLINEAR FUNDAMENTAL FREQUENCY OF SYMMETRIC ANGLE -PLY  $[\pm 45]_S$  LAMINATED COMPOSITE SQUARE PLATE WITH RISE IN TEMPERATURE ( $\Delta T$ ). PLATE THICKNESS RATIO ( $A/H = 10$ ).  $\omega_L$  IS LINEAR FUNDAMENTAL FREQUENCY.

BCs	$W_{max}/h$	$\delta T=100$			$\delta T=200$		
		Mean $\omega_{nl}$	COV, $\omega_{nl}^2$		Mean $\omega_{nl}$	COV, $\omega_{nl}^2$	
			$b_i, i=1, \dots, 8$	$b_i, i=7, 8$		$b_i, i=1, \dots, 8$	$b_i, i=7, 8$
SSSS	0.3	17.8120	0.0670	0.0015	17.7241	0.0691	0.0030
	0.6	19.8566	0.0712	0.0012	19.7650	0.0731	0.0024
	0.9	22.5515	0.0748	9.238e-04	21.2648	0.0724	0.0022
	$\omega_L$	(17.0086)			(16.9250)		
CCCC	0.3	22.8071	0.0601	9.446e-04	22.7070	0.0613	0.0019
	0.6	26.0220	0.0620	7.038e-04	25.9317	0.0631	0.0021
	0.9	26.6363	0.0597	8.701e-04	26.5088	0.0608	0.0022
	$\omega_L$	(21.5997)			(21.5023)		
CSCS	0.3	20.0160	0.0617	0.0012	19.9224	0.0633	0.0024
	0.6	22.3299	0.0646	9.585e-04	22.2368	0.0661	0.0019
	0.9	23.7000	0.0638	9.129e-04	23.5888	0.0655	0.0015
	$\omega_L$	(19.1249)			(19.0339)		

The effects of aspect ratios with amplitude ratios on the dimensionless mean and coefficient of variations of  $[00/900/00]$  and  $[00/900]_2T$  cross ply laminated composite plate resting on Winkler and Pasternak elastic foundation subjected to uniform constant temperature (U.T), in-plane bi-axial compression, simple support S2 boundary conditions and  $b/h=60$  for  $b_i, [(i=1 \text{ to } 8), (7,8) \text{ and } (9, 10)] = 0.10$  is shown in Table (13)& (14). The effect of amplitude ratio increases the mean thermal post buckling temperature and decreases the coefficient of variations of the plate in both TID and TD cases. But when the number of layer increases the mean thermal post buckling temperature increases and coefficient of variations decreases, whereas when aspect ratio is increased the dimensionless mean thermal post buckling temperature decreases and coefficient of variations increases. The effect of random thermal expansion coefficients on the coefficient of variations of thermal buckling load is significant in TID and TD condition while foundation parameters show fewer effects in both TID and TD cases of plate supported with either Winkler or Pasternak elastic foundation. The result is more prominent for the plate with Winkler elastic foundation TD case.

TABLE 13 EFFECTS OF ASPECT RATIOS ( $A/B$ ), LAMINA LAY-UP AND AMPLITUDE RATIOS ( $W_{max}/h$ ) FOR  $b_i, [(i=1 \text{ TO } 8), (7,8) \text{ AND } (9, 10)] = 0.10$  ON THE DIMENSIONLESS EXPECTED MEAN ( $T_{crnl}$ ) AND COEFFICIENT OF VARIATIONS ( $\lambda_{crnl}$ ) OF  $[00/900/00]$  AND  $[00/900]_2T$  CROSS PLY LAMINATED COMPOSITE PLATE RESTING ON WINKLER ELASTIC FOUNDATION ( $k_1=100, k_2=0$ ), SUBJECTED TO UNIFORM CONSTANT TEMPERATURE (U.T), IN-PLANE BI-AXIAL COMPRESSION AND SIMPLE SUPPORT S2 BOUNDARY CONDITIONS. PLATE THICKNESS RATIO ( $B/H=60$ ).  $T_{crL}$  - LINEAR SOLUTION.

Lay-up	a/b	$W_{max}/h$	(TID)				(TD)			
			Mean $T_{crnl}$	COV, $\lambda_{crnl}$			Mean $T_{crnl}$	COV, $\lambda_{crnl}$		
				bi				bi		
				(i=1, \dots, 8)	i=(7, 8)	(i=9, 10)		(i=1, \dots, 8)	i=(7, 8)	(i=9, 10)
$[0^0/90^0]_{2T}$	1	0.2	0.2663	0.3324	0.2659	0.0342	0.1724	0.5195	0.3740	0.0333
		0.4	0.3047	0.2892	0.2325	0.0298	0.1973	0.4525	0.3267	0.0290
		0.6	0.3633	0.2402	0.1950	0.0246	0.2373	0.3742	0.2717	0.0236
		$T_{crL}$	(0.2499)				(0.1620)			
$[0^0/90^0]_{3T}$	2	0.2	0.1537	0.6107	0.4180	0.4606	0.0999	0.9105	0.6453	0.0057
		0.4	0.1694	0.5517	0.4180	0.0049	0.1156	0.7851	0.5578	0.0047
		0.6	0.1821	0.5115	0.0043	0.0043	0.1260	0.7181	0.5116	0.0044
		$T_{crL}$	(0.1398)				(0.0907)			
$[0^0/90^0]_{3T}$	1	0.2	0.2831	0.3092	0.2502	0.0322	0.1826	0.4845	0.3532	0.0314
		0.4	0.3223	0.2702	0.2197	0.0282	0.2080	0.4238	0.3099	0.0275
		0.6	0.3747	0.2308	0.1890	0.0241	0.2483	0.3529	0.2597	0.0227
		$T_{crL}$	(0.2666)				(0.1721)			
$[0^0/90^0]_{3T}$	2	0.2	0.1679	0.3215	0.4216	0.0055	0.1085	0.8314	0.5943	0.0053
		0.4	0.1873	0.4938	0.3781	0.0045	0.1266	0.7100	0.5091	0.0044
		0.6	0.1541	0.6041	0.4594	0.0040	0.1310	0.6849	0.4922	0.0038
		$T_{crL}$	(0.1539)				(0.0993)			

TABLE 14 EFFECTS OF ASPECT RATIOS (A/B) , LAMINA LAY-UP AND AMPLITUDE RATIOS (W<sub>MAX/H</sub>) FOR BI, [(i=1 to 8), (7,8) AND (9, 10)] = 0.10] ON THE DIMENSIONLESS EXPECTED MEAN (T<sub>CRNL</sub>) AND COEFFICIENT OF VARIATIONS (λ<sub>CRNL</sub>) OF [00/900/00] AND [00/900]2T CROSS PLY LAMINATED COMPOSITE PLATE RESTING ON PASTERNAK ELASTIC FOUNDATION (κ<sub>1</sub>=100, κ<sub>2</sub>=10), SUBJECTED TO UNIFORM CONSTANT TEMPERATURE (U.T), IN-PLANE BI-AXIAL COMPRESSION AND SIMPLE SUPPORT S2 BOUNDARY CONDITIONS. PLATE THICKNESS RATIO (B/H=60) .T<sub>CRNL</sub> - LINEAR SOLUTION.

Lay-up	a/b	W <sub>max/h</sub>	(TID)				(TD)			
			Mean T <sub>crnl</sub>	COV, λ <sub>crnl</sub>			Mean T <sub>crnl</sub>	COV, λ <sub>crnl</sub>		
				bi				bi		
				(i=1,..,8)	i=(7, 8)	(i=9,10)		(i=1,..,8)	i=(7,8)	(i=9,10)
[0°/90°] <sub>2T</sub>	1	0.2	0.4462	0.1834	0.1587	0.0452	0.2857	0.3174	0.2257	0.0444
		0.4	0.4846	0.1684	0.1461	0.0416	0.3106	0.2914	0.2076	0.0409
		0.6	0.5432	0.1492	0.1304	0.0370	0.3506	0.2578	0.1839	0.0361
		T <sub>crnl</sub>	(0.4299)				(0.2753)			
	2	0.2	0.1987	0.4599	0.3563	0.0231	0.1282	0.7020	0.5027	0.0225
		0.4	0.2144	0.4245	0.3303	0.0213	0.1439	0.6243	0.4480	0.0200
0.6		0.2271	0.3994	0.3118	0.0201	0.1543	0.5806	0.4177	0.0187	
T <sub>crnl</sub>		(0.1848)				(0.1190)				
[0°/90°] <sub>3T</sub>	1	0.2	0.4630	0.1750	0.1530	0.0436	0.2959	0.3019	0.2179	0.0429
		0.4	0.5023	0.1608	0.1410	0.0401	0.3213	0.2773	0.2007	0.0395
		0.6	0.5546	0.1449	0.1277	0.0363	0.3616	0.2457	0.1783	0.0350
		T <sub>crnl</sub>	(0.4465)				(0.2854)			
	2	0.2	0.2129	0.4250	0.3326	0.0216	0.1368	0.6518	0.4712	0.0211
		0.4	0.2323	0.3877	0.3049	0.0197	0.1550	0.5739	0.4160	0.0186
0.6		0.2422	0.3705	0.2923	0.0189	0.1593	0.5574	0.4047	0.0180	
T <sub>crnl</sub>		(0.1989)				(0.1276)				

Table (15)&(16) shows the effect of plate thickness ratios (a/h=10 and 20) with amplitude ratios on the mean and coefficient of variations for SD/mean, bi, {i = (1,..., 8) and (7,8)} = 0.10 of nonlinear fundamental frequency of two layer cross-ply [0°/90°] and angle-ply [±45°] square plate subjected to various temperature changes simply supported. The thin plate (a/h=20) shows higher nonlinear frequency as compare to moderately thick plate (a/h=10). As revealed by numerical results, for the same amplitude ratio and temperature increments thin plate shows higher coefficient of variations to random change in both all random input variables and thermal expansion coefficients. However, increase the temperature sensitivity of thermal expansion coefficients for the plate increases with increase the a/h ratio. It is true in both of the cross-ply and angle-ply plates. As the amplitude ratio and temperature increases the coefficient of variations of nonlinear frequency of the plate decreases in both of thin and moderately thick plate for cross-ply plate, while, in the case of angle-ply plate the coefficient of variations of nonlinear frequency of the plate increases at lower temperature. However increases the temperature coefficient of variations of the plate decreases to random change in both all random variables and thermal expansion coefficients with increase the amplitude ratio.

TABLE 15 EFFECT OF PLATE THICKNESS RATIOS (A/H), RISE IN TEMPERATURE(ΔT) FOR BI, [(i=1,..,8 & 7, 8)= 0.10 ] WITH AMPLITUDE RATIOS (W<sub>MAX/H</sub>) ON THE DIMENSIONLESS EXPECTED MEAN (ω<sub>NL</sub>) AND COEFFICIENT OF VARIATIONS (ω<sub>NL2</sub>) OF NONLINEAR FUNDAMENTAL FREQUENCY OF ANTI-SYMMETRIC CROSS-PLY [00/900]2T LAMINATED COMPOSITE SQUARE PLATE. ω<sub>L</sub> IS LINEAR FUNDAMENTAL FREQUENCY.

a/h	W <sub>max/h</sub>	δT=100			δT=200		
		Mean ω <sub>nl</sub>	COV, ω <sub>nl</sub> <sup>2</sup>		Mean ω <sub>nl</sub>	COV, ω <sub>nl</sub> <sup>2</sup>	
			bi, i=1,..,8	bi, i=7,8		bi, i=1,..,8	bi, i=7,8
10	0.3	10.6602	0.0645	0.0040	10.6064	0.0694	0.0080
	0.6	11.0746	0.0635	0.0037	11.0184	0.0680	0.0074
	0.9	11.7033	0.0624	0.0033	11.6443	0.0664	0.0066
	ω <sub>l</sub>	(10.5154)			(10.4622)		
20	0.3	11.0881	0.0824	0.0148	10.8546	0.1048	0.0310
	0.6	11.5077	0.0801	0.0138	11.2654	0.1008	0.0287
	0.9	12.1594	0.0774	0.0123	11.9033	0.0958	0.0257
	ω <sub>l</sub>	(10.9432)			(10.7128)		

Table (17)&(18) show the effects of support conditions (SSSS (S1), SSSS(S2), CCCC, CSCS) with amplitude ratios on the dimensionless mean and coefficient of variations of thermal post buckling temperature for bi,[(i =1 to 8),

(7,8) and (9, 10)} = 0.10],  $b/h=60$ , of angle ply  $[\pm 45]_2T$  laminated square composite plate resting on Winkler and Pasternak elastic foundations subjected to in-plane bi-axial compression. The effects of amplitude ratios increases the dimensionless mean values and decreases the dimensionless coefficient of variations values in both TID and TD cases, but when support conditions are changed the effects are seen significant in clamp support conditions. The buckling load coefficient of variations is highest for the plate resting on either Winkler elastic foundation or Pasternak foundation with SSSS (S2) support condition while lowest with CCCC support conditions. It is observed that the plate with all system properties subjected to TD is more sensitive than TID. In general, the thermal buckling load for the plate resting on Winkler elastic foundation is higher than the plate resting on Pasternak elastic foundations. The effect of random thermal expansion coefficients on the coefficient of variations of thermal buckling load is significant in TD condition for simple support S2, while foundation parameters show fewer effects for clamp support condition in both TID and TD cases of plate with Winkler and Pasternak elastic foundation. The result is more prominent for the plate with Winkler elastic foundation subjected to TD case.

TABLE 16 EFFECT OF PLATE THICKNESS RATIOS (A/H), RISE IN TEMPERATURE( $\Delta T$ ) FOR BI, [(i=1,...,8 & 7, 8) = 0.10 ] WITH AMPLITUDE RATIOS (WMAX/H) ON THE DIMENSIONLESS EXPECTED MEAN ( $\omega_{nl}$ ) AND COEFFICIENT OF VARIATIONS ( $\omega_{nl}^2$ ) OF NONLINEAR FUNDAMENTAL FREQUENCY OF ANGLE PLY  $[\pm 45]_2$  LAMINATED COMPOSITE SQUARE PLATE.  $\omega_L$  IS LINEAR FUNDAMENTAL FREQUENCY.

a/h	$W_{max}/h$	$\delta T=100$			$\delta T=200$		
		Mean $\omega_{nl}$	COV, $\omega_{nl}^2$		Mean $\omega_{nl}$	COV, $\omega_{nl}^2$	
			bi, i=1,...,8	bi, i=7,8		bi, i=1,...,8	bi, i=7,8
10	0.3	16.0254			15.9447		
	0.6	17.4523	0.0698	0.0053	17.3637	0.0762	0.0107
	0.9	19.4098	0.0705	0.0044	19.3238	0.0760	0.0090
	$\omega_1$	(15.4897)	0.0709	0.0036	(15.4119)	0.0753	0.0073
20	0.3	17.9306			17.5563		
	0.6	19.5795	0.0839	0.0058	19.1710	0.0941	0.0121
	0.9	21.9626	0.0843	0.0048	21.5482	0.0934	0.0101
	$\omega_1$	(17.3279)	0.0845	0.0038	(16.9660)	0.0918	0.0079

TABLE 17 EFFECTS OF BOUNDARY SUPPORT CONDITIONS(BCs) WITH AMPLITUDE RATIOS (WMAX/H) FOR BI,[(i=1 TO 8), (7,8) AND (9, 10)} = 0.10], ON THE DIMENSIONLESS EXPECTED MEAN ( $T_{crnl}$ ) AND COEFFICIENT OF VARIATIONS ( $\lambda_{crnl}$ ) OF THERMAL POST BUCKLING TEMPERATURE FOR PLATE THICKNESS RATIO (A/H=60), ANGLE PLY  $[\pm 45]_2T$  LAMINATED SQUARE COMPOSITE PLATE RESTING ON WINKLER ELASTIC FOUNDATION ( $\kappa_1=100$ ,  $\kappa_2=0$ ), SUBJECTED TO UNIFORM CONSTANT TEMPERATURE (U.T), IN-PLANE BI-AXIAL COMPRESSION.  $T_{crL}$  - LINEAR SOLUTION.

BCs	$W_{max}/h$	(TID)				(TD)			
		Mean $T_{crnl}$	COV, $\lambda_{crnl}$			Mean $T_{crnl}$	COV, $\lambda_{crnl}$		
			bi				bi		
		(i=1,...,8)	i=(7, 8)	(i=9,10)	(i=1,...,8)	i=(7, 8)	(i=9,10)		
SSSS (S1)	0.2	0.3755			0.2411				
	0.4	0.4068	0.2218	0.1886	0.2617	0.3575	0.2674	0.0129	
	0.6	0.4512	0.2041	0.1741	0.2919	0.3285	0.2464	0.0119	
	$T_{crL}$	(0.3640)	0.1831	0.1570	(0.2337)	0.2934	0.2209	0.0106	
SSSS (S2)	0.2	0.3716			0.2389				
	0.4	0.4022	0.2247	0.1906	0.2586	0.3622	0.2699	0.0130	
	0.6	0.4480	0.2070	0.1761	0.2864	0.3338	0.2493	0.0120	
	$T_{crL}$	(0.3602)	0.1849	0.1581	(0.2314)	0.3003	0.2251	0.0108	
CCCC	0.2	0.6529			0.4342				
	0.4	0.7102	0.1215	0.1085	0.4725	0.2146	0.1485	0.0053	
	0.6	0.7938	0.1114	0.0997	0.5303	0.1966	0.1365	0.0049	
	$T_{crL}$	(0.6322)	0.0994	0.0892	(0.4207)	0.1744	0.1216	0.0044	
CSCS	0.2	0.4835			0.3154				
	0.4	0.5390	0.1678	0.1465	0.3516	0.2784	0.2044	0.0083	
	0.6	0.6174	0.1499	0.1314	0.4079	0.2494	0.1834	0.0075	
	$T_{crL}$	(0.4636)	0.1302	0.1147	(0.3025)	0.2147	0.1581	0.0065	

TABLE 18 EFFECTS OF BOUNDARY SUPPORT CONDITIONS(BCs) WITH AMPLITUDE RATIOS ( $W_{max}/h$ ) FOR  $b_i, [(i=1 \text{ to } 8), (7,8) \text{ AND } (9, 10)] = 0.10$ , ON THE DIMENSIONLESS EXPECTED MEAN ( $T_{crnl}$ ) AND COEFFICIENT OF VARIATIONS ( $\lambda_{crnl}$ ) OF THERMAL POST BUCKLING TEMPERATURE FOR PLATE THICKNESS RATIO ( $A/h=60$ ), ANGLE PLY  $[\pm 450]_{2T}$  LAMINATED SQUARE COMPOSITE PLATE RESTING ON PASTERNAK ELASTIC FOUNDATION ( $k_1=100, k_2=10$ ), SUBJECTED TO UNIFORM CONSTANT TEMPERATURE (U.T), IN-PLANE BI-AXIAL COMPRESSION.  $T_{crL}$  - LINEAR SOLUTION.

BCs	$W_{max}/h$	(TID)				(TD)			
		Mean $T_{crnl}$	COV, $\lambda_{crnl}$			Mean $T_{crnl}$	COV, $\lambda_{crnl}$		
			bi				bi		
			(i=1,...,8)	i=(7, 8)	(i=9,10)		(i=1,...,8)	i=(7, 8)	(i=9,10)
SSSS (S1)	0.2	0.4710				0.3027			
	0.4	0.5020	0.1715	0.1504	0.0227	0.3228	0.2919	0.2130	0.0228
	0.6	0.5483	0.1604	0.1411	0.0213	0.3512	0.2731	0.1998	0.0213
	$T_{crL}$	(0.4595)	0.5483	0.1292	0.0195	(0.2952)	0.2500	0.1836	0.0196
SSSS (S2)	0.2	0.4671				0.3004			
	0.4	0.4977	0.1733	0.1516	0.0229	0.3201	0.2955	0.2147	0.0229
	0.6	0.5435	0.1623	0.1423	0.0215	0.3479	0.2767	0.2014	0.0215
	$T_{crL}$	(0.4557)	0.1480	0.1303	0.0196	(0.2929)	0.2538	0.1854	0.0198
CCCC	0.2	0.7484				0.4957			
	0.4	0.8056	0.1065	0.0946	0.0136	0.5340	0.2014	0.1301	0.0132
	0.6	0.8893	0.0988	0.0879	0.0127	0.5918	0.1866	0.1207	0.0123
	$T_{crL}$	(0.7276)	0.0894	0.0796	0.0115	(0.4821)	0.1678	0.1090	0.0111
CSCS	0.2	0.5789				0.3769			
	0.4	0.6345	0.1376	0.1223	0.0179	0.4130	0.2440	0.1711	0.0177
	0.6	0.7128	0.1253	0.1116	0.0164	0.4694	0.2225	0.1561	0.0162
	$T_{crL}$	(0.5590)	0.1111	0.0994	0.0146	(0.3640)	0.1961	0.1374	0.0143

The effect of plate aspect ratios ( $a/b=1$  and  $1.5$ ) with amplitude ratios on the mean and coefficient of variations of the nonlinear fundamental frequency of four layers anti-symmetric cross-ply  $[00/900]_{2T}$  and angle-ply  $[\pm 450]_{2T}$  laminated composite plates with  $b_i$   $\{i = (1, \dots, 8) \text{ and } (7, 8)\} = 0.10$ ,  $a/h=20$  is shown in Table (19)-(20). As revealed by numerical results, for the same amplitude ratio and temperature increments rectangular plate ( $a/b=1.5$ ) shows higher mean and coefficient of variations to both random change in all random input variables and thermal expansion coefficients as compared to square plate ( $a/b=1$ ).

TABLE 19 EFFECT OF PLATE ASPECT RATIO ( $A/B$ ), RISE IN TEMPERATURE ( $\Delta T$ ) WITH AMPLITUDE RATIOS ( $W_{max}/h$ ) FOR  $b_i, [(i=1, \dots, 8 \text{ \& } 7, 8)] = 0.10$  ON THE DIMENSIONLESS EXPECTED MEAN ( $\omega_{nl}$ ) AND COEFFICIENT OF VARIATIONS ( $\omega_{nl2}$ ) OF NONLINEAR FUNDAMENTAL FREQUENCY OF ANTI SYMMETRIC CROSS-PLY  $[00/900]_{2T}$  LAMINATED COMPOSITE PLATE. PLATE THICKNESS RATIO ( $A/h = 20$ ).  $\omega_L$  IS LINEAR FUNDAMENTAL FREQUENCY.

a/b	$W_{max}/h$	$\delta T=100$			$\delta T=200$		
		Mean $\omega_{nl}$	COV, $\omega_{nl}^2$		Mean $\omega_{nl}$	COV, $\omega_{nl}^2$	
			bi, i=1,...,8	bi, i=7,8		bi, i=1,...,8	bi, i=7,8
1	0.3	16.3874			16.0424		
	0.6	16.6736	0.0911	0.0068	16.3225	0.1028	0.0142
	0.9	17.1318	0.0894	0.0066	16.7711	0.1008	0.0137
	$\omega_L$	(16.2901)	0.0871	0.0062	(15.9471)	0.0979	0.0130
1.5	0.3	28.3766			27.7791		
	0.6	28.7415	0.0954	0.0083	28.1364	0.1092	0.0172
	0.9	29.3361	0.0944	0.0080	28.7185	0.1079	0.0168
	$\omega_L$	(28.2594)	0.0926	0.0077	(27.6644)	0.1057	0.0161

The effect of uniform constant temperature rise and transverse temperature gradient with amplitude ratios on dimensionless mean and coefficient of variations of thermal post buckling load for  $b_i, [(i=1 \text{ to } 8), (7,8) \text{ and } (9, 10)] = 0.10$  of angle ply  $[\pm 450]_{2T}$  laminated square composite plate resting on elastic foundation subjected to uni-axial and bi-axial in-plane compression, uniform temperature or transverse temperature gradients (linearly varying thickness across the thickness of the plates), simply supported SSSS (S2) boundary conditions and  $b/h=100$  is studied in Table (21)&(22). There is decrease in buckling strength of the plate when subjected to uniform in-plane temperature induced loading along with in-plane edge compressive loading but in the case of transverse

temperature the effect is insignificant. It is expected that the mean post buckling load with TID is more than TD case subjected to either under in-plane uniform temperature or combination of transverse temperature gradient and uniform constant temperature. Coefficient of variations in the thermal post buckling load with U.T is higher than T.T with random change in all system properties. The effects of random foundation parameters and thermal expansion coefficients on the coefficient of variations of thermal buckling load resting on either Winkler or Pasternak elastic foundations is higher in the U.T condition compared to T.T condition. The thermal post buckling load coefficient of variations is higher with the random change in all system properties (whether considered as combined or separately). The buckling load coefficient of variations of the laminated plate with random system properties subjected to biaxial compression is higher than uni-axial compression however the mean thermal buckling temperature shows the opposite effect.

TABLE 20 EFFECT OF PLATE ASPECT RATIO (A/B), RISE IN TEMPERATURE ( $\Delta T$ ) WITH AMPLITUDE RATIOS ( $W_{max}/h$ ) FOR  $b_i$ , [( $i=1, \dots, 8$  & 7, 8) = 0.10] ON THE DIMENSIONLESS EXPECTED MEAN ( $\omega_{nl}$ ) AND COEFFICIENT OF VARIATIONS ( $\omega_{nl2}$ ) OF NONLINEAR FUNDAMENTAL FREQUENCY OF ANGLE-PLY  $[\pm 45]_2 T$  LAMINATED COMPOSITE PLATE. PLATE THICKNESS RATIO ( $A/h = 20$ ).  $\omega_L$  IS LINEAR FUNDAMENTAL FREQUENCY.

a/b	$W_{max}/h$	$\delta T=100$			$\delta T=200$		
		Mean $\omega_{nl}$	COV, $\omega_{nl}^2$		Mean $\omega_{nl}$	COV, $\omega_{nl}^2$	
			$b_i, i=1, \dots, 8$	$b_i, i=7, 8$		$b_i, i=1, \dots, 8$	$b_i, i=7, 8$
1	0.3	22.5777	0.0898	0.0036	22.1023	0.0976	0.0075
	0.6	24.0681	0.0905	0.0032	23.5610	0.0979	0.0066
	0.9	26.2722	0.0913	0.0027	25.7194	0.0981	0.0056
	$\omega_L$	(22.0460)			(21.5819)		
1.5	0.3	35.8252	0.0935	0.0052	35.0709	0.1034	0.0108
	0.6	36.6930	0.0924	0.0049	35.9201	0.1020	0.0103
	0.9	38.0526	0.0908	0.0046	37.2508	0.0999	0.0095
	$\omega_L$	(35.5262)			(34.7784)		

TABLE 21 EFFECTS OF TYPE OF COMPRESSION, TEMPERATURE RISE CONDITIONS WITH AMPLITUDE RATIOS ( $W_{max}/h$ ) FOR  $b_i$ , [( $i=1$  TO 8), (7,8) AND (9, 10)] = 0.10] ON THE DIMENSIONLESS EXPECTED MEAN ( $T_{crl}$ ) AND COEFFICIENT OF VARIATIONS ( $\lambda_{crl}$ ) OF THERMAL POST BUCKLING TEMPERATURE OF ANGLE PLY  $[\pm 45]_2 T$  LAMINATED SQUARE COMPOSITE PLATE RESTING ON WINKLER ELASTIC FOUNDATION ( $k_1=100, k_2=0$ ) WITH SSSS (S2) BOUNDARY CONDITIONS, SUBJECTED TO IN-PLANE UNI-AXIAL AND BI-AXIAL COMPRESSIONS. PLATE THICKNESS RATIO ( $A/h=100$ ).  $T_{crl}$  - LINEAR SOLUTION.

Type of compression	Conditions	$W_{max}/h$	(TID)				(TD)			
			Mean $T_{crl}$	COV, $\lambda_{crl}$			Mean $T_{crl}$	COV, $\lambda_{crl}$		
				$b_i$				$b_i$		
				( $i=1, \dots, 8$ )	( $i=7, 8$ )	( $i=9, 10$ )		( $i=1, \dots, 8$ )	( $i=7, 8$ )	( $i=9, 10$ )
uniaxial	U.T	0.2	0.2736	0.6864	0.5167	0.0127	0.1747	1.0411	0.7371	0.0128
		0.4	0.2917	0.6383	0.4813	0.0117	0.1875	0.9699	0.6873	0.0119
		0.6	0.3042	0.4995	0.3841	0.0074	0.1958	0.7709	0.5516	0.0077
		$T_{crl}$	(0.2652)				(0.1693)			
	T.T	0.2	0.2732	0.6854	0.5159	0.0126	0.1745	1.0402	0.7365	0.0128
		$T_{crl}$	(0.2648)				(0.1692)			
biaxial	U.T	0.2	0.1369	0.6874	0.5173	0.0127	0.0874	1.0421	0.7378	0.0128
		0.4	0.1483	0.6338	0.4777	0.0117	0.0947	0.9607	0.6809	0.0118
		0.6	0.1646	0.5696	0.4303	0.0105	0.1053	0.8626	0.6123	0.0106
		$T_{crl}$	(0.1327)				(0.0847)			
	T.T	0.2	0.1368	0.6871	0.5171	0.0127	0.0874	1.0419	0.7377	0.0128
		$T_{crl}$	(0.1326)				(0.0847)			

TABLE 22 EFFECTS OF TYPE OF COMPRESSION, TEMPERATURE RISE CONDITIONS WITH AMPLITUDE RATIOS ( $W_{max}/h$ ) FOR BI,  $\{i=1 \text{ TO } 8, (7,8) \text{ AND } (9, 10)\} = 0.10$ ] ON THE DIMENSIONLESS EXPECTED MEAN ( $T_{CRNL}$ ) AND COEFFICIENT OF VARIATIONS ( $\lambda_{CRNL}$ ) OF THERMAL POST BUCKLING TEMPERATURE OF ANGLE PLY  $[\pm 45]_2 T$  LAMINATED SQUARE COMPOSITE PLATE RESTING ON PASTERNAK ELASTIC FOUNDATION ( $k_1=100, k_2=10$ ) WITH SSSS (S2) BOUNDARY CONDITIONS, SUBJECTED TO IN-PLANE UNI-AXIAL AND BI-AXIAL COMPRESSIONS. PLATE THICKNESS RATIO ( $A/H=100$ ).  $T_{CRNL}$  - LINEAR SOLUTION.

Type of compression	Conditions	$W_{max}/h$	(TID)				(TD)			
			Mean $T_{CRNL}$	COV, $\lambda_{CRNL}$			Mean $T_{CRNL}$	COV, $\lambda_{CRNL}$		
				bi				bi		
				(i=1,..,8)	(i=7, 8)	(i=9,10)		(i=1,..,8)	(i= 7, 8)	(i=9,10)
Uniaxial	U.T	0.2	0.3417	0.5051	0.3898	0.0209	0.2187	0.8149	0.5812	0.0223
		0.4	0.3563	0.5068	0.3899	0.0211	0.2255	0.7464	0.5338	0.0202
		0.6	0.3531	0.3738	0.2961	0.0151	0.2419	0.7364	0.5260	0.0202
	$T_{CRNL}$	(0.3339)				(0.2135)				
	T.T	0.2	0.3411	0.5065	0.3908	0.0210	0.2185	0.8144	0.5809	0.0223
		0.4	0.3481	0.4560	0.3546	0.0187	0.2240	0.7283	0.5215	0.0197
0.6		0.3519	0.3554	0.2831	0.0143	0.2298	0.6699	0.4809	0.0179	
$T_{CRNL}$	(0.3332)				(0.2133)					
biaxial	U.T	0.2	0.1712	0.5389	0.4135	0.0225	0.1095	0.8258	0.5887	0.0226
		0.4	0.1826	0.5047	0.3878	0.0211	0.1168	0.7734	0.5519	0.0212
		0.6	0.1989	0.4622	0.3560	0.0193	0.1274	0.7079	0.5060	0.5060
	$T_{CRNL}$	(0.1670)				(0.1068)				
	T.T	0.2	0.1712	0.5386	0.4134	0.0225	0.1095	0.8256	0.5886	0.0226
		0.4	0.1825	0.5044	0.3876	0.0211	0.1168	0.7731	0.5517	0.0212
0.6		0.1989	0.4618	0.3557	0.0193	0.1274	0.7076	0.5058	0.0194	
$T_{CRNL}$	(0.1670)				(0.1068)					

TABLE 23 EFFECT OF RISE IN TEMPERATURE ( $\Delta T$ ), PLATE THICKNESS RATIOS ( $A/H$ ), ASPECT RATIOS ( $A/B$ ) WITH AMPLITUDE RATIOS ( $W_{max}/h$ ) FOR BI,  $\{i=9\} = 0.10$ ] ON THE DIMENSIONLESS NONLINEAR EXPECTED MEAN ( $\omega_{NL}$ ) AND THE COEFFICIENT OF VARIATIONS ( $\omega_{NL2}$ ) OF FUNDAMENTAL FREQUENCY ON ANTI SYMMETRIC ANGLE-PLY  $[\pm 45]_2 T$  LAMINATED C PLATES.  $\omega_L$  IS LINEAR MEAN FUNDAMENTAL FREQUENCY.

a/h	a/b	$W_{max}/h$	$\delta T=50$		$\delta T=150$	
			Mean, $\omega_{NL}$	COV, $\omega_{NL}^2$	Mean, $\omega_{NL}$	COV, $\omega_{NL}^2$
				bi, i=9		bi, i=9
10	1	0.3	15.6203	0.0416	15.5422	0.0396
		0.6	15.8696	0.0408	15.7901	0.0388
		0.9	16.2120	0.0396	16.1305	0.0377
	$\omega_L$	(15.5285)		(15.4509)		
	2	0.3	38.9618	0.0420	38.7669	0.0385
		0.6	39.7049	0.0410	39.5060	0.0376
0.9		40.7480	0.0396	40.5435	0.0364	
$\omega_L$	(38.6935)		(38.5000)			
20	1	0.3	17.5948	0.0469	17.2349	0.0408
		0.6	17.8539	0.0461	17.4886	0.0402
		0.9	18.2498	0.0447	17.8761	0.0392
	$\omega_L$	(17.5060)		(17.1480)		
	2	0.3	42.0292	0.0422	41.1693	0.0297
		0.6	42.8042	0.0408	41.9279	0.0289
0.9		43.9927	0.0391	43.0911	0.0278	
$\omega_L$	(41.7638)		(40.9095)			

Tables (23) examines the effect of plate thickness ratio ( $a/h=10$  &  $20$ ) and aspect ratio ( $a/b=1$  and  $2$ ) on the dimensionless mean and the coefficient of variations for  $b_i, \{i = 9\} = 0.10$  of the nonlinear fundamental frequency with amplitude ratio of two layer angle-ply anti-symmetric  $[\pm 45]_2$  laminated composite square plate with simply supported SSSS boundary conditions subjected to uniform temperature change ( $\delta T = 50$  and  $150$ ). For the same amplitude ratio, aspect ratio and thermal loading, moderately thick square plate ( $a/h=20$ ) show the largest coefficient of variations to random change in lamina plate thickness input variables, while moderately thick rectangular plate laminate shows highest mean dimensionless nonlinear fundamental frequency. Apart from other side, at the same amplitude ratio, thickness ratio and thermal loading, rectangular plate ( $a/b=2$ ) show the largest coefficient of variations to random change in lamina plate thickness input variables for small temperature changes

( $\delta T = 50$ ). However, when temperature on increasing from ( $\delta T = 50$ ) to ( $\delta T = 150$ ) the square plate is more sensitive.

## Conclusions

A C0 nonlinear finite element method in conjunction with Taylor series based mean centered first order perturbation technique combined with direct iterative method is developed to examine the second order statistics of thermal post buckling load and thermal nonlinear free vibration. The following conclusions can be drawn from the limited study.

The coefficient of variation of thermal post buckling temperature is significant when the plate is supported on Winkler and Pasternak elastic foundations. The numerical results are significantly influenced by different amplitude ratios, support conditions, plate thickness ratios, aspect ratios and temperature changes. The buckling strength of laminated composite plate decreases when subjected to uniform in-plane temperature induced loading along with in-plane edge compressive loading.

The coefficient of variation in thermal post buckling temperature for square plate is less as compared to rectangular plate with temperature dependent material properties and resting on Winkler foundation. Moderately thick plate shows lower coefficient of variation to random change in all random input variables as compared to moderately thin plate.

The thermal post buckling temperature is significant for plate with simple SSSS (S2) boundary support conditions compared to clamped support conditions. Mean and coefficient of variation of Thermal post buckling of the plate is more subjected to temperature dependent as compared to temperature independent random system properties. Increase in temperature results in decrease in nonlinear mean fundamental frequency and increase in coefficient of variation of nonlinear fundamental frequency of the plate .

## Notations

$A_{ij}, B_{ij}, etc :$	Laminate stiffnesses
$BB :$	Strain-displacement matrix
$a, b :$	Plate length and breadth
$bi :$	Basic random system properties
$E_{11}, E_{22} :$	Longitudinal and Transverse elastic moduli
$G_{12}, G_{13}, G_{23} :$	Shear moduli
$h :$	Thickness of the plate
$Kl :$	Linear bending stiffness matrix
$Kg :$	Thermal geometric stiffness matrix
$M, m :$	Mass and inertia matrices
$NE, NL :$	Number of elements, number of layers in the laminated plate
$N_x, N_y, N_{xy}$	In-plane thermal buckling loads
$NN :$	Number of nodes per element
$\phi_i$	Shape function of ith node
$Q_{ij} :$	Reduced elastic material constants
$\{\Lambda\}^{(e)}, \{\Lambda\}^{(e)}$	Vector of unknown displacements, displacement vector of eth element
$U,$	Strain energy due to bending

$u, v, w$ :	Displacements of a point on the mid plane of plate
$u, v, w$ :	Displacement of a point $(x, y, z)$
$\{\sigma\}, \{\varepsilon\}$ :	Stress vector, Strain vector
$y, x$ :	Rotations of normal to mid plane about the x and y axis respectively
$x, y, k$ :	Two slopes and angle of fiber orientation wrt x-axis for kth layer
$x, y, z$ :	Cartesian coordinales
$Var()$ :	Variance
$RVs$ :	Random variables
$T$ :	Difference in temperatures
$\alpha_1, \alpha_2$ :	Thermal expansion coefficients along x and y direction
$\beta_1, \beta_2$ :	Coefficients of hygroscopic expansion along x and y direction.

### Appendix (A)

$$(A_{ij}, B_{ij}, D_{ij}, E_{ij}, F_{ij}, H_{ij}) = \int_{-h/2}^{h/2} Q_{ij}(1, z, z^2, z^3, z^4, z^6) dz; \quad (i,j=1,2,6)$$

$$(A_{ij}, D_{ij}, F_{ij}) = \int_{-h/2}^{h/2} Q_{ij}(1, z^2, z^4) dz; \quad (i,j=4,5) [K_b] = \sum_{i=1}^n \int_{A^{(e)}} [B_b]^T [D_b] [B_b] dA; [K_s] = \sum_{i=1}^n \int_{A^{(e)}} [B_s]^T [D_s] [B_s] dA$$

$$[K_g] = \sum_{i=1}^n \int_{A^{(e)}} [B_g]^T [N_0] [B_g] dA, \{q\} = \sum_{e=1}^{NE} \{\Lambda\}$$

$$[F^T] = \sum_{i=1}^n \int_{A^{(e)}} \left[ [B_{li}]^T [N^T] + [B_{bli}]^T [M^T] + [B_{b2i}]^T [P^T] \right] dA$$

$$[D_b] = \begin{bmatrix} \varphi_{i,x} & 0 & 0 & 0 & 0 & 0 & 0 \\ \varphi_{i,y} & 0 & 0 & 0 & 0 & 0 & 0 \\ 0 & \varphi_{i,x} & 0 & 0 & 0 & 0 & 0 \\ 0 & \varphi_{i,y} & 0 & 0 & 0 & 0 & 0 \\ 0 & 0 & \varphi_{i,x} & 0 & 0 & 0 & 0 \\ 0 & 0 & \varphi_{i,y} & 0 & 0 & 0 & 0 \\ 0 & 0 & 0 & C_1 \varphi_{i,x} & 0 & 0 & 0 \\ 0 & 0 & 0 & 0 & C_1 \varphi_{i,y} & 0 & 0 \\ 0 & 0 & 0 & C_1 \varphi_{i,y} & C_1 \varphi_{i,x} & 0 & 0 \\ 0 & 0 & 0 & -C_2 \varphi_{i,x} & 0 & -C_2 \varphi_{i,x} & 0 \\ 0 & 0 & 0 & 0 & -C_2 \varphi_{i,y} & 0 & -C_2 \varphi_{i,y} \\ 0 & 0 & 0 & -C_2 \varphi_{i,y} & -C_2 \varphi_{i,x} & -C_2 \varphi_{i,y} & -C_2 \varphi_{i,x} \end{bmatrix} \{q\}$$

$$[D_s] = \begin{bmatrix} 0 & 0 & \varphi_{i,x} & 1 & 0 & 0 & 0 \\ 0 & 0 & \varphi_{i,x} & 0 & 1 & 0 & 0 \\ 0 & 0 & 0 & -3 & 0 & -3 & 0 \\ 0 & 0 & 0 & 0 & -3 & 0 & -3 \end{bmatrix} \{q\} [B_{li}] = \begin{bmatrix} \varphi_{i,x} & 0 & 0 & 0 & 0 & 0 & 0 \\ 0 & \varphi_{i,y} & 0 & 0 & 0 & 0 & 0 \\ 0 & 0 & 0 & 0 & 0 & 0 & 0 \\ \varphi_{i,y} & \varphi_{i,x} & 0 & 0 & 0 & 0 & 0 \end{bmatrix}$$

$$[B_{bi}] = \begin{bmatrix} 0 & 0 & 0 & 0 & 0 & C_1 \varphi_{i,x} & 0 \\ 0 & 0 & 0 & 0 & 0 & 0 & C_1 \varphi_{i,y} \\ 0 & 0 & 0 & 0 & 0 & C_1 \varphi_{i,y} & C_1 \varphi_{i,x} \end{bmatrix} [B_{si}] = \begin{bmatrix} 0 & 0 & \varphi_{i,x} & 0 & 0 & C_1 \varphi_i & 0 \\ 0 & 0 & \varphi_{i,y} & 0 & 0 & 0 & C_1 \varphi_i \end{bmatrix}$$

$$[B_{gi}] = \begin{bmatrix} 0 & 0 & \varphi_{i,x} & 0 & 0 & 0 & 0 \\ 0 & 0 & \varphi_{i,y} & 0 & 0 & 0 & 0 \end{bmatrix}, [N_0] = \begin{bmatrix} N_x & N_{xy} \\ N_{xy} & N_y \end{bmatrix}, [B_{li}] = [B_{li}]; [B_{bii}] = [B_{bi}]; [B_{b2i}] = [B_{si}];$$

### Appendix (B)

The non-dimensional parameters for elastic foundations used are as follows:

$$k_1 = K_1 b^4 / E_{22}^d h^3; \quad k_2 = K_2 b^2 / E_{22}^d h^3 .$$

## REFERENCES

- [1] Chen L.W and Chen L.Y., "Thermal buckling behavior of laminated composite plates with temperature-dependent properties", *Composite Structures*, vol. 13(4) pp 275–287, 1989.
- [2] Huang T.R, Tauchert Lexington and Kentucky, "Post buckling response of antisymmetric angle-ply laminates to uniform temperature loading", *Acta Mechanica*, vol.72 pp173-183, 1988.
- [3] Chen L.W and Chen L.Y., "Thermal post buckling behaviors of laminated composite plates with temperature-dependent properties", *Composite Structures*, vol. 19 pp 267-283, 1991.
- [4] Shen H.S, "Thermal post buckling behaviors of imperfect shear deformable laminated composite plates with temperature-dependent properties", *Comput Methods Appl Mech Engg* vol.190 pp 5377-5390, 2001.
- [5] Sita.V, Thankam, Singh G., Venkateswara G Rao and Rath A.K, "Thermal post buckling behaviors of laminated composite plates using shear flexible element based on coupled-displacement field", *Composite Structures*, vol.59 pp 351-359, 2003.
- [6] Shariyat M, "Thermal buckling analysis of rectangular composite plates with temperature-dependent properties, based on a layer wise theory", *Thin wall structure*, vol. 45(4) pp 439-452, 2007.
- [7] Pandey. Ramesh, Shukla K.K and Jain. Anuj, "Thermoelastic stability analysis of laminated composite plates, An analytical approach", *Communications in Nonlinear Science and Numerical Simulation*, vol. 14(4) pp 1679-1699, 2009.
- [8] Nigam N.C and Narayana S, "Application of random vibrations", Narosa, New Delhi, 1994.
- [9] Handa K and Anderson K, "Application of Finite Element Methods in the statistical analysis of structures", *Int Conf on Structl, Safety and Reliability*, pp 409-417, 1981.
- [10] Nakagiri S, Tani H and Tatabatake S, "Uncertain eigen value analysis of composite laminated plates by SFEM", *Compo. Strut*, vol. 14 pp 9-12, 1990.
- [11] Lin S.C and Kam T .Y, "Buckling analysis of imperfect frames using a stochastic finite element method", *Comput Struct.*, vol. 42(6) pp 895–901, 1992.
- [12] Englested S.P and Reddy J.N, "Probabilistic methods for the analysis of matrix composite," vol.50 pp 91-107, 1994.
- [13] Zhang J and Ellingwood B, "Effects of uncertain material properties on structural stability", *J Struct Engg*, vol. 121(4) pp 705-716, 1995.
- [14] Graham L.L and Siragy E.F, "Stochastic finite element analysis for elastic buckling of stiffened panels", *J Engrg. Mech*, vol. 127 pp 91-97, 2001.
- [15] Singh B.N, Iyengar N.G.R and Yadav D, "Effects of random material properties on buckling of composite plates," *ASCE J Engrg Mech*, vol. 127 (9) pp 873-879, 2001.
- [16] Singh B.N, Iyengar N.G.R and Yadav D, "A C0 finite element investigation for buckling analysis of composite plates with random material properties", *Struct Engg and Mech* vol. 13(1) pp 53-74, 2002.
- [17] Ankara A.K, Upadhyay C.S and Yadav D. "Generalized buckling analysis of laminated plates with random material properties using stochastic finite elements," *Int J Mech Sci*, vol. 48 pp 780-798, 2006.
- [18] Liu W.K, Belytschko T and Mani. A, "Random field finite elements," *Int J Numer. Meth Engrg*, vol. 23 pp 1831–1845, 1986.
- [19] Yamin Z, Chen S and Lue Q, "Stochastic perturbation finite elements," *Comp and Struct* vol. 59 (3) pp 425-429, 1996
- [20] Liu F.C and Huang C.H, "Free vibration of composite laminated Plates subjected to temperature change," *Computers & Structures* , vol. 60(1) pp 95-101, 1996.
- [21] Bailey C.D, "Vibration and local instability of thermally stressed plates," *Comput Method Appl. Mech. Eng*, vol.25( 3) pp 263-278, 1981.
- [22] Tauchert T.R, "Thermally induced flexure buckling and vibration of plates", *Applied Mechanics Review Thermal and nonlinear matrices*, vol. 44(8) pp 347-360, 1991.

- [23] Chang W.P and Jen S.C, " Nonlinear free vibration of heated orthotropic rectangular plates", *Int. J. Solids Struct*, vol.22 pp 267–281, 1986.
- [24] Collins J.D and Thomson W.T, "The Eigen value problems in structural system with statistical properties", *A.I.A.A. J*, vol. 7(4) pp 170-173, 1969.
- [25] Leissa A.W and Martin A.F, "Vibration and buckling of rectangular composite plates with variable fiber spacing", *Composite Structures* vol. 14 pp 339–357, 1990.
- [26] Zhang Z and Chen S, "The standard deviation of the Eigen solutions for random multi degree freedom systems", *Computers & Structures*, vol. 39(6) pp 603-607, 1990.
- [27] Zhang J and Ellingwood B, "Effects of uncertain material properties on structural stability", *Journal of Structural Engineering ASCE*, vol. 121 pp 705-716, 1993.
- [28] Zhang Y, Chen S and Liu Q, " Stochastic perturbation finite elements", *Computers & Structures*, vol. 59(3) pp 425- 429, 1996.
- [29] Manohar C.S and Ibrahim R.A, "Progress in structural dynamics with stochastic parameter variations", *applied mechanics review*, vol. 52 pp 177–196, 1999.
- [30] Salim S, Iyengar N.G.R and Yadav D, "Natural frequency characteristics of composite plates with random properties", *Structural Engineering and Mechanics*, vol. 6(6) pp 659-671, 1998.
- [31] Venini P and Mariani J, "Free vibration of uncertain composite plates via Raleigh-Ritz approaches", *Computer and Structures*, vol. 64(1-4) pp 407-423, 2002.
- [32] Yadav D and Verma N, "Free vibration of composite circular cylindrical shells with random material properties Part 2: Applications", *Composite Structures*, vol. 51 pp 371–380, 2001.
- [33] Singh B.N, Yadav D and Iyengar N.G.R, "Natural frequencies of composite plates with random material properties using higher order shear deformation theory", *International Journal Mechanical Sciences*, vol. 43 pp 2193–2214, 2001.
- [34] Singh B.N, Yadav D and Iyengar N.G.R, "A C0 finite element for free vibration of laminated composite plates with uncertain material properties", *advanced composite materials*, vol. 11(4) pp 331–350, 2003.
- [35] Onkar A.K and Yadav D, " Non-linear free vibration of laminated composite plate with random material properties", *Journal of Sound and Vibration*, vol. 27 pp 627–641, 2004.
- [36] Kitipornchai S, Yang J and Liu KM, "Random vibration of the functionally graded laminates in thermal environments", *Comput. Methods appl. mech. Engg*, vol. 195 pp 1075–1095, 2006.
- [37] Tripathi Vivek, Singh B.N and Shukla K.K, "Free vibration of laminated composite conical shells with random material properties", *Composite Structures*, vol. 81 pp 96–104, 2007.
- [38] Reddy J.N, "A simple higher order theory for laminated composite plates", *J Appld Mech Trans ASME*, vol. 51 pp 745-752, 1984.
- [39] Shankara C.A and Iyengar N.G.R, "A C0 element for the buckling analysis of laminated composite plates", *Journal of sound and vibration*, vol. 191 (5) pp 721-738, 1996 .
- [40] Chia C.Y, "Nonlinear analysis of plates", McGraw-Hill New York, 1980.
- [41] Reddy J.N, "Mechanics of laminated composite plate", CRC Press Florida, 1996
- [42] Franklin J.N, "Matrix theory", Englewood cliffs J.N. Prentice Hall, 1968.
- [43] Klieber M and Hien T.D, "stochastic finite element method", Wiley Chichester, 1992.
- [44] Jones R.M, "Mechanics of composite materials", Mc Graw Hill New York, 1975.
- [45] Reddy J.N, "Energy and variational methods in applied mechanics", John Wiley & Sons, 1984.
- [46] Zang Z and Chen S, "Standard deviations of the Eigen solutions for random dof systems", *Comp Struct*, vol. 39 pp 603–607, 1991.

- [47] Chen W.J, Lin P.D and Chen L.W, "Thermal Buckling Behavior of Thick Laminated Plates under Non-Uniform Temperature Distribution", *Comput Struct*, vol. 41(4) pp 637–645, 1991.
- [48] Boley B.A and Weiner J.J, "Theory of thermal stress", John Wiley New York, pp 307-335,1960.
- [49] Lal A, Singh B.N and Rajesh Kumar, "Effects of random system properties on thermal buckling analysis of laminated composite plates", *Int. Journal of computer and Structure*, vol. 87(17-18) pp 1119-1128, 2009.
- [50] Singh B.N, Lal A, "Stochastic analysis of laminated composite plates on elastic foundations: The cases of postbuckling behavior and nonlinear free vibration", *Int. Journal of Pressure vessel and piping*, vol. 87(10) pp 559-574, 2010.

# Experimental and Numerical Investigation on Compressive Stability of Stiffened Composite Panel with Multiple Stringers and Frames

Tianliang Qin<sup>1</sup>, Lei Peng<sup>2</sup>, Bo Ma<sup>3</sup>, Yanan Chai<sup>4</sup>, Feng Yao<sup>5</sup>, Jifeng Xu<sup>\*6</sup>

<sup>1,2,3,\*6</sup>Beijing Key Laboratory of Commercial Aircraft Structures and Composite Materials, Beijing Aeronautical Science & Technology Research Institute, Beijing, 102211 P.R. China

<sup>4</sup>China Aircraft Strength Research Institute, Xi'an, 610113 P.R. China

<sup>5</sup>AVIC Composite Corporation Ltd., Beijing 101300, PR China

<sup>1</sup>qintianliang@comac.cc; <sup>2</sup>penglei@comac.cc; <sup>3</sup>mabo2@comac.cc; <sup>4</sup>yanan.chai@263.net; <sup>5</sup>yf\_ly2003@126.com;

<sup>\*6</sup>xujifeng@comac.cc

## Abstract

The stability of stiffened composite panels is the primary problem in aircraft design. This work investigates the compressive buckling and postbuckling behaviors of a stiffened composite panel with seven hat stringers and three frames. Both the compressive experiment and Finite Element (FE) analysis are carried out for the buckling and postbuckling responses of the stiffened composite panel under compressive load. A new test setup is designed for the compressive experiment, where the transverse deflections of the frame ends are constrained by six in-plane movable jigs when compressive load is applied. The Digital Image Correlation (DIC) technique is used to measure the buckling modes and strain distributions of the skin in the experiment. The detailed buckling developments are recorded by DIC technique at different load levels. In addition, the strains on different sections of the skin and stringers are recorded by strain gauges to monitor the strain changes during the postbuckling process. Meanwhile, the nonlinear FE analysis using the Riks method is carried out in Abaqus. The skin, stringers and frames are modeled using shell elements. The adhesive bonded joints are simulated by Tie constraints. The bolted joints are simulated by the combination of beam elements and distributing coupling elements. The maximum strain criterion is used to predict the ultimate failure. The numerical model is validated by comparing the predicted buckling load, buckling mode developments and ultimate failure region with the experimental results.

## Keywords

*Stiffened Composite Structures; Buckling; FE Analysis; Mechanical Testing*

## Introduction

The stiffened panels are main structural components to build the aircraft fuselage and wings, because of the lesser structural weight penalty of using stiffener than increasing panel thickness. The stability of such panels, when subjected to compression or shear loads, is a primary design problem. With increasing use of composite materials in aircraft primary structures, the stability of stiffened composite panels has received a lot of research studies from the researchers and designers.

Lots of research work on the metal panel stability has been done both in analysis and experiments, and relatively reliable analysis and design methods have been developed. However, the methods for metal panels cannot be applied to composite panels directly, as the anisotropic properties of composite materials lead to more complex responses of composite panels, such as the bending-extension coupling effects in unsymmetrical laminated plates. Many studies by Sundaresan, Singh and Rao indicate that the bending-extension coupling effects may lead the laminated plate to buckling in a way similar to the buckling responses of eccentrically loaded plates rather than the buckling patterns of bifurcation in stability. For complex stiffened composite panels with multiple stringers and frames, the stability problems are quite complicated due to their complex configurations. Various local buckling patterns may occur before the global buckling for a stiffened panel, such as the skin local buckling, the stringer

local buckling, etc., reported by Stevens, Ricci and Davies, Kong, Lee, Kim and Hong. The postbuckling capability significantly influences the structural safety and design. Therefore, it is essential to carry out some studies to understand the stability of complex stiffened panels both experimentally and numerically.

Experimental method is a direct and important way to study the buckling characteristics and postbuckling capability of the composite panels, such as the works by Chryssanthopoulos, Elghazouli, and Esong, Simites, Shaw and Sheinman. However, only few published papers are found to focus on the compressive experiments of stiffened composite panels. Stevens, Ricci and Davies studied the compressive postbuckling behaviors of I-stiffened composite panels by the experimental method. Kong, Lee, Kim and Hong conducted the compressive experiments on the I- and T-stiffened composite panels. Orifici, Alberdi, Thomson and Bayandor investigated the postbuckling behaviors of T-stiffened composite panels under compressive load. Jegley conducted the experiments and finite element analysis for the compressive stability of Pultruded Rod Stitched Efficient Unitized Structure (PRSEUS) panels which have multiple rod-frames and stiffeners. The stability of stiffened composite panels with multiple frames and stiffeners is quite complex. More specific research work is necessary to be performed for better understanding such buckling and postbuckling behaviors. In this study, great efforts have been made in the design of the equipment and fixtures for the compressive buckling testing of complex stiffened panels, and the support conditions of frames have been incorporated into the finite element modeling. Besides, some advanced monitoring techniques are employed to observe the buckling development in the experiment.

The buckling analysis methods of composite panels include the analytical methods and FE methods. The analytical methods of buckling analysis mainly focus on the laminated panels with the simple geometries, and they are usually not available for complex stiffened panels as the corresponding analytical buckling expressions are extremely difficult to be obtained. The FE methods become widely used in stability analysis of the stiffened panels. Eigenvalue buckling analysis and nonlinear stability analysis are two FE methods for buckling analysis. The Eigenvalue buckling analysis is generally used to estimate the critical load of stiff structures, which exhibit bifurcation instability and have very little deformation prior to buckling. For the complex stiffened panels, bifurcation buckling may not occur due to the out-of-plane deformations developed from bending-extension coupling effects and eccentric loading in some local regions. The out-of-plane deformations may further induce serious geometric nonlinearity. Therefore, the nonlinear FE analysis is an acceptable way to investigate the buckling and postbuckling behaviors of complex composite panels.

In this paper, complex composite panels with seven hat stringers and three frames are both studied experimentally and numerically. In the experiment, the transverse deflections of the frame ends are constrained by six jigs. These jigs can only move in the plane parallel with the skin. The DIC technique is used to monitor the skin deformation development at different load levels. Strain gauges are set on different sections of the skin and stringers to monitor the buckling point. The numerical analysis is conducted in Abaqus. The skin, stringers and frames are modeled using shell elements. The tie constraints are used to join the skin and stringers models together. The bolted joints in the structures are modeled by the combination of beam elements and distributing coupling elements. Nonlinear FE analysis is performed using the Riks method to predict the postbuckling behaviors of the stiffened composite panels. The numerical model is validated by comparing the experimental and numerical results of buckling load, buckling mode development and ultimate failure load.

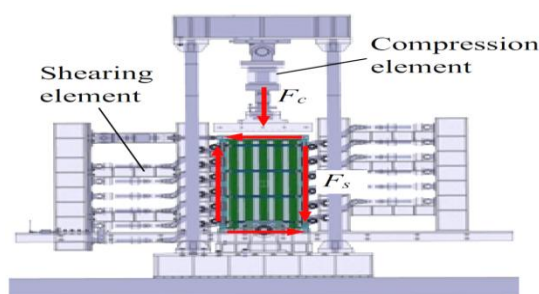


FIG.1 EXPERIMENT LOADING SYSTEM FOR ARBITRARY COMPRESSION-SHEARING RATIO

**Experiment**

A study on the stiffened composite panel stability is conducted for the understanding of complex stiffened

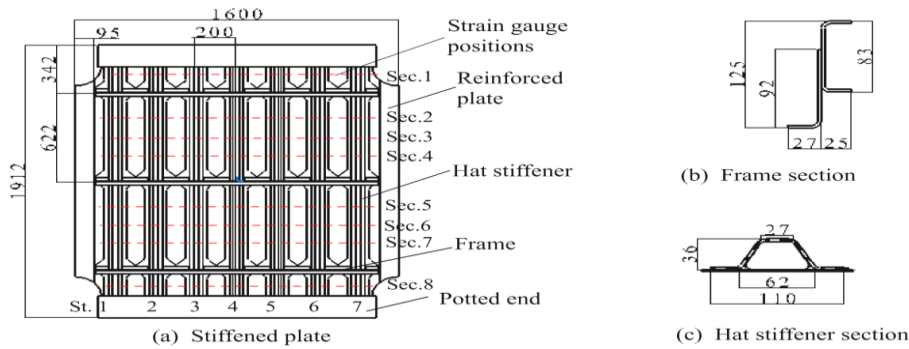


FIG.2 CONFIGURATION AND DIMENSIONS OF STIFFENED COMPOSITE PANEL

panel stabilities and for the validation of numerical analysis methods. Various stability experiments of the flat and curved composite panels are carried out. The compressive buckling experiment of flat stiffened panel in this paper is part of the study. In addition to the typical loading conditions such as compressive and shearing loads, the mixed compression-shearing loads are also considered in the study. A new experiment loading system has been designed as shown in Fig.1. The vertical and horizontal loading elements of the experiment loading system can apply compression and shearing loads in coordination. As a result, arbitrary ratio of the mixed compression-shearing loads could be obtained using this experiment loading system. In this paper, we focus on the compressive properties and behaviors of stiffened composite panels.

The stiffened composite panel consists of the skin, seven hat stringers and three frames, as shown in Fig.2 (a). All parts are made of carbon/epoxy composite materials. The thickness of each layer is 0.191mm. The ply sequence of the skin is  $[\pm 45/0/0/90/0]_s$ . The frame includes an L laminate and a C laminate, bolted together, as shown in Fig.2 (b). Both of them have 16 plies with lay-ups of  $[\pm 45/0/0/0/90/\pm 45]_s$ . The hat stringer is formed with an  $\Omega$  laminate of  $[\pm 45/0/0/0/90/\pm 45]_s$  and an inner U laminate of  $[\pm 45]_s$ . The junction parts of stringer are filled with unidirectional composite fillers. The stringers and skin are adhesive bonded together. The frames and skin are fastened by titanium alloy bolts. The main dimensions of each part are given in Fig.2.

The mechanical properties of carbon/epoxy composite materials are listed in Table 1.

The stiffened composite panel is loaded to first buckling under different load cases before loaded to ultimate failure in compression. The stiffened composite panel is designed to be suitable for both the compressive and shearing load cases. The left and right sides of the skin are extended as the connection regions joined with the shearing fixtures. Two pieces of laminates are bonded at the connection regions front and back for reinforcement. The reinforced plates have the same lay-up as the skin. The top and bottom ends are potted in aluminum boxes filled with resin, as shown in Fig.2. The loading faces of the boxes are machined flat to achieve uniform compressive load condition.

TABLE 1 PROPERTIES OF CARBON/EPOXY COMPOSITE MATERIALS

Elastic Modulus /GPa	$E_{11}$	$E_{22}$	$G_{12}$	$\nu_{12}$	-
	164	9.0	4.14	0.32	-
Failure Strain / $\mu\epsilon$	$\epsilon_{11t}$	$\epsilon_{11c}$	$\epsilon_{22t}$	$\epsilon_{22c}$	$\gamma_{2\%}$
	15000	7900	10000	24000	12000

The experiment setup is shown in Fig.3. The lower end of the specimen is placed on the platform and fixed to the platform by two L-jigs and bolts. The compressive load is applied to the upper end of the specimen with a thick metal plate. No shearing load is applied by separating the shearing fixtures from the shearing loading element. The

frame ends are connected with six out-of-plane supports as shown in Fig.4. The out-of-plane supports can freely move in the plane parallel with skin, so that only the transverse deflections of the frame ends are constrained in the experiments.

The DIC technique is used to monitor the displacement and strain responses of the skin in this paper. The DIC technique is a non-contact optical technique for measuring the strain and displacement. It works by comparing digital photographs of a test piece at different stages of deformation. By tracking blocks of pixels, the system can measure surface displacement and build up 2D and 3D deformation vector fields and strain maps. The DIC technique is simple to use and accurate for the measurement. It has been widely used in the characterization of materials as well as in many practices in civil engineering.



FIG.3 EXPERIMENT SETUP OF STIFFENED COMPOSITE PANELS



FIG.4 OUT-OF-PLANE CONSTRAINTS OF FRAME ENDS

The outer surface of the skin is painted white strewn with black spots as shown in Fig. 3, which would be used to measure the displacements and strain fields of the skin by the DIC technique. Meanwhile, the strain gages are placed on eight sections of the skin and stringers as shown in Fig.2. Fig.5 gives the setting scheme of strain gauges on different sections. Five 0° strain gauges are bonded on each section of the hat stringers. The strain rosette gauges are placed on the skin front and back. To make the measuring areas of DIC as continuous as possible, the front skin surfaces on Sec. 2, 4, 5 and 7 are free of any gauges.

The compressive load is applied at a rate of 0.5kN/s until ultimate failure. The strains and DIC photos are recorded in every increase of 1.0 kN. The sounds and damages in the experiment are recorded with digital videos for the analysis.

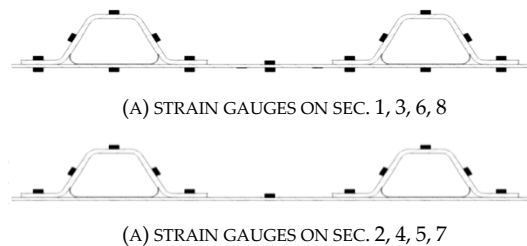


FIG.5 THE SETTING SCHEME OF STRAIN GAUGES

## Numerical Analysis Model

All composite parts of the specimen are modeled using S4 shell elements in Abaqus. The fixtures for shear experiment are also modeled with S4 shell elements. The finite element model mesh is shown in Fig.6. The hat stringer models are tied to the skin model to simulate the adhesive bonded joints. The bolts to fasten the L and C laminates, skin and frames, and skin and fixtures are simulated using B31 beam elements. The beam element nodes are connected to the shell elements using distributing coupling elements.

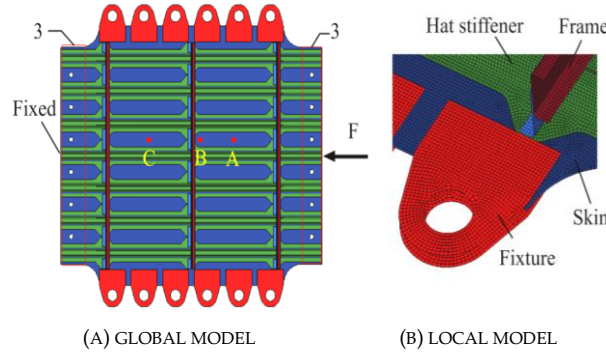


FIG.6 FINITE ELEMENT MODEL, BOUNDARY AND LOAD OF STIFFENED PANEL IN COMPRESSION

Figure 6 indicates the boundary and load of the stiffened panel that the finite element model adopts in the analysis. The supported end is completely fixed. The nodes of skin and hat stringers in the pot are constrained in transverse deflection. A concentrated compressive force of 1750kN is applied on the loading end.

The geometrically nonlinear analysis associated with the modified Riks method is carried out for the compressive buckling and postbuckling process of the stiffened composite panel. The Riks method discovers a single equilibrium path in a space defined by the displacement and loading parameters. It is generally used to predict unstable, geometrically nonlinear collapse of a structure. A very tight convergence tolerance is set to prevent the load floating back because of the existence of local buckling.

## Results and Discussions

### Local Buckling and Postbuckling Behaviors

Figure 7 shows the out-of-plane deformations of the skin during the loading process obtained by the DIC technique and FE method. The bumps are first observed between stringers along the frames. With the load increasing, more bumps appear along the frames. When the load increases to 1000 kN, new buckling waves have filled the middle area of each bay. The detailed buckling mode is given in Fig. 8. It can be seen that the buckling waves are symmetric about the stringers. There are about three and a half of waves in each bay. The predicted buckling shape developments agree well with the experiential results.

To explain the phenomena in Fig.7 that the bumps of the skin first occur near the frames, the detail configurations of the stiffened panel are observed. As shown in Fig.9, there are flange extensions in the conjunctions of stringers and frames. The laminate thicknesses between two stringers are not uniform along the longitudinal direction. The changes of the laminate section near the flange extensions will induce local eccentricity under compression. Bending deformations occur as soon as the compressive load is applied in the nearby region such as Point B in Fig.9.

In the middle area marked as Point A in Fig.9, the eccentricity effects decrease. The transverse deflections don't appear obviously until buckling at Point A.

Figure 10 shows the experimental and numerical load-strain curves of the skin at point C front and back. The point C is at the same locations as point A in each bay, as shown in Fig. 6. The strains increase linearly since the beginning. When the load increases to a certain level, the curves become nonlinear, which indicate the appearance of buckling. The experimental buckling load at point C is about 820 kN. The numerical result is about 850 kN,

which is 3.7% higher than the experiment result.

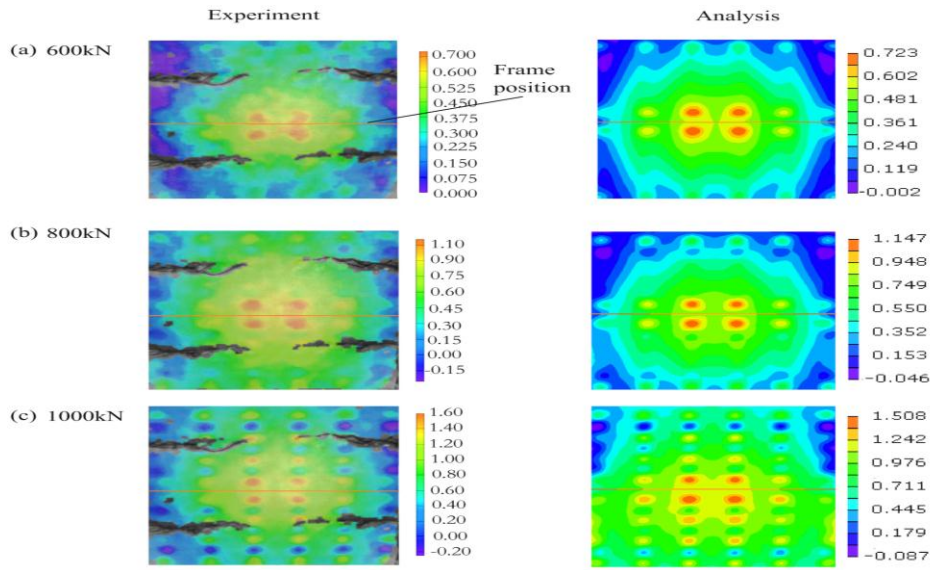


FIG.7 OUT-OF-PLANE DEFORMATION OF THE STIFFENED PANEL UNDER COMPRESSION

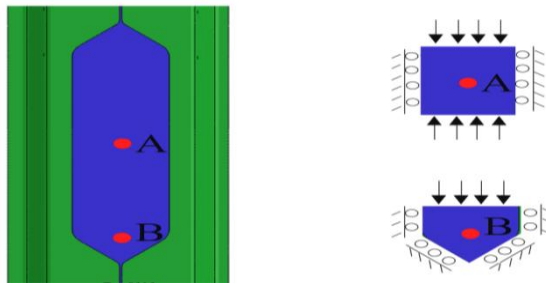
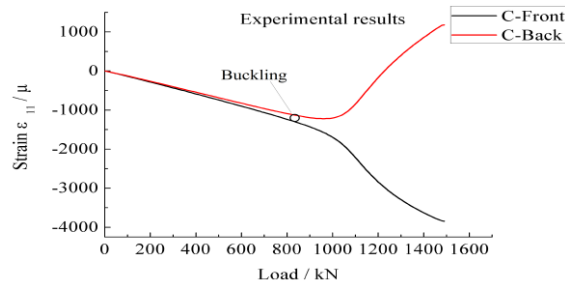
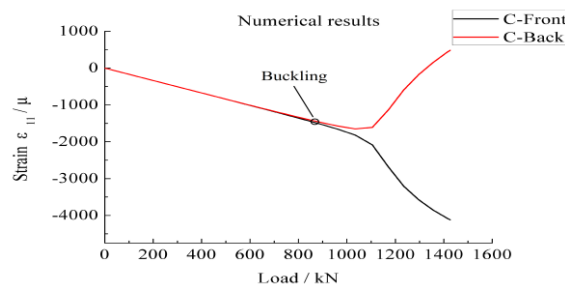


FIG.9 CONFIGURATION AND EQUIVALENT CONSTRAINT CONDITIONS OF THE LOCAL SKIN



(A) EXPERIMENTAL RESULTS



(B) NUMERICAL RESULTS

FIG.10 LOAD-STRAIN CURVES OF THE SKIN ON BOTH SIDES AT POINT C

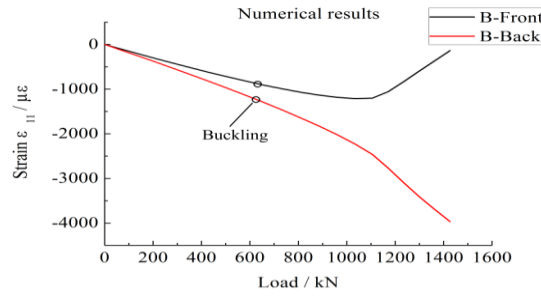


FIG.11 LOAD-STRAIN CURVES OF THE SKIN ON BOTH SIDES AT POINT B

As no strain gauges are set at point B in the experiment, there are no experimental load-strain curves at point B offered in this paper. The numerical results of load-strain curves at point B are given in Fig.11. The curves become nonlinear at about 580 kN. It is about 32% lower than the buckling load at A and C, which indicates that the local eccentricity significantly affect the skin first buckling load.

When local buckling occurs in the skin, the skin may withstand higher load. The local postbuckling capability of the skin depends on its support conditions. In the stiffened composite panels, the hat stiffeners act as the local support conditions of the skin. According to Fig.9, the local support conditions can be grouped into two categories: one is the two-edge simply support condition at points A and C, the other is three-edge simply support condition at point B. Because the average strains of the laminate are relative with the in-plane load, they could reflect the local load withstood by the skin under compression. To investigate the local postbuckling capability of the skin, the average strains at points A, B and C are calculated by  $\bar{\epsilon}_{11} = (\bar{\epsilon}_{11}^{front} + \bar{\epsilon}_{11}^{back}) / 2$ . It can be seen that, all the average strains keep increasing after buckling. The postbuckling capability at point B is much higher than that at points A and C due to the stronger support conditions, although the buckling load at point B is lower. The postbuckling load at points A and C is around 1050 kN in the experimental, The numerical result is 1170 kN, which is 11.4% higher than the experiment load. The average strain of C keeps increasing until the ultimate failure load. As a result, the postbuckling loads are about 25% higher than the buckling values at A and C, while above 100% higher at B.

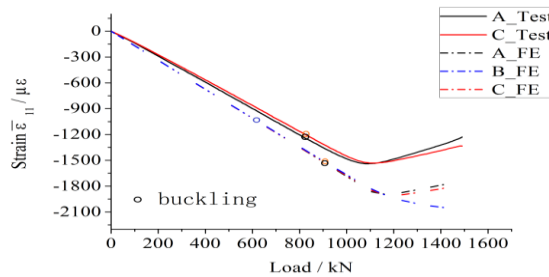


FIG.12 LOAD-AVERAGE STRAIN CURVES OF THE SKIN AT POINTS A, B AND C

**Global Buckling and Ultimate Failure**

Figure 13 gives the global deformations of the stiffened panel at 600 kN obtained experimentally and numerically. Because the panel section changes at the four corners, the bending neutral axis of the stiffened panel changes. The distance between the compressive load and bending neutral axis will cause eccentricity in the stiffened panel. Both the experimental and numerical results show that the center of the panel begins to bulge as soon as the compressive load is applied. With the compressive load increasing, the effects of the eccentricity decrease due to the frame constraints. When the load increases to a certain level, the global buckling appears. The global buckling mode at 1200 kN is shown in Fig.14. The buckling mode presents a full sine wave. The frames are at the wave nodes. The results indicate that the laterally supported frames divide the stiffened panels and could improve the structural stability by decreasing the effective compression length of the panels.

Figure 15 shows experimental results of load-strain curves of the 1<sup>st</sup> and 3<sup>rd</sup> stringers at Sec.6. The flange strain curves marked as 1 and 5 become nonlinear first among the five curves, at the load of about 970 kN. At this

moment, the curves 2, 3 and 4 are still straight, which means the stringers don't reach the buckling yet. The nonlinearity of curves 2, 3 and 4 indicate the stringer buckling. The buckling loads for the 1<sup>st</sup> stringer is 1030 kN, while for the 3<sup>rd</sup> stringer is 1110 kN. After buckling, the strains on the 1<sup>st</sup> stringer increase rapidly, while those on the 3<sup>rd</sup> stringer indicate slight nonlinearity. It reveals that the stringers near the panel edges have lower postbuckling capability than that in the center of the panel.

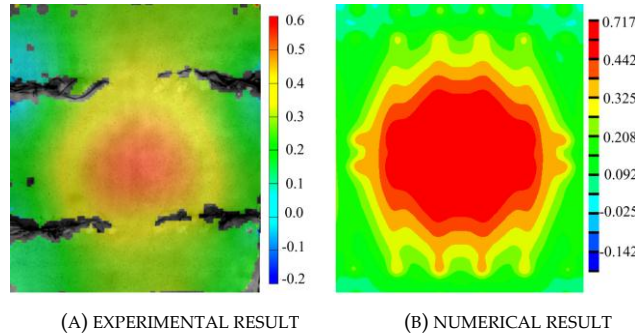


FIG.13 GLOBAL DEFORMATION OF THE STIFFENED PANEL AT 600 kN

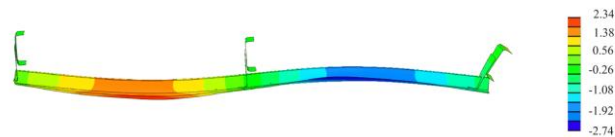


FIG.14 GLOBAL BUCKLING MODE OF THE STIFFENED PANEL AT 1200 kN

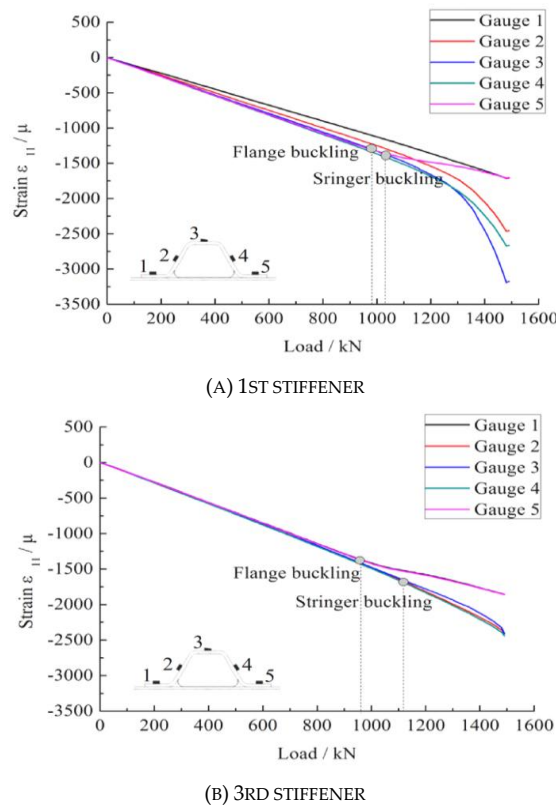


FIG.15 EXPERIMENTAL RESULTS OF LOAD- STRAIN CURVES OF THE 1<sup>ST</sup> AND 3<sup>RD</sup> STRINGERS AT SEC.6

Figure 16 gives numerical results of load-strain curves of the 1<sup>st</sup> and 3<sup>rd</sup> stringers at Sec.6. The numerical curves have the similar shapes with the experimental ones. The predicted buckling load of the 1<sup>st</sup> stringer is 970 kN, 5.8% lower than experiment results. The predicted buckling load of the 3<sup>rd</sup> stringer is 1180 kN, 7.3% higher than experiment results.

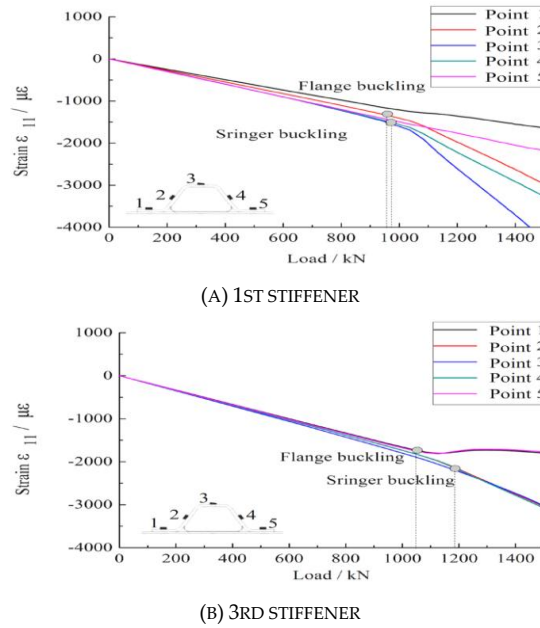


FIG.16 NUMERICAL RESULTS OF LOAD- STRAIN CURVES OF THE 1ST AND 3RD STRINGERS AT SEC.6

The stiffened panel failed in a sudden collapse before any visible local damage is observed. The ultimate failure appears between the lower frame and the potted end, as shown in Fig.17(a). The ultimate failure load is 1490kN. Fig.17(b) gives the predicted failure region using the maximum strain criterion. The predicted failure location is near the fillet, which is the same as the experiment results.

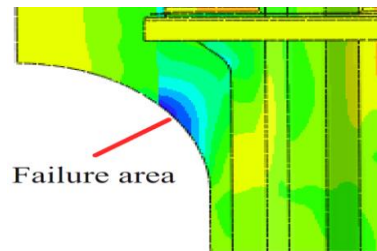
**Conclusions**

The compressive buckling and postbuckling behaviors of a complex composite panel with multiple stringers and frames are studied in this paper. The compressive experiment was conducted on a new test setup. The frame ends are constrained in the transverse deflection by six in-plane movable jigs. The DIC technique is used to monitor the deformation development of the skin at different load levels. The strain gauges are set on the skin and stringers to monitor the strain changes in the loading process. The local buckling in the skin was first observed. Due to the eccentricity induced by local reinforcement, the buckling load of the skin near the frames is lower than that in the middle areas. However, the local postbuckling capability of the skin near the frames is higher than that in the middle areas, because of the stronger constraint conditions near the frames. In the middle of each bay, the local postbuckling loads of the skin are about 25% higher than their buckling values. Near the frames, the local postbuckling loads of the skin are above 100% higher than their buckling values. The global buckling appears when the skin becomes unstable. The stringers near the panel edges buckling at lower load than those in the center of the panel.

A nonlinear FE model is established for the compressive buckling and postbuckling analysis of the complex stiffened composite panel. The structure details including the bonded joints, bolted joints and jigs are modeled. The Riks method is used to solve the nonlinear FE model. The predicted local buckling, global buckling and ultimate failure are compared with the experiment results. The numerical results show good agreement with experimental ones.



(A) ULTIMATE FAILURE IN EXPERIMENT



(B) PREDICTED FAILURE IN FINITE ELEMENT MODEL

FIG.17 EXPERIMENTAL AND NUMERICAL RESULTS OF ULTIMATE FAILURE

## REFERENCES

- [1] ABAQUS Theory and user's manuals. Hibbit, Karlsson, Sorensen. Providence, 2012.
- [2] Bisagni, C. "Numerical analysis and experimental correlation of composite shell buckling and post-buckling." *Composites Part B Engineering* 31(2000): 655-667.
- [3] Chen, F., and Qiao, P. "Buckling of delaminated bi-layer beam-columns." *International Journal of Solids and Structures* 48(2011): 2485-2495.
- [4] Chryssanthopoulos, M.K., Elghazouli, A.Y., and Esong, I.E. "Compression tests on anti-symmetric two-ply GFRP cylinders." *Composites Part B: Engineering* 30(1999): 335-350.
- [5] Dash, P., and Singh, B.N. "Buckling and post-buckling of laminated composite plates." *Mechanics Research Communications* 46(2012): 1-7.
- [6] Featherston, C.A., and Watson, A. "Buckling of optimized flat composite plates under shear and in-plane bending." *Composites Science and Technology* 65( 2005): 839-853.
- [7] Gabriella, T., and Laszlo, P.K. "Buckling of axially loaded composite plates with restrained edges." *Journal of Reinforced Plastics and Composites* 29(2010): 3521-3529.
- [8] Hosseini-Toudeshky, H., Loughlan, J., and Kharazi, M. "The buckling characteristics of some integrally formed bead stiffened composite panels." *Thin-Walled Structure* 43( 2005): 629-445.
- [9] Ibrahim, S.M., Carrera, E., Petrolo, M., and Zappino, E. "Buckling of composite thin walled beams by refined theory." *Composite Structures* 94(2012): 563-570.
- [10] Jegley, D.C. "Structural efficiency and behavior of pristine and notched stitched structure." Paper presented at SAMPE 2011 Fall Technical Conference, Fort Worth, TX, United States, Oct. 17-20, 2011.
- [11] Kharazi, M., Ovesy, H.R., and Taghizadeh, M. "Buckling of the composite laminates containing through-the-width delaminations using different plate theories." *Composite Structures* 92( 2010): 1176-1183.
- [12] Kim, S.E., Thai, H.T., and Lee, J. "Buckling analysis of plates using the two variable refined plate theory." *Thin-Walled Structures* 47(2009): 455-462.
- [13] Kong, C.W., Lee, I.C., Kim, C. G., and Hong, C.S. "Postbuckling and failure of stiffened composite panels under axial compression." *Composite Structures* 42(1998): 13-21.
- [14] Lei, Z., Bai, R., Qiu, W., and Zhan, L. "Optical evaluation of the buckling behavior of stiffened composite laminates." *Composites: Part A* 43(2012): 1850-1859.
- [15] Lancaster, E.R., Calladine, C.R., and Palmer, S.C. "Paradoxical buckling behaviour of a thin cylindrical shell under axial compression." *International Journal of Mechanical Sciences* 42(2000): 843-865.
- [16] McCormick, N., and Lord, J. "Digital imaging correlation." *Materials today* 13(2010): 52-54.
- [17] Orifici, A.C., Alberdi, I.O.Z., Thomson, R.S., and Bayandor, J. "Compression and post-buckling damage growth and collapse analysis of flat composite stiffened panels." *Composites science and technology* 68(2008): 3150-3160.
- [18] Riks, E. "The Application of Newtons Method to the Problem of Elastic Stability." *Journal of Applied Mechanics* 39(1972): 1060-1065.

- [19] Riks, E. "An incremental approach to the solution of snapping and buckling problems." *International Journal of Solids & Structures* 15(1979): 529-551.
- [20] Shufrin, I., Rabinovitch, O., and Eisenberger, M. "Buckling of symmetrically laminated rectangular plates with general boundary conditions – A semi analytical approach." *Composite Structures* 82(2008): 521-531.
- [21] Simitse, G.J., Shaw, D., and Sheinman, I. "Stability of imperfect laminated cylinders - A comparison between theory and experiment." *AIAA Journal* 23(2015): 1086-1092.
- [22] Stevens, K.A., Ricci, R., and Davies, G.A.O. "Buckling and postbuckling of composite structures." *Composites* 26(1995): 189-199.
- [23] Sundaresan, P., Singh, G., and Rao, G.V. "Buckling and post-buckling analysis of moderately thick laminated rectangular plates." *Computers & Structures* 61(1996): 79-86.

# Effects of Hygrothermomechanical Loading and Uncertain System Environments on Flexural and Free Vibration Response of Shear Deformable Laminated Plates:

Stochastic Finite Element Method Micromechanical Model Investigation

Rajesh Kumar

School of Mechanical Engineering, JIT, Jimma University, ETHIOPIA

rajeshtripathi63@gmail.com

## *Abstract*

Present paper investigates the effects of hygrothermomechanical loading and uncertain system environments on flexural and free vibration response of shear deformable laminated plates. System parameters such as the lamina material properties, coefficients of thermal expansion and coefficients of hygroscopic expansion, lamina plate thickness, geometric property and lateral load are modeled as basic random variables. A C0 finite element method in conjunction with the first order perturbation technique procedure for the plate subjected to lateral loading and free vibration is employed to obtain the second order response statistics of the transverse deflection and natural frequency of the plates. Typical numerical results for the second order statistics of the transverse central deflection and free vibration of geometrically linear composite plates subjected to uniform temperature distribution are investigated. The performance of the stochastic laminated composite model is demonstrated through comparison of mean transverse central deflection and free vibration with those results available in literature and standard deviation of the deflection and natural frequency with an independent Monte Carlo simulation before data generation.

## *Keywords*

*Hygrothermomechanical Loading; Uncertain System Properties; Micromechanical Model; Perturbation Technique*

## **Introduction**

Composite materials are being nowadays widely used in critical structural members such as light weight components, ability to tailor structural properties through appropriate lamination scheme for achieving high strength and stiffness to weight ratio and with good energy and sound absorption and often also low production cost. The structural plates made of the composite material are increasingly used in many industrial applications such as aerospace, automotive and shipbuilding industries. The plates are often subjected to vibration and combination of lateral pressure in hygrothermomechanical loading environments. The capability to predict the structural response which enables a better understanding and characterization of the actual behavior of laminated composite plate in terms of structural response when subjected to combined loads is of prime interest to structural analysis.

A considerable volume of literature is available on the static response of geometrically linear and nonlinear composite laminated plates under various thermal and mechanical loads or combination of two. Whitney et al. [1971] studied the effect of environment on the elastic response of layered composite plates. They used deterministic finite element method with macro mechanical model for the buckling, vibration and static bending response of laminated composite plates. Sai Ram and Sinha [1991] investigated the hygrothermal effects on the bending characteristics of laminated composite plates by using first order shear deformation theory and deterministic finite element method. They found that there are appreciable effects of hygrothermal on the bending

characteristics of laminated composite plates. Shen [2000, 2002] Non-linear bending of shear deformable laminated plates under lateral pressure and thermal loading and resting on elastic foundations and hygrothermal effects on the nonlinear bending of shear deformable laminated plates. Lee et al. [1992] analyzed the hygrothermal effects on the linear and nonlinear analysis of symmetric angle-ply laminated plates by using deterministic finite element macro mechanical model. Patel et al. [2002] investigated the hygrothermal effects on the structural behavior of thick composite laminates using higher-order theory. They also used macro mechanical model to find out the effects on buckling, vibration and bending response of laminated composite plates. Onkar and Yadav [2003] have investigated the non-linear response statistics of composite laminated flat panel with random material properties subjected to transverse random loading based on CLT in conjunction with FOPT. Singh et al. [2000] is extended to random environments. They presented  $C^0$  linear and nonlinear finite element method (FEM) in conjunction with a FOPT to obtain the second order response statistics of bending deflection of laminated composite plate supported with and without elastic foundation. They included the transverse shear effects in the system equation using HSDT.

A few literatures is available on the static linear and nonlinear bending response of laminated composite plates using deterministic micromechanical model. Upadhyay et al. [2010] investigated the nonlinear flexural response of laminated composite plates under hygro-thermo-mechanical loading using deterministic finite element method and micromechanical model. Rajesh et al.[2011, 2012] investigated the hygrothermal effects on the flexural response of laminated composite plates with random material properties and nonlinear response.

Chen and Chen [1988] investigated the vibrations of hygrothermal elastic composite plates using deterministic finite element method. The investigated the different behavior of plates when exposed to moisture and temperature environments. Ram and Sinha [1992] investigated the the hygrothermal effects on the free vibration of laminated composite plates using deterministic finite element approach with first order shear deformation theory. Huang and Zheng [2003,2004] studied the nonlinear vibration and dynamic response of simply supported shear deformable laminated plates on elastic foundations and in hygrothermal environments by using deterministic finite element approach. Lal A et al.[2009] investigated the Stochastic Nonlinear free vibration response of laminated composite plates resting on elastic foundation in thermal environments. Rajesh et al.[2011,2013] studied the hygrothermoelastic free vibration response of laminated composite plates resting on elastic foundations with random system properties using micromechanical model and nonlinear responses. Zhang et al. [1996] have applied the stochastic perturbation method to vector-valued and matrix-valued function for the response and reliability of uncertain structures. Liu et al. [1986] developed the probabilistic finite element method (PFEM) for linear and nonlinear continua with homogeneous random fields of a one dimensional elastic plastic wave propagation problems and a two dimensional plane-stress beam bending problem. Zhang and Ellingwood [1993] examined the effect of random material field characteristics on the instability of a simply supported beam on elastic foundation and a frame using perturbation technique.

It is evident from the literature review presented and observations, there is no literature covering the flexural and free vibration responses of laminated composite plates, subject to hygrothermo-mechanical loading involving randomness in material properties and micromechanical model to the best of the authors' knowledge.

In the present study, the stochastic flexural and free vibration responses of laminated composite plates in the presence of small random variation in the material variables, taking into account the transverse shear strain using higher order shear deformation theory (HSDT) is studied. The  $C^0$  finite element method (FEM) and mean centered first order perturbation technique (FOPT) is employed to determine the second order statistics (mean and standard deviation) of transverse central deflection of laminated composite plates subjected to hygrothermo-mechanical loading with a linearly varying transverse moisture and temperature distribution across the thickness. The numerical illustrations concerned the stochastic bending and free vibration responses of laminated composite plates for individual random input variables, plate thickness ratio, aspect ratio, boundary conditions; lamina lay up, load deflection, fiber volume fraction under different sets of environmental conditions. It is observed that small amount of random material properties, coefficient of hygroscopic expansion; coefficients of thermal expansion variations and geometric parameters of the composite plate significantly affect the transverse central deflection and natural frequency of the laminates. The proposed probabilistic procedure would be valid for small random

coefficient of variations compared to their mean values. The condition is satisfied by most engineering materials and it hardly puts any limitation on the approach.

### Mathematical Formulations

Consider geometry of laminated composite rectangular plate of length  $a$ , width  $b$ , and thickness  $h$ , which consists of  $N$  plies located in three dimensional Cartesian coordinate system  $(X, Y, Z)$  where  $X$ - and  $Y$ -plane passes through the middle of the plate thickness with its origin placed at the corner of the plate as shown in Figure. 1. Let  $(\bar{u}, \bar{v}, \bar{w})$  be the displacements parallel to the  $(X, Y, Z)$  axes, respectively. The thickness coordinate  $Z$  of the top and bottom surfaces of any  $k$ th layer are denoted by  $Z(k-1)$  and  $Z(k)$ , respectively. The fiber of the  $K$ th layer is oriented with angle  $\theta_k$  to the  $X$ - axes. The plate is assumed to be subjected to uniformly distributed transverse static load is defined as  $q(x, y) = q_0$ .

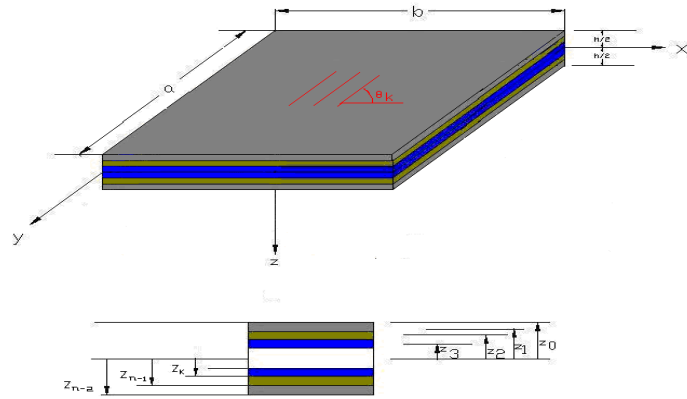


FIGURE.1. GEOMETRY OF LAMINATED COMPOSITE PLATE

### Displacement Field Model

In the present study, the assumed displacement field is based on the Reddy's higher order shear deformation theory [1996], which requires C1 continuous element approximation. In order to avoid the usual difficulties associated with these elements the displacement model has been slightly modified to make the suitability for C0 continuous element [1997]. In modified form, the derivatives of out-of-plane displacement are themselves considered as separate degree of freedom (DOFs). Thus five DOFs with C1 continuity are transformed into seven DOFs with C0 due to conformity with the HSDT. In this process, the artificial constraints are imposed which should be enforced variationally through a penalty approach.

However, the literature demonstrates that without enforcing these constraints the accurate results using C0 can be obtained. The modified displacement field along the  $X$ ,  $Y$ , and  $Z$  directions for an arbitrary composite laminated plate is now written as [1990]:

$$\begin{aligned}\bar{u} &= u + f_1(z)\psi_x + f_2(z)\theta_x; \\ \bar{v} &= v + f_1(z)\psi_y + f_2(z)\theta_y; \\ \bar{w} &= w;\end{aligned}\tag{1}$$

where  $\bar{u}$ ,  $\bar{v}$  and  $\bar{w}$  denote the displacements of a point along the  $(x, y, z)$  coordinates  $u$ ,  $v$ , and  $w$  are corresponding displacements of a point on the mid plane.  $\psi_x$  and  $\psi_y$  are the rotations of normal to the mid plane about the  $y$ -axis and  $x$ -axis respectively, with  $\theta_x = w_{,x}$  and  $\theta_y = w_{,y}$

$$f_1(z) = C_1 z - C_2 z^3; \quad f_2(z) = -C_4 z^3 \quad \text{with } C_1 = 1, C_2 = C_4 = 4h^2/3.$$

The displacement vector for the modified models is

$$\{\Lambda\} = [u \quad v \quad w \quad \theta_y \quad \theta_x \quad \psi_y \quad \psi_x]^T, \quad (2)$$

where, comma (,) denotes partial differential.

### Strain Displacement Relations

For the structures considered here, the relevant strain vector consisting of strains in terms of mid-plane deformation, rotation of normal and higher order terms associated with the displacement for kth layer are as

$$\{\varepsilon\} = \{\varepsilon_l\} - \{\bar{\varepsilon}_{HT}\} \quad (3)$$

where  $\{\varepsilon_l\}$  and  $\{\bar{\varepsilon}_{HT}\}$  are the linear strain vectors, hygrothermal strain vector, respectively.

Using Eq. (3) the linear strain vector can be obtained using linear strain displacement relations [1990], which can be written as

$$\{\varepsilon_l\} = \begin{Bmatrix} \varepsilon_P^L \\ 0 \end{Bmatrix} + \begin{Bmatrix} z\varepsilon_b^L \\ \varepsilon_s \end{Bmatrix} + \begin{Bmatrix} 0 \\ z^2\varepsilon_s^* \end{Bmatrix} + \begin{Bmatrix} z^3\varepsilon^* \\ 0 \end{Bmatrix} \quad (4)$$

where,

$$\{\varepsilon_P^L\} = \begin{Bmatrix} u_{0,x} \\ v_{0,y} \\ u_{0,y} + v_{0,x} \end{Bmatrix}, \quad \{\varepsilon_b^L\} = C_1 \begin{Bmatrix} \psi_{x,x} \\ \psi_{y,y} \\ \psi_{x,y} + \psi_{y,x} \end{Bmatrix}, \quad (5)$$

$$\{\varepsilon^*\} = -C_2 \begin{Bmatrix} \psi_{x,x} \\ \psi_{y,y} \\ \psi_{x,y} + \psi_{y,x} \end{Bmatrix} - C_4 \begin{Bmatrix} \theta_{x,x} \\ \theta_{y,y} \\ \theta_{x,y} + \theta_{y,x} \end{Bmatrix}, \quad (6)$$

$$\{\varepsilon_s\} = C_1 \begin{Bmatrix} \psi_y \\ \psi_x \end{Bmatrix} + \begin{Bmatrix} w_{,y} \\ w_{,x} \end{Bmatrix}, \quad \{\varepsilon_s^*\} = -C_2 \begin{Bmatrix} \psi_y \\ \psi_x \end{Bmatrix} - C_4 \begin{Bmatrix} w_{,y} \\ w_{,x} \end{Bmatrix},$$

The hygrothermal strain vector  $\{\bar{\varepsilon}_{HT}\}$  is represented as

$$\{\bar{\varepsilon}_{HT}\} = \begin{Bmatrix} \bar{\varepsilon}_x \\ \bar{\varepsilon}_y \\ \bar{\varepsilon}_{xy} \\ \bar{\varepsilon}_{yz} \\ \bar{\varepsilon}_{zx} \end{Bmatrix} = \Delta T \begin{Bmatrix} \alpha_1 \\ \alpha_2 \\ \alpha_{12} \\ 0 \\ 0 \end{Bmatrix} + \Delta C \begin{Bmatrix} \beta_1 \\ \beta_2 \\ \beta_{12} \\ 0 \\ 0 \end{Bmatrix} \quad (7)$$

$\alpha_1$ ,  $\alpha_2$  and  $\alpha_{12}$  are coefficients of thermal expansion and  $\beta_1$ ,  $\beta_2$  and  $\beta_{12}$  are coefficients of hygroscopic expansion along the x, y, z direction respectively which can be obtained from the thermal coefficients in the longitudinal ( $\alpha_l$ ) and transverse ( $\alpha_t$ ) directions of the fibers using transformation matrix and  $\Delta T$  is the change in temperature and hygroscopic coefficients in the longitudinal ( $\beta_l$ ) and transverse ( $\beta_t$ ) directions of the fibers using transformation matrix and  $\Delta C$  is the change in moisture in percentage in the plate subjected with uniform moisture ( $\Delta C=C_0$  in percentage) and temperature ( $\Delta T=T_0$ ) rise (U.T).

### Stress-strain Relation

The constitutive law of thermo-elasticity for the materials under considerations relates the stresses with strains in a plane stress state for the kth lamina oriented as an arbitrary angle with respect to reference axis for the orthotropic layers is given by [1996, 1997, 1992]

$$\{\sigma\}_k = [\bar{Q}]_k \{\varepsilon\}_k$$

$$\text{Or } \begin{Bmatrix} \sigma_{xx} \\ \sigma_{yy} \\ \sigma_{xy} \\ \sigma_{yz} \\ \sigma_{xz} \end{Bmatrix}_k = \begin{bmatrix} \bar{Q}_{11} & \bar{Q}_{12} & \bar{Q}_{16} & 0 & 0 \\ \bar{Q}_{12} & \bar{Q}_{22} & \bar{Q}_{26} & 0 & 0 \\ \bar{Q}_{16} & \bar{Q}_{26} & \bar{Q}_{66} & 0 & 0 \\ 0 & 0 & 0 & \bar{Q}_{44} & \bar{Q}_{45} \\ 0 & 0 & 0 & \bar{Q}_{45} & \bar{Q}_{55} \end{bmatrix}_k \begin{Bmatrix} \varepsilon_{xx} - \alpha_{xx}\Delta T - \beta_{xx}\Delta C \\ \varepsilon_{yy} - \alpha_{yy}\Delta T - \beta_{yy}\Delta C \\ \varepsilon_{xy} - \alpha_{xy}\Delta T - \beta_{xy}\Delta C \\ \varepsilon_{yz} \\ \varepsilon_{zx} \end{Bmatrix}_k [X, Y, Z] \quad (8)$$

where  $\{\bar{Q}\}_k$ ,  $\{\sigma\}_k$  and  $\{\varepsilon\}_k$  are transformed stiffness matrix, stress and strain vectors of the  $k^{\text{th}}$  lamina, respectively and  $(\alpha_x, \alpha_y, \alpha_{xy})$ ,  $(\beta_{xx}, \beta_{yy}, \beta_{xy})$  are the thermal and hygroscopic expansion coefficients along  $x$ ,  $y$ ,  $z$ , direction, respectively which can be obtained from the thermal coefficients in the longitudinal ( $\alpha_l$ ) and transverse ( $\alpha_t$ ) directions of the fibers using transformation matrix.  $T(X, Y, Z)$  is the uniform temperature field distribution.

### Strain Energy of the Plate

The strain energy ( $\Pi$ ) of the laminated composite plate is given by

$$\Pi = \frac{1}{2} \int_V \{\varepsilon\}^T [\sigma] dV. \quad (9)$$

The strain energy as given above can be written as

$$\Pi = \Pi_l \quad (10)$$

Where  $\Pi_l$  and  $\Pi_{nl}$  are the linear and the nonlinear strain energy respectively which are expressed as

$$\Pi_l = \frac{1}{2} \int_A \{\bar{\varepsilon}_l\}^T [\bar{Q}] \{\varepsilon_l\} dA \quad (11)$$

Using linear strain displacement relations the linear elastic strain energy as given in Eq. (11) can be expressed as

$$\Pi_l = \frac{1}{2} \int_A \{\bar{\varepsilon}_l\}^T [\bar{Q}] \{\varepsilon_l\} dA \quad (12)$$

Where  $\{\bar{\varepsilon}_l\}$  is the linear strain vector at the reference plane, i.e.,  $z=0$  and  $[D]$  is the laminate stiffness matrix.

### Strain Energy Due to Hygrothermal Stresses

The Strain energy ( $\Pi_2$ ) storage by hygrothermal (combined temperature and moisture) load is written as

$$\begin{aligned} \Pi_2 &= \frac{1}{2} \int_A \left[ N_x (w_{,x})^2 + N_y (w_{,y})^2 + 2N_{xy} (w_{,x})(w_{,y}) \right] dA \\ &= \frac{1}{2} \int_A \begin{Bmatrix} w_{,x} \\ w_{,y} \end{Bmatrix}^T \begin{bmatrix} N_x & N_{xy} \\ N_{xy} & N_y \end{bmatrix} \begin{Bmatrix} w_{,x} \\ w_{,y} \end{Bmatrix} dA \end{aligned} \quad (13)$$

where,  $N_x$ ,  $N_y$  and  $N_{xy}$  are pre-buckling hygrothermal stresses.

### External Work Done

The potential energy due to distributed transverse static load  $q(x, y)$  can be expressed as

$$\Pi_3 = W_{ext} = -W_q = \int_A q(x, y) w dA \quad (14)$$

where,  $q(x, y)$  is the intensity of distributed transverse static load which is defined as

$$q(x, y) = \frac{QE_{22}h^3}{b^4}, \quad \text{here } Q \text{ is represented as uniform lateral load.}$$

### Kinetic Energy of the Laminate

The kinetic energy ( $T$ ) of the vibrating laminated plate can be expressed as

$$T = \frac{1}{2} \int_V \rho^{(k)} \left\{ \dot{\mathbf{u}} \right\}^T \left\{ \dot{\mathbf{u}} \right\} dV \quad (15)$$

where  $\rho$  and  $\left\{ \dot{\mathbf{u}} \right\} = \left\{ \dot{u} \quad \dot{v} \quad \dot{w} \right\}^T$  are the density and velocity vector of the plate respectively.

In the present study a C0 nine-noded isoparametric finite element with 7 DOFs per node is employed. For this type of element, the displacement vector and the element geometry are expressed as

$$\left\{ \Lambda \right\} = \sum_{i=1}^{NN} \varphi_i \left\{ \Lambda \right\}_i; \quad x = \sum_{i=1}^{NN} \varphi_i x_i; \quad \text{and} \quad y = \sum_{i=1}^{NN} \varphi_i y_i \quad (16)$$

where  $\varphi_i$  is the interpolation function for the  $i$ th node,  $\left\{ \Lambda \right\}_i$  is the vector of unknown displacements for the  $i$ th node, NN is the number of nodes per element and  $x_i$  and  $y_i$  are Cartesian Coordinate of the  $i$ th node.

The linear mid plane strain vector can be expressed in terms of mid plane displacement field and then the energy is computed for each element and then summed over all the elements to get the total strain energy Following this, and using Eq. (16), can be written as

$$\Pi_1 = \sum_{e=1}^{NE} \Pi_1^{(e)} \quad (17)$$

where, NE is the number of elements and  $\Pi_1^{(e)}$  is the elemental total potential energy which can be expressed as

$$\Pi_1 = \sum_{e=1}^{NE} \left[ \frac{1}{2} \left\{ \Lambda^{(e)} \right\}^T \left[ K^{*(e)} \right] \left\{ \Lambda^{(e)} \right\} - \left\{ \Lambda^{(e)} \right\}^T \left[ F_t^{(e)} \right] \right] = \frac{1}{2} \{q\}^T [K] \{q\} - \{q\}^T [F^T] \quad (18)$$

with

$$[K_t] = [K_b] + [K_s]$$

where global bending stiffness matrix  $[K_b]$ , shear stiffness matrix  $[K_s]$ , global displacement vector  $\{q\}$  and hydrothermal load vector  $[F]$  are defined as appendix.

### Work Done Due to External Transverse Load

Using finite element model equation may be written as

$$\Pi_2 = \sum_{e=1}^{NE} \Pi_2^{(e)}, \quad \Pi_3^{(e)} = - \int_{A^{(e)}} \left\{ \Lambda \right\}^{(e)T} \left\{ P_M \right\}^{(e)} dA = - \{q\}^{(e)T} \left\{ P_M \right\}^{(e)} \quad (19)$$

Adopting Gauss quadrature integration numerical rule, the element stiffness and geometric stiffness, hydrothermal and mechanical load respectively can be obtained by transforming expression in  $x, y$  coordinate system to natural coordinate system  $\xi, \eta$ .

### Governing Equations

The governing equation for the static analysis can be derived using Variational principle [Reddy1997] which is generalization of the principle of virtual displacement. The equation does not change in the random environment. This gives

$$\Delta(U_{SE} + U_{TH} - W) = 0 \quad (20)$$

The governing equation for hydrothermal free vibration analysis of the laminated plate can be derived using the Lagrange's equation of motion [26] in terms of global matrices. This gives

$$\delta \int_{t_1}^{t_2} (\Pi_1 - W - T) dt \quad (21)$$

$$[M] \{q\} + [K] \{q\} = 0, [K] = \{[K_t] - \lambda_{HT} [Kg]\} \quad (21a)$$

where

$\{q\}, [K], [M]$  and  $\lambda_{HT}$  are defined as the global displacement vector, the global linear stiffness matrix, the global mass matrix and the critical hygrothermal buckling parameter respectively. The above equation can be expressed in the form of linear generalized eigen value problem for hygrothermal linear free vibration as:

$$[K]\{q\} = \lambda[M]\{q\} \quad (22a)$$

Substituting equations. one obtains as

$$[K]\{q\} = \{F\}, \quad \text{with} \quad [F] = [P_M] + [P_T] \quad (22)$$

where  $[K]$ , and  $[P_M]$  and  $[P_T]$  are defined in appendix.

The stiffness matrix  $[K]$  is random in nature, being dependent on the hygrothermo-elastic properties. Therefore the eigenvalues and eigenvectors also become random. The Eq. (22) can be solved with the help of perturbation technique or Monte Carlo simulation (MCS) to obtain the mean and variance of the transverse central deflection.

### **Solution Approach –Perturbation Technique**

In the present analysis, the lamina material properties are treated as independent random variables (RVs). The governing equation (22) can be written in the most general form as:

$$[K_{ij}^R]\{W_i^R\} = \{F_i\} \quad (23)$$

where  $[K_{ij}^R]$ ,  $[W_i^R]$  and  $\{F_i\}$  are represented as the random stiffness matrix, the random response vector and the deterministic forcing vector. Here  $[K_{sij}^R]$  are the known functions of a set of primary RVs  $[b_i^R]$  and  $[W_i^R]$  is unknown and treated as random, also being dependent on RVs  $[b_i^R]$ .

In the present study, our aim is to find the second order statistics of  $[W_i^R]$  when the second order statistics of primary RVs  $[b_i^R]$  are known. Any random variable can be expressed as the sum of its mean and the zero mean random variable which is expressed. The expression only up to the first-order terms and neglecting the second- and higher-order terms are given as random variable  $(RV^R) = \text{mean}(RV^d) + \text{zero-mean random variable}(RV^r)$

The operating random variables in the present case are defined as:

$$b_i^R = b_i^d + b_i^r; K_{sij}^R = K_{sij}^d + K_{sij}^r; W_i^R = W_i^d + W_i^r \quad (24)$$

We can express the above relations in the form:

$$b_i^R = b_i^d + \epsilon b_i^r; K_{sij}^R = K_{sij}^d + \epsilon K_{sij}^r; W_i^R = W_i^d + \epsilon W_i^r \quad (25)$$

where  $\epsilon$  is a scaling parameter, and is small in magnitude. We consider a class of problems where the zero-mean random variation is very small as compared to the mean part of random variables. i.e.,  $RV^d \gg \epsilon RV^r$ . Using the Taylor series expansion and neglecting the second and higher-order terms since first order approximation is sufficient to yield results with desired accuracy with low variability which are the cases in most of the sensitive application. Substituting Eq. (25) in Eq. (23) we get:

$$[K_{sij}^d + \epsilon K_{sij}^r]\{W_i^d + \epsilon W_i^r\} = \{F_i\}; \quad (26)$$

Equating the terms of same order, we obtain the zeroth order perturbation equation and first order perturbation equation as follows [21].

Zeroth order perturbation equation ( Flexural)

$$(\epsilon^0): [K_{sij}^d]\{W_i^d\} = \{F_i\} \quad (27)$$

Zeroth order perturbation equation (Free Vibration)

$$[K^d]\{q_i^d\} = \lambda[M]\{q_i^d\} \quad (27a)$$

First order perturbation equation (Flexural)

$$(\epsilon^1): [K_{sij}^d]\{W_i^r\} + [K_{sij}^r]\{W_i^d\} = \{F_i\} \quad (28)$$

First order perturbation equation (Free Vibration)

$$[K^d]\{q_i^r\} + [K^r]\{q_i^d\} = \lambda_i^r[M]\{q_i^d\} + \lambda_i^d[M]\{q_i^r\} \quad (28a)$$

Using this Eq. (28a) can be decoupled and the expression for hygrothermal free vibration is obtained. Eq. (27, 27a) is the deterministic equation relating to the mean response, which can be determined by conventional solution procedures Eq. (28, 28a) is the random equation, defining the stochastic nature of the bending characteristics and free vibration which cannot be solved using conventional method. For this a further analysis is required.

Using Taylor's series expansion the system matrix and response vector can be expressed as;

$$[K_{sij}^r] = \sum_l \frac{\partial K_{sij}^d}{\partial b_l^R} b_l^r, [W_i^r] = \sum_l \frac{\partial W_i^d}{\partial b_l^R} b_l^r \quad (29)$$

Substituting Eq.(29) in Eq.(28)and equating the coefficients of  $b_l^r$ .

$$[K_{sij}^d]\left\{\frac{\partial W_l^d}{\partial b_l^R}\right\} + \left[\frac{\partial K_{sij}^d}{\partial b_l^R}\right]\{W_i^d\} = 0, l = 1, 2, \dots \quad (30)$$

Using Eq. (25) we can solve the only unknown  $\left\{\frac{\partial W_l^d}{\partial b_l^R}\right\}$ , for each  $l$ . So the sensitivity matrix of eigenvectors can be found out.

The total deflection response and its variance can be written as:

$$W = W^d + \left\{\frac{\partial W_l^d}{\partial b_l^r}\right\} b_l^r \text{ and } \text{var}(W) = E \left[ \sum_l \frac{\partial W_l^d}{\partial b_l^R} b_l^r \right]^2 \quad (31)$$

Where  $E[\ ]$  is the expectation. The variance can be written as:

The total free vibration response and its variance can be written as:

$$\text{var}(W) = \sum_l^N \sum_l^N \text{diag} \left[ \frac{\partial W_l^d}{\partial b_l^R} \left( \frac{\partial W_l^d}{\partial b_l^R} \right)^T \right] E(b_l^r, b_l^r) \quad (32)$$

$$\lambda_i^r = \sum_{j=1}^q \lambda_{i,j}^d b_j^r; \{q_i^r\} = \sum_{j=1}^p q_{i,j}^d b_j^r; [K^r] = \sum_{j=1}^q [K_{,j}^d] b_j^r; \quad (33)$$

Using the above and decoupled equations, the expressions for  $\lambda_{i,j}^d$  is obtained.

Using Eq. (33) the variances of the Eigen values can now be expressed as

$$\text{Var}(\lambda_{i_i}) = \sum_{j=1}^p \sum_{k=1}^p \lambda_{i,j}^d \lambda_{i,k}^d \text{Cov}(b_j^r, b_k^r) \quad (34)$$

where  $\text{Cov}(b_j^r, b_k^r)$  is the cross variance between  $b_j^r$  and  $b_k^r$ . The standard deviation (SD) is obtained by the square root of the variance [26].

## Numerical Results and Discussions

A finite element code in MATLAB environment is developed to compute the second-order statistics (expected mean and coefficient of variations). The stochastic finite element method (SFEM) approach outlined for the static

bending and free vibration response of the laminated composite plates, subjected to uniform moisture and temperature changes with among all random input variables including material properties, coefficients of hygroscopic expansion and coefficients of thermal expansion and load deflections has been illustrated through numerical examples. The approach has been validated by comparing the results with those available in literatures and independent Monte Carlo simulation. A nine noded Lagrangian isoparametric element with 63 degrees of freedom (DOFs) for the present HSDT model has been used for discretizing the laminate. Based on convergence study, a (5×5) mesh has been used. The influence of scattering in the system properties on the static bending and free vibration in the following text has been examined for the laminated composite plate with various moisture and temperature increments. The mean and standard deviation of the static bending and natural frequency are obtained considering the all random input variables and coefficients of hygroscopic expansion as well as thermal expansion coefficients taking separately as basic random variables (RVs) as stated earlier. However, the results are only presented taking coefficient of variations of the system property equal to 0.10 [22]. as the nature of the SD (Standard deviation) variation is linear and passing through the origin. The basic random variables such as  $E_{11}$ ,  $E_{22}$ ,  $G_{12}$ ,  $G_{13}$ ,  $G_{23}$ ,  $\nu_{12}$ ,  $\alpha_1$ ,  $\alpha_2$ ,  $\beta_2$ ,  $h$  and  $Q$  are sequenced and defined as:

$$b_1 = E_{11}, b_2 = E_{22}, b_3 = G_{12}, b_4 = G_{13}, b_5 = G_{23}, b_6 = \nu_{12}, b_7 = \alpha_1, b_8 = \alpha_2, b_9 = \beta_2, b_{10} = h \text{ and } b_{11} = Q.$$

The following dimensionless linear load deflection parameters have been used in this study:  $Q = q b^4 / E_{22} h^4$ . The following dimensionless linear fundamental frequency and thermal buckling load parameters have been used in this study:  $\varpi = (\omega a^2 \sqrt{\rho / E_{22}^d}) / h$

The dimensionless parameters used are as follows:  $T = T_0 + \Delta T$ ; where  $T$  = total temperature,  $T_0$  = Initial Temperature,  $\Delta T$  = rise in temperature.  $C = C_0 + \Delta C$  where  $C$  = total moisture concentration,  $C_0$  = Initial moisture concentration,  $\Delta C$  = rise in moisture concentration.

The following material properties are used for computation Shen [2002].

$$T_0 = 25; C_0 = 0; \Delta T = 0; \Delta C = 0.0; V_f = 0.5; E_f = 230.0 \times 10^9; G_f = 9.0 \times 10^9; c_{fm} = 0; \rho_c = 1.5; \nu_f = 0.203; \alpha_f = -0.54 \times 10^{-6}; Q_f = 1750; c_{fm} = 0; \nu_m = 0.34; \alpha_m = 45 \times 10^{-6}; \rho_m = 1200; \beta_m = 2.68 \times 10^{-3}; \beta_f = 0; E_m = (3.51 - 0.003 \times T - 0.142 \times C) \times 10^9; G_m = E_m \times (2 \times (1 + \nu_m))^{-1}, E_{10} = (V_f \times E_f + V_m \times E_m).$$

Coefficients of thermal expansion and hygroscopic expansion are expressed as Shen [2002] and Hunget al.[2004].

$$\alpha_{11} = \frac{V_f E_f \alpha_f + V_m E_m \alpha_m}{V_f E_f + V_m E_m}, \quad \alpha_{22} = (1 + \nu_f) V_f \alpha_f + (1 + \nu_m) V_m \alpha_m - \nu_{12} \alpha_{11}, \quad \beta_{11} = \frac{V_f E_f c_{fm} \beta_f + V_m E_m \beta_m}{E_{11} (V_f \rho_f c_{fm} + V_m \rho_m)} \rho, \\ \beta_{22} = \frac{V_f (1 + \nu_f) c_{fm} \beta_f + V_m (1 + \nu_m) \beta_m}{(V_f \rho_f c_{fm} + V_m \rho_m)} \rho - \nu_{12} \beta_{11}, \quad \frac{1}{E_{22}} = \frac{V_f}{E_f} + \frac{V_m}{E_m} - V_f V_m \frac{V_f^2 \frac{E_m}{E_f} + \nu_m^2 \frac{E_f}{E_m} - 2 \nu_f \nu_m}{V_f E_f + V_m E_m}, \quad \rho = V_f \rho_f + V_m \rho_m, \quad E_{11} = V_f E_f + V_m E_m \\ \frac{1}{G_{12}} = \frac{V_f}{E_f} + \frac{V_m}{G_m}, \quad \nu_{12} = V_f \nu_f + V_m \nu_m, \quad V_m + V_f = 1$$

### **Temperature Independent Material Properties (TID)**

$$E_{111} = 0; \quad E_{21} = 0; G_{121} = 0; G_{131} = 0; G_{231} = 0; \alpha_{11} = 0; \alpha_{21} = 0; \beta_{11} = 0; \beta_{21} = 0;$$

### **Temperature Dependent Material Properties (TD)**

$$E_{111} = -0.5 \times 10^{-3}; \quad E_{21} = -0.2 \times 10^{-3}; \quad G_{121} = -0.2 \times 10^{-3}; \quad G_{131} = -0.2 \times 10^{-3}; \quad G_{231} = -0.2 \times 10^{-3};$$

$$\alpha_{11} = 0.5 \times 10^{-3}; \alpha_{21} = 0.5 \times 10^{-3}; \quad \beta_{11} = 0.5 \times 10^{-3}; \quad \beta_{21} = 0.5 \times 10^{-3};$$

$$E_1 = (E_{10} \times (1 + E_{111} \times (T + C))); \quad E_2 = (E_{20} \times (1 + E_{21} \times (T + C))); \quad G_{12} = (G_{120} \times (1 + G_{121} \times (T + C)));$$

$$G_{13} = (G_{130} \times (1 + G_{131} \times (T + C))); \quad G_{23} = (G_{230} \times (1 + G_{231} \times (T + C))); \quad \alpha_1 = \alpha_{110} \times (1 + \alpha_{11} \times T);$$

$$\alpha_2 = \alpha_{210} \times (1 + \alpha_{21} \times T); \quad \beta_1 = \beta_{11} \times (1 + \beta_{11} \times C); \quad \beta_2 = \beta_{21} \times (1 + \beta_{21} \times C);$$

The boundary conditions for simply supported, clamped and combination of both used for the present analysis are given as Figure 2.

All edges simply supported (SSSS):

$$v = w = \theta_y = \psi_y = 0, \text{ at } x = 0, a; \quad u = w = \theta_x = \psi_x = 0 \text{ at } y = 0, b$$

All edges clamped (CCCC):

$$u = v = w = \psi_x = \psi_y = \theta_x = \theta_y = 0, \text{ at } x = 0, a \quad \text{and } y = 0, b;$$

Two opposite edges clamped and other two simply supported (CSCS):

$$u = v = w = \psi_x = \psi_y = \theta_x = \theta_y = 0, \text{ at } x = 0 \quad \text{and } y = 0; \quad v = w = \theta_y = \psi_y = 0, \text{ at } x = a \quad u = w = \theta_x = \psi_x = 0, \text{ at } y = b;$$

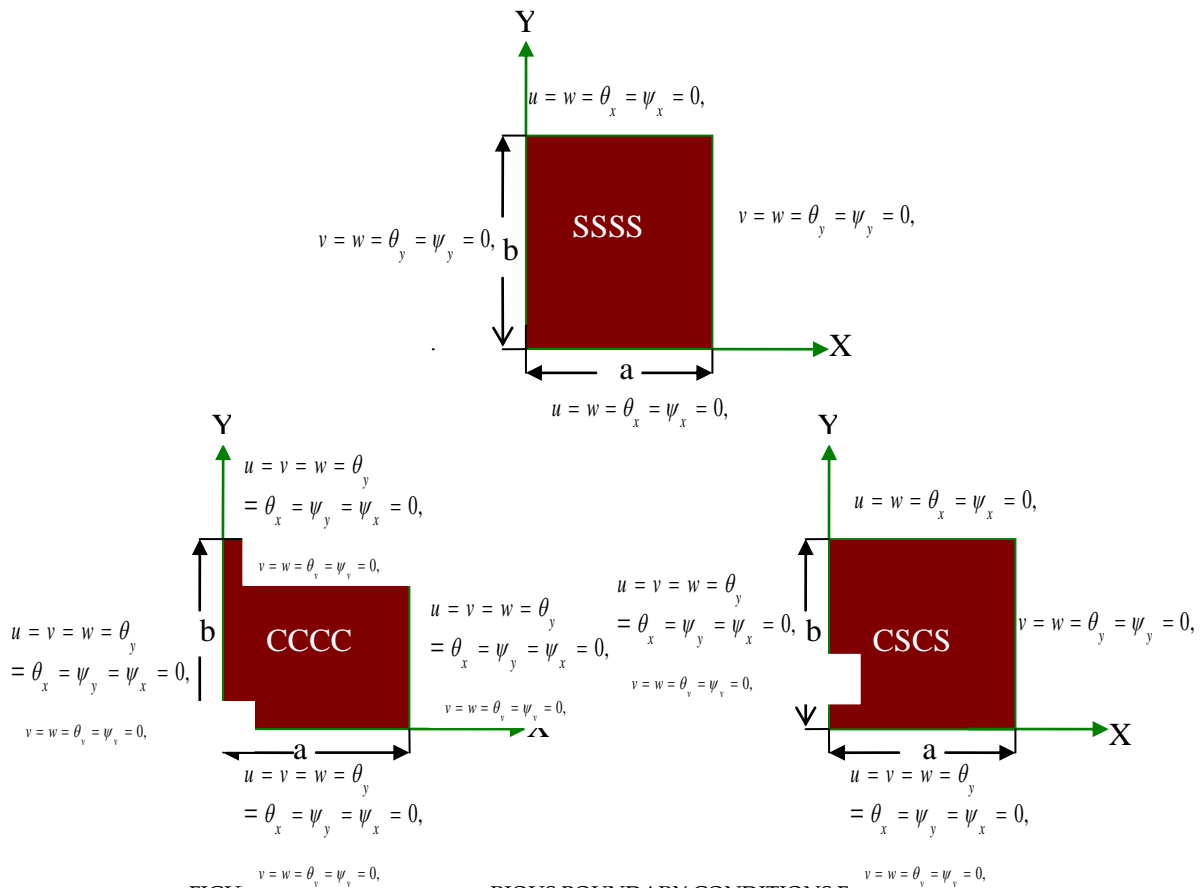


FIGURE 2 SCHEMATIC OF VARIOUS BOUNDARY CONDITIONS FOR THE PLATE

TABLE 1 COMPARISON OF HYGROTHERMAL EFFECTS ON THE LINEAR AND NONLINEAR BENDING BEHAVIOR OF (±45)2T LAMINATED SQUARE PLATE LOAD DEFLECTION Q WHERE  $Q = Q_0 b^4 / E_2^2 h^4$ , FIBER VOLUME FRACTION (VF)=0.6, PLATE THICKNESS RATIO (A/H)=10, SIMPLE SUPPORT SSSS(S2) BOUNDARY CONDITIONS.

Q	Non-dimensional Hygrothermal static bending load					
	Shen [2002]	Present		Shen [2002]	Present	
	$\Delta T=100, \Delta C=1\%$	$\Delta T=100, \Delta C=1\%$		$\Delta T=200, \Delta C=2\%$	$\Delta T=200, \Delta C=2\%$	
	Non-linear	Linear	Non-linear	Non-linear	Linear	Non-linear
100	0.6683	1.1707	0.6685	0.6483	1.0431	0.6444
150	0.8248	1.3954	0.8262	0.7716	1.2400	0.7744
200	0.9296	1.5242	0.9171	0.8583	1.3435	0.8406

**Validation Study for Random Hygrothermal Static Bending Load**

Comparison for present [FOPT] with present [MCS] for material property ( $E_{11}$ ) plate thickness ratio ( $a/h=10$ ), geometric property ( $h$ ) plate thickness ratio ( $a/h=30$ ), aspect ratio ( $a/b=1$ ), expected mean ( $W_0$ )= $1.0431$ ,  $\Delta T=2000C$ ,  $\Delta C=2\%$ , simple support SSSS ( $S_2$ ), angle ply ( $\pm 450$ ) $2T$ , fiber volume fraction ( $V_f=0.6$ ), load deflection  $Q = q b_4/E_{22}h_4 =100$ . Present [FOPT] results are in good agreement with present [MCS] results as shown in Figure 3.

Table 2. shows the effects of the variation of individual random system property  $b_i$ , [ $i=1$  to  $11$ ], =  $0.10$ ] on the dimensionless expected mean ( $W_0$ ) and coefficient of variation ( $W_1$ ) of hygrothermally induced central deflection of angle ply ( $\pm 450$ ) $2T$  square laminated composite plates in-plane bi-axial compression,  $a/h=20$ , with simple support  $S_2$  boundary conditions. The dimensionless mean load deflections are given in brackets. Dimensionless deflection load ( $Q$ )= $q b_4/E_{22}h_4 =100$  and fibre volume fraction ( $V_f =0.6$ ). It is noticed that expected mean ( $W_0$ ) value of individual random variables of hygrothermal deflection decreases with increase of temperature and moisture conditions. The expected mean ( $W_0$ ) further increases for TD material properties, the coefficient of variation ( $W_1$ ) of hygrothermal deflection increases on rise in temperature and moisture concentration for both TID and TD material properties.

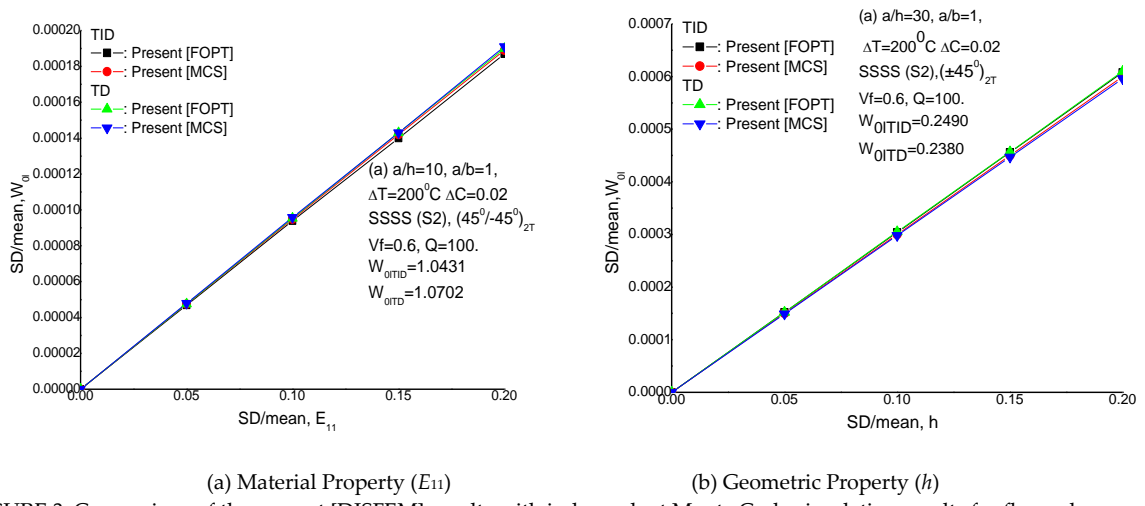


FIGURE 3. Comparison of the present [DISFEM] results with independent Monte Carlo simulation results for flexural response.

TABLE 2 EFFECTS OF THE VARIATION OF INDIVIDUAL RANDOM SYSTEM PROPERTY  $b_i$ , [ $i=1$  TO  $11$ ], =  $0.10$ ] ON THE DIMENSIONLESS EXPECTED MEAN ( $W_0$ ) AND COEFFICIENT OF VARIATION ( $W_1$ ) OF HYGROTHERMALLY INDUCED CENTRAL DEFLECTION OF ANGLE PLY ( $\pm 450$ ) $2T$  SQUARE LAMINATED COMPOSITE PLATES, IN-PLANE BI-AXIAL COMPRESSION,  $A/H=20$ , WITH SIMPLE SUPPORT  $S_2$  BOUNDARY CONDITIONS. THE DIMENSIONLESS MEAN LOAD DEFLECTIONS ARE GIVEN IN BRACKETS. DIMENSIONLESS DEFLECTION LOAD ( $Q$ )= $Q b_4/E_{22}H_4 =100$  AND FIBRE VOLUME FRACTION ( $V_F =0.6$ ).

$b_i$	(TID)				(TD)			
	COV, $W_1$				COV, $W_1$			
	$\Delta T=0^\circ C$ $\Delta C=0.0$	$\Delta T=100^\circ C$ $\Delta C=0.01$	$\Delta T=200^\circ C$ $\Delta C=0.02$	$\Delta T=300^\circ C$ $\Delta C=0.03$	$\Delta T=0^\circ C$ $\Delta C=0.0$	$\Delta T=100^\circ C$ $\Delta C=0.01$	$\Delta T=200^\circ C$ $\Delta C=0.02$	$\Delta T=300^\circ C$ $\Delta C=0.03$
$E_{11}$ ( $i=1$ )	(0.8359) 1.70e-04	(0.6223) 1.36e-04	(0.4821) 1.09e-04	(0.3832) 8.65e-05	(0.8400) 1.70e-04	(0.6319) 1.35e-04	(0.4882) 1.06e-04	(0.3820) 7.95e-05
$E_{22}$ ( $i=2$ )	0.0026	6.65e-05	2.44e-04	2.82e-04	0.0012	8.10e-04	1.58e-04	2.61e-04
$G_{12}$ ( $i=3$ )	2.74e-07	6.60e-07	1.20e-06	1.92e-06	2.75e-07	6.94e-07	1.35e-06	2.33e-06
$G_{13}$ ( $i=4$ )	3.02e-05	3.08e-05	3.44e-05	4.10e-05	3.01e-05	3.02e-05	3.39e-05	4.15e-05
$G_{23}$ ( $i=5$ )	1.51e-05	1.54e-05	1.72e-05	2.05e-05	1.50e-05	1.51e-05	1.69e-05	2.07e-05
$\nu_{12}$ ( $i=6$ )	0.0162	9.58e-04	1.44e-04	4.69e-05	0.0082	0.0050	4.52e-04	1.27e-04
$\alpha_{11}$ ( $i=7$ )	7.20e-09	8.83e-09	1.03e-08	1.19e-08	7.27e-09	9.21e-09	1.10e-08	1.29e-08
$\alpha_{22}$ ( $i=8$ )	7.85e-08	6.16e-08	5.01e-08	4.17e-08	7.97e-08	6.62e-08	5.66e-08	4.92e-08
$\beta_2$ ( $i=9$ )	1.50e-05	1.17e-05	9.57e-06	7.95e-06	1.51e-05	1.19e-05	9.72e-06	8.06e-06
$h$ ( $i=10$ )	0.0011	0.0010	8.97e-04	7.24e-04	0.0011	0.0010	8.87e-04	6.86e-04
$Q$ ( $i=11$ )	2.53e-04	2.66e-04	2.81e-04	2.97e-04	2.53e-04	2.68e-04	2.87e-04	3.12e-04

Effects of plate thickness ratios ( $a/h$ ) with random input variables  $b_i$ , [ $\{(i=1..9), (7..9),(10) \text{ and } (11)\} = 0.10$ ] on the dimensionless expected mean ( $W_{0l}$ ) of hygrothermally induced central deflection of angle ply  $(\pm 45^\circ)_{2T}$  square laminated composite plate subjected to in-plane bi-axial compression with simple support S2 boundary conditions. Dimensionless deflection load  $Q = 100$  and fibre volume fraction ( $V_f = 0.6$ ) as shown in Table 3. It is seen that on variations of thickness ratio the mean ( $W_{0l}$ ) hygrothermal deflection decreases when thickness ratio is increased; however it is higher for TD conditions, whereas coefficient of variation ( $W_l$ ) of hygrothermal deflection decreases with different combinations of input random variables it is further higher for TD conditions as shown in Figure.4.

TABLE 3 EFFECTS OF PLATE THICKNESS RATIOS ( $A/H$ ) WITH RANDOM INPUT VARIABLES  $b_i$ , [ $\{(i=1..9), (7..9),(10) \text{ AND } (11)\} = 0.10$ ] ON THE DIMENSIONLESS EXPECTED MEAN ( $W_{0l}$ ) OF HYGROTHERMALLY INDUCED CENTRAL DEFLECTION OF ANGLE PLY  $(\pm 45^\circ)_{2T}$  SQUARE LAMINATED COMPOSITE PLATE SUBJECTED TO IN-PLANE BI-AXIAL COMPRESSION WITH SIMPLE SUPPORT S2 BOUNDARY CONDITIONS. DIMENSIONLESS DEFLECTION LOAD  $Q = 100$  AND FIBRE VOLUME FRACTION ( $V_F = 0.6$ ).

a/h	(TID)		(TD)	
	Mean, $W_{0l}$		Mean, $W_{0l}$	
	$\Delta T = 0^\circ C, \Delta C = 0.0$	$\Delta T = 100^\circ C, \Delta C = 0.01$	$\Delta T = 0^\circ C, \Delta C = 0.0$	$\Delta T = 100^\circ C, \Delta C = 0.01$
5	3.1159	2.8971	3.1210	2.9195
10	1.3280	1.1707	1.3327	1.1894
30	0.6965	0.4030	0.6996	0.4031
50	0.4965	0.1362	0.4973	0.1266

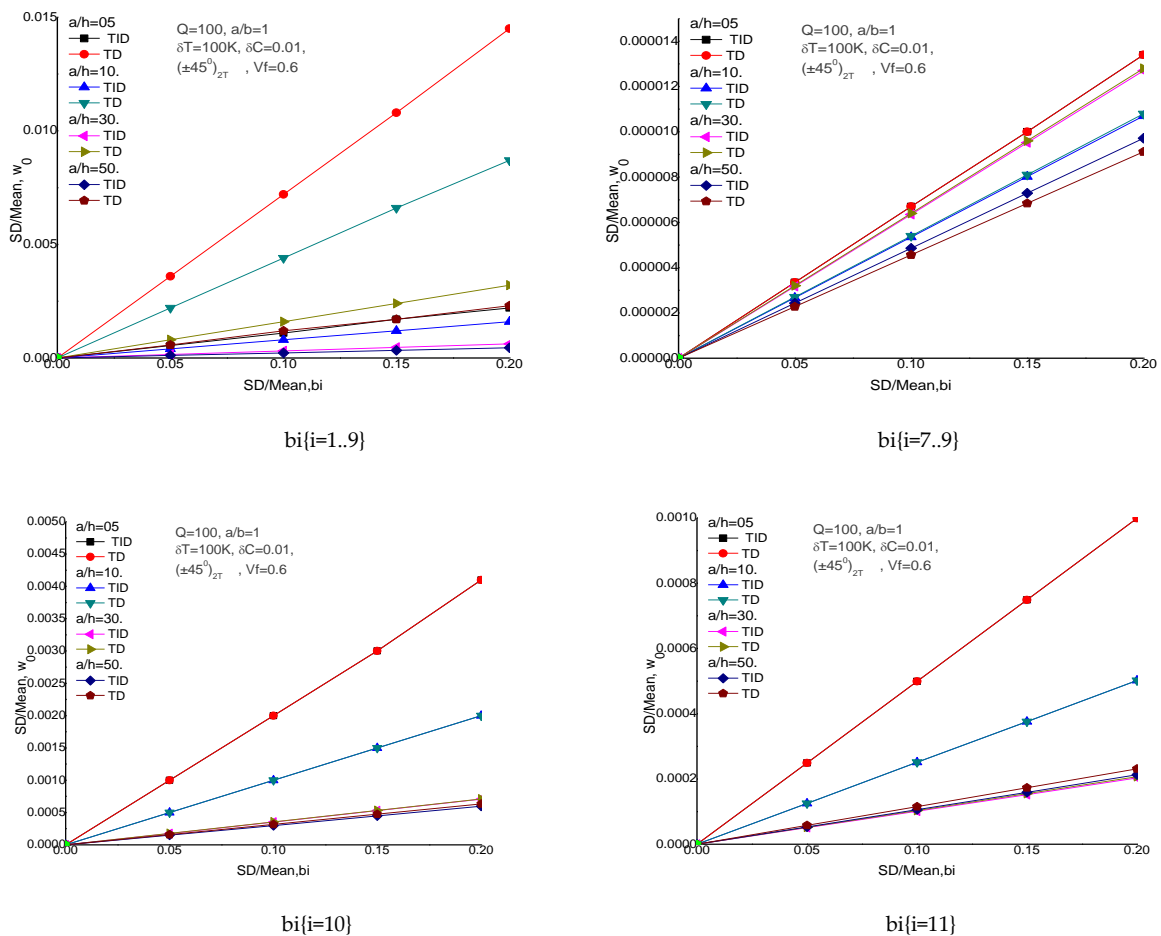


FIGURE. 4 RANDOM COV RESULTS FOR FLEXURAL RESPONSE

Table 4. Presents the effects of aspect ratios ( $a/b$ ) with random input variables  $b_i$ , [ $\{(i=1 \text{ to } 9), (7..9),(10) \text{ and } (11)\} = 0.10$ ] on the dimensionless expected mean ( $W_{0l}$ ) of hygrothermally induced central deflection of angle ply

(±450)2T laminated composite plates subjected to in-plane bi-axial compression with simple support S2 boundary conditions, plate thickness ratio (a/h=40), dimensionless deflection load Q = 100 and fibre volume fraction (Vf =0.6). It is noticed that on increase of aspect ratio the mean (W0l) hygrothermal deflection value increases whereas coefficient of variation (Wl) of hygrothermal deflection decreases for all different combinations of input random variables, mean and COV are higher for TD conditions as shown in Figure.5.

TABLE 4 EFFECTS OF ASPECT RATIOS (A/B) WITH RANDOM INPUT VARIABLES BI, [(i=1 TO 9), (7..9),(10) AND (11)] = 0.10] ON THE DIMENSIONLESS EXPECTED MEAN (W0L) OF HYGROTHERMALLY INDUCED CENTRAL DEFLECTION OF ANGLE PLY (±450)2T LAMINATED COMPOSITE PLATES SUBJECTED TO IN-PLANE BI-AXIAL COMPRESSION WITH SIMPLE SUPPORT S2 BOUNDARY CONDITIONS, PLATE THICKNESS RATIO (A/H=40), DIMENSIONLESS DEFLECTION LOAD Q = 100 AND FIBRE VOLUME FRACTION (VF =0.6).

a/b	(TID)		(TD)	
	Mean, W <sub>0l</sub>		Mean, W <sub>0l</sub>	
	ΔT= 0°C, ΔC= 0.0	ΔT =100°C, ΔC =0.01	ΔT= 0°C, ΔC= 0.0	ΔT =100°C, ΔC =0.01
1.0	0.5942	0.2480	0.5962	0.2417
1.5	1.4122	0.8405	1.4190	0.8471
2.0	2.2301	1.5071	2.2416	1.5305

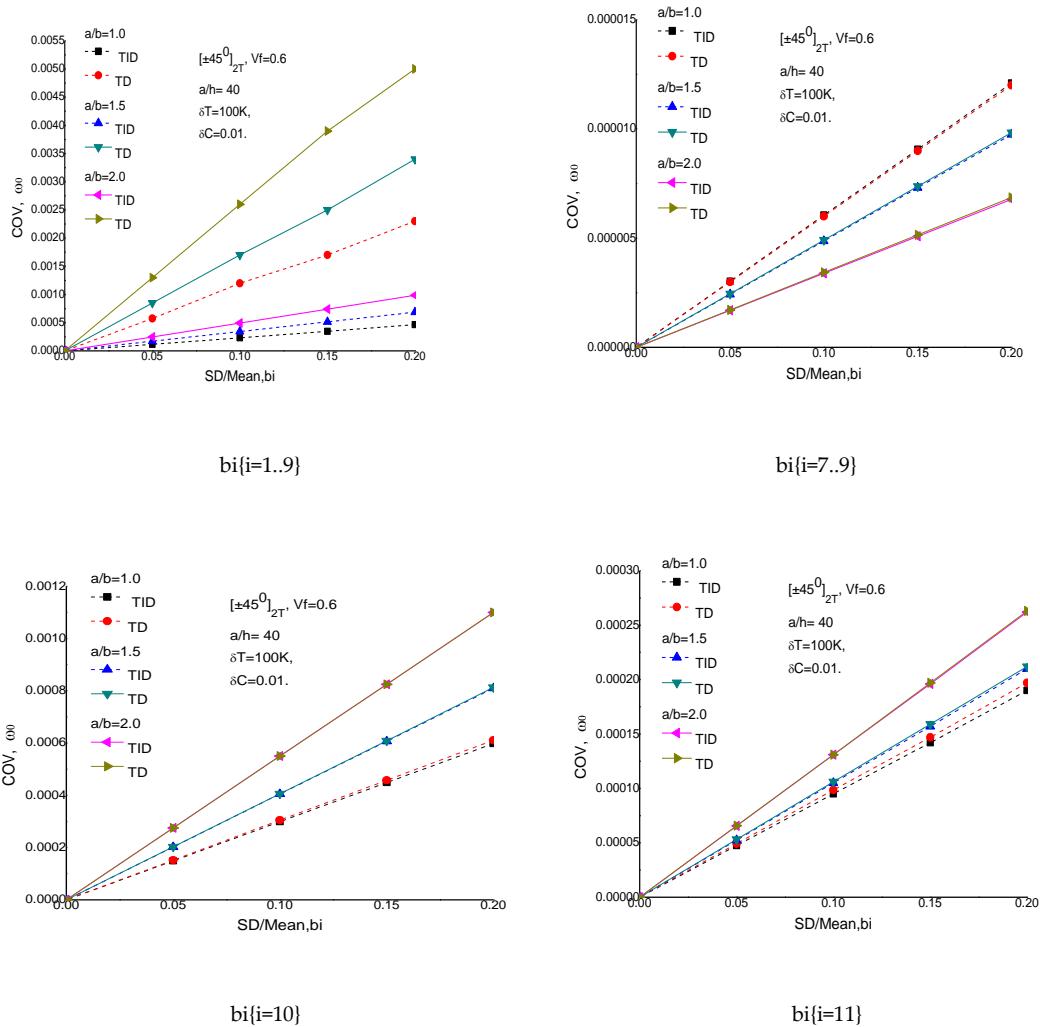


FIGURE. 5. RANDOM COV RESULTS FOR FLEXURAL RESPONSE

Effects of support conditions with random input variables bi, [(i =1 to 9), (7..9),(10) and (11)] = 0.10] on the dimensionless expected mean (W0l) of hygrothermally induced central deflection, plate thickness ratio (a/h=60), of angle ply (±450)2T laminated square composite plates subjected to in-plane bi-axial compression. Dimensionless

deflection load  $Q = 100$  and fibre volume fraction ( $V_f = 0.6$ ) is shown in Table 5. It is noticed that combined simple support and clamped support CSCS have significance effects on mean ( $W_{0l}$ ) hygrothermal deflection with different combinations of input random variables under environmental conditions. However the coefficient of variation ( $W_l$ ) of hygrothermal deflection also varies accordingly under given environmental conditions and different combinations of input random variables as shown in Figure.6.

TABLE 5 EFFECTS OF SUPPORT CONDITIONS WITH RANDOM INPUT VARIABLES  $b_i$ ,  $\{i=1 \text{ TO } 9\}$ ,  $(7..9)$ ,  $(10)$  AND  $(11) = 0.10$  ON THE DIMENSIONLESS EXPECTED MEAN ( $W_{0l}$ ) OF HYGROTHERMALLY INDUCED CENTRAL DEFLECTION, PLATE THICKNESS RATIO ( $A/H=60$ ), OF ANGLE PLY  $(\pm 45^\circ)_{2T}$  LAMINATED SQUARE COMPOSITE PLATES SUBJECTED TO IN-PLANE BI-AXIAL COMPRESSION. DIMENSIONLESS DEFLECTION LOAD  $Q = 100$  AND FIBRE VOLUME FRACTION ( $V_f = 0.6$ )

BCs	(TID)		(TD)	
	Mean, $W_{0l}$		Mean, $W_{0l}$	
	$\Delta T = 0^\circ\text{C}, \Delta C = 0.0$	$\Delta T = 100^\circ\text{C}, \Delta C = 0.01$	$\Delta T = 0^\circ\text{C}, \Delta C = 0.0$	$\Delta T = 100^\circ\text{C}, \Delta C = 0.01$
SSSS (S1)	0.3993	0.0590	0.3991	0.0481
SSSS(S2)	0.4027	0.0590	0.4026	0.0483
CCCC	0.2496	0.1785	0.2506	0.1822
CSCS	0.4468	0.4526	0.4494	0.4753

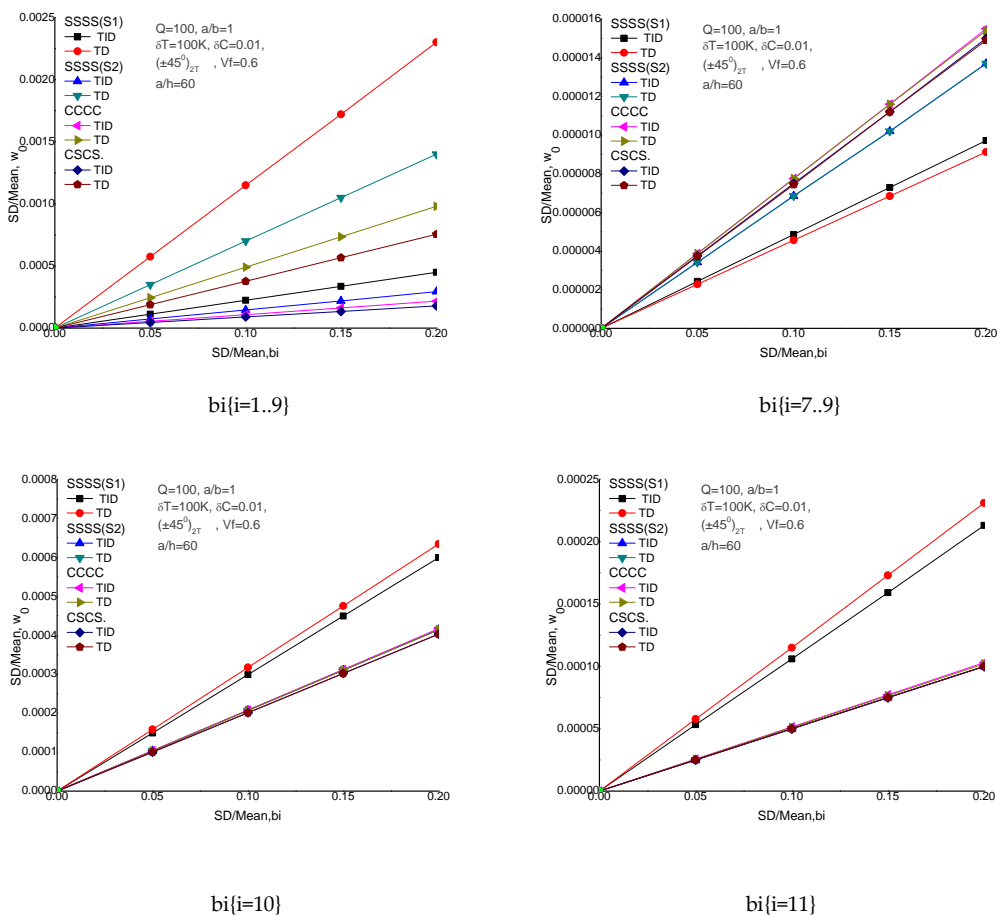


FIGURE. 6. RANDOM COV RESULTS FOR FLEXURAL RESPONSE

Table 6. Presents the effects of lamina lay-up with random input variables  $b_i$ ,  $\{i=1 \text{ TO } 9\}$ ,  $(7..9)$ ,  $(10)$  and  $(11) = 0.10$  on the dimensionless expected mean ( $W_{0l}$ ) of hygrothermally induced central deflection, plate thickness ratio ( $a/h=50$ ), dimensionless deflection load  $Q = 100$ , of laminated square composite plate, simple support S2 boundary conditions subjected to in-plane bi-axial compression and fibre volume fraction ( $V_f = 0.6$ ). It is observed that on

change of lamina layup the mean ( $W_{01}$ ) of hygrothermal central deflection increases significantly for cross ply symmetric plates and it is lower for angle ply laminates. The coefficient of variation ( $W_1$ ) of hygrothermal central deflection also decreases for different combinations of input random variables.

Effects of dimensionless load deflection ( $Q$ ) with random input variables  $bi$ ,  $\{(i=1 \text{ to } 9), (7..9), (10) \text{ and } (11)\} = 0.10$  on the dimensionless expected mean ( $W_{01}$ ) of hygrothermally induced central deflection, plate thickness ratio ( $a/h=30$ ), angle ply ( $\pm 45^\circ$ )<sub>2T</sub> laminated square composite plate, simple support S2 boundary conditions subjected in-plane bi-axial compression. fibre volume fraction ( $V_f=0.6$ ). It is seen that on increasing load deflection the mean ( $W_{01}$ ) hygrothermal central deflection increases in given environmental conditions and different combinations of input random variables are shown in Table 7. The coefficient of variation ( $W_1$ ) of hygrothermal central deflection decreases in similar conditions for both TID and TD conditions as shown in Figure 7.

TABLE 6 EFFECTS OF LAMINA LAY-UP WITH RANDOM INPUT VARIABLES  $bi$ ,  $\{(i=1 \text{ TO } 9), (7..9), (10) \text{ AND } (11)\} = 0.10$  ON THE DIMENSIONLESS EXPECTED MEAN ( $W_{01}$ ) OF HYGROTHERMALLY INDUCED CENTRAL DEFLECTION, PLATE THICKNESS RATIO ( $A/H=50$ ), DIMENSIONLESS DEFLECTION LOAD  $Q=100$ , OF LAMINATED SQUARE COMPOSITE PLATE, SIMPLE SUPPORT S2 BOUNDARY CONDITIONS SUBJECTED TO IN-PLANE BI-AXIAL COMPRESSION AND FIBRE VOLUME FRACTION ( $V_f=0.6$ ).

Lay-up	(TID)		(TD)	
	Mean, $W_{01}$		Mean, $W_{01}$	
	$\Delta T=0^\circ C, \Delta C=0.0$	$\Delta T=100^\circ C, \Delta C=0.01$	$\Delta T=0^\circ C, \Delta C=0.0$	$\Delta T=100^\circ C, \Delta C=0.01$
$(\pm 45^\circ)_{2T}$	0.4965	0.1362	0.4973	0.1266
$(\pm 45^\circ)_S$	0.6040	0.2999	0.6057	0.3013
$[0^\circ/90^\circ]_{2T}$	0.8177	0.3446	0.8190	0.3468
$[0^\circ/90^\circ]_S$	0.7343	0.3398	0.7358	0.3404

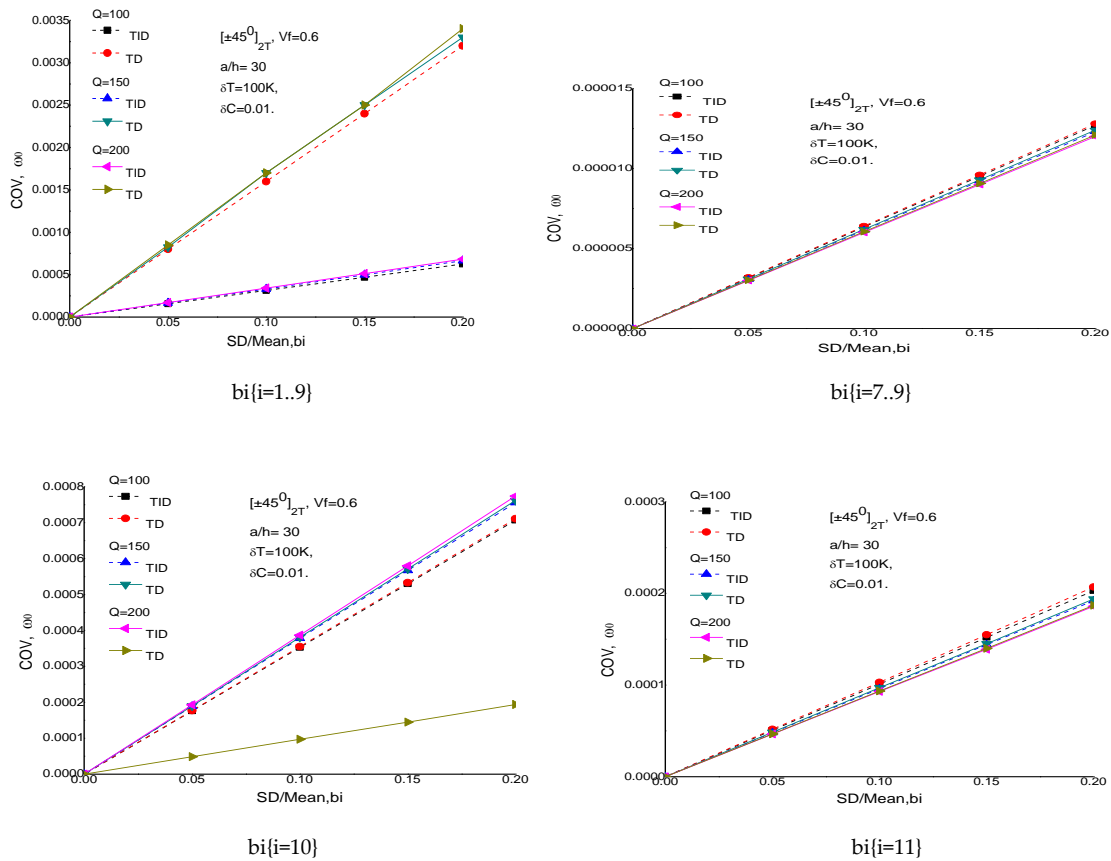


FIGURE 7. RANDOM COV RESULTS FOR FLEXURAL RESPONSE

TABLE 7 EFFECTS OF DIMENSIONLESS LOAD DEFLECTION (Q) WITH RANDOM INPUT VARIABLES BI, [(i=1 TO 9), (7..9),(10) AND (11)] = 0.10] ON THE DIMENSIONLESS EXPECTED MEAN (W0L) OF HYGROTHERMALLY INDUCED CENTRAL DEFLECTION , PLATE THICKNESS RATIO (A/H=30), ANGLE PLY (±450)2T LAMINATED SQUARE COMPOSITE PLATE, SIMPLE SUPPORT S2 BOUNDARY CONDITIONS SUBJECTED TO IN-PLANE BI-AXIAL COMPRESSION AND FIBRE VOLUME FRACTION (VF =0.6).

Q	(TID)		(TD)	
	Mean, W <sub>0l</sub>		Mean, W <sub>0l</sub>	
	ΔT= 0°C, ΔC= 0.0	ΔT =100°C, ΔC =0.01	ΔT= 0°C, ΔC= 0.0	ΔT =100°C, ΔC =0.01
100	0.6965	0.4030	0.6996	0.4031
150	1.0128	0.6211	1.0179	0.6262
200	1.3158	0.8354	1.3228	0.8457

Shows the effects of fibre volume fraction (Vf) with random input variables bi, [(i=1 to 9), (7..9),(10) and (11)] = 0.10] on the dimensionless expected mean (W0l) of hygrothermally induced central deflection of angle ply(±450)2T laminated composite plates subjected to in-plane bi-axial compression with simple support S2 boundary conditions , plate thickness ratio (a/h=40) and dimensionless deflection load(Q) =100. It is observed that on varying fibre matrix volume fraction the mean (W0l) hygrothermal central deflection increases in given environmental conditions and different combinations of input random variables whereas the value of coefficient of variation (Wl) of hygrothermal central deflection also varies in similar conditions for both TID and TD conditions as shown in Figure 8.

TABLE 8 EFFECTS OF FIBRE VOLUME FRACTION (VF) WITH RANDOM INPUT VARIABLES BI, [(i=1 TO 9), (7..9),(10) AND (11)] = 0.10] ON THE DIMENSIONLESS EXPECTED MEAN (W0L) OF HYGROTHERMALLY INDUCED CENTRAL DEFLECTION OF ANGLE PLY (±450)2T LAMINATED SQUARE COMPOSITE PLATE SUBJECTED TO IN-PLANE BI-AXIAL COMPRESSION , PLATE THICKNESS RATIO (A/H=40) AND DIMENSIONLESS DEFLECTION LOAD(Q) =100.

V <sub>f</sub>	(TID)		(TD)	
	Mean, W <sub>0l</sub>		Mean, W <sub>0l</sub>	
	ΔT= 0°C, ΔC= 0.0	ΔT =100°C, ΔC =0.01	ΔT= 0°C, ΔC= 0.0	ΔT =100°C, ΔC =0.01
0.50	0.5518	0.2224	0.5533	0.2145
0.55	0.5681	0.2326	0.5699	0.2255
0.60	0.5942	0.2480	0.5962	0.2417
0.65	0.6327	0.2699	0.6349	0.2645
0.70	0.6878	0.3001	0.6904	0.2959

Effects of temperature and moisture rise (ΔT, ΔC) , with random input variables bi, [(i=1 to 9), (7..9),(10) and (11)] = 0.10] on the dimensionless expected mean (W0l) of central deflection, fibre volume fraction (Vf=0.6), plate thickness ratio (a/h=20), dimensionless deflection load(Q) =150, of angle ply (±450)2T laminated square composite plate subjected to uniform constant temperature and moisture (U.T) with in-plane bi-axial compression are shown in Table 9. It is noticed that on increasing temperature and moisture the mean (W0l) hygrothermal central deflection decreases in given environmental conditions and different combinations of input random variables whereas the value of coefficient of variation (Wl) of hygrothermal central deflection increases in similar conditions as shown in Figure 9.

TABLE 9 EFFECTS OF TEMPERATURE AND MOISTURE RISE (ΔT, ΔC) WITH RANDOM INPUT VARIABLES BI, [(i=1 TO 9), (7..9),(10) AND (11)] = 0.10] ON THE DIMENSIONLESS EXPECTED MEAN (W0L) OF HYGROTHERMALLY INDUCED CENTRAL DEFLECTION, FIBRE VOLUME FRACTION (VF=0.6), PLATE THICKNESS RATIO (A/H=20), DIMENSIONLESS DEFLECTION LOAD(Q) =150, OF ANGLE PLY (±450)2T LAMINATED SQUARE COMPOSITE PLATE SUBJECTED TO UNIFORM CONSTANT TEMPERATURE AND MOISTURE (U.T) WITH IN-PLANE BI-AXIAL COMPRESSION.

Environmental conditions	Mean, W <sub>0l</sub>	
	(TID)	(TD)
ΔT= 0°C, ΔC= 0.0	1.1548	1.1612
ΔT=100°C, ΔC= 0.01	0.8754	0.8928
ΔT=200°C, ΔC= 0.02	0.6860	0.7023
ΔT= 300°C, ΔC= 0.03	0.5481	0.5581
ΔT= 400°C, ΔC= 0.04	0.4424	0.4431
ΔT= 500°C, ΔC= 0.05	0.3578	0.3477

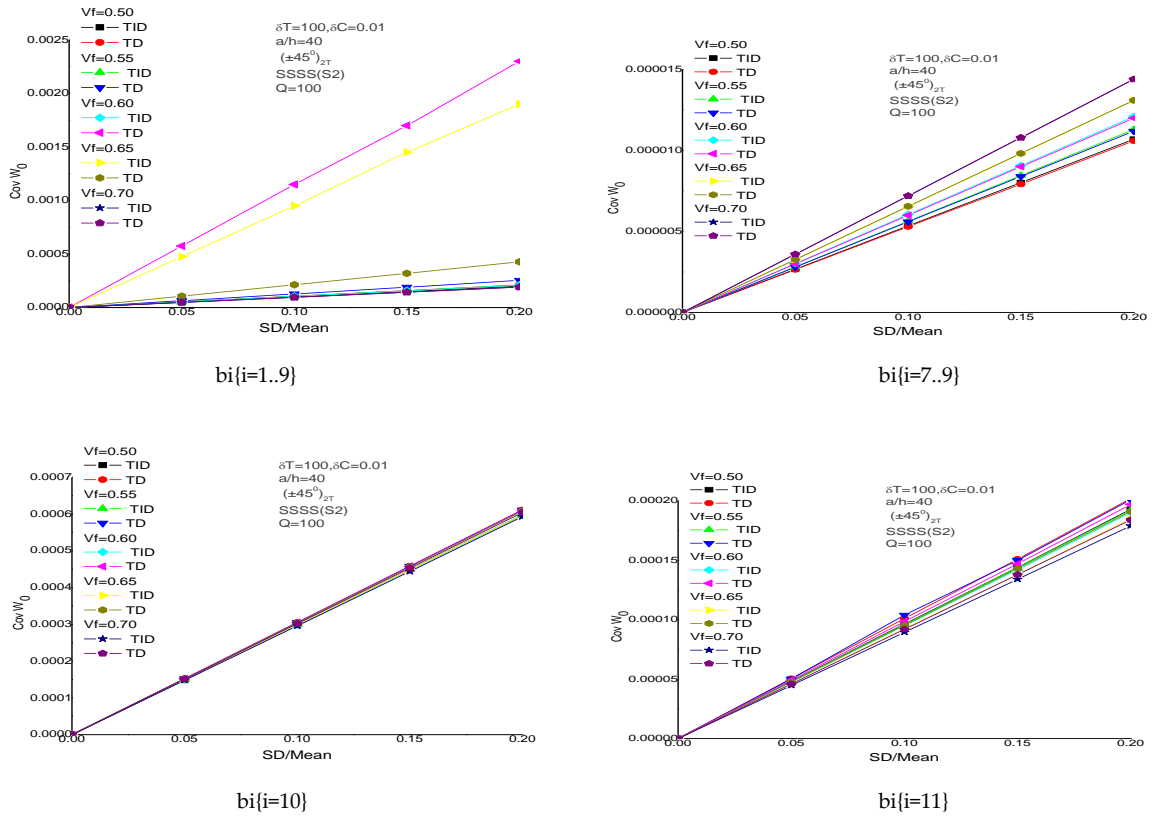


FIGURE 8. RANDOM COV RESULTS FOR FLEXURAL RESPONSE

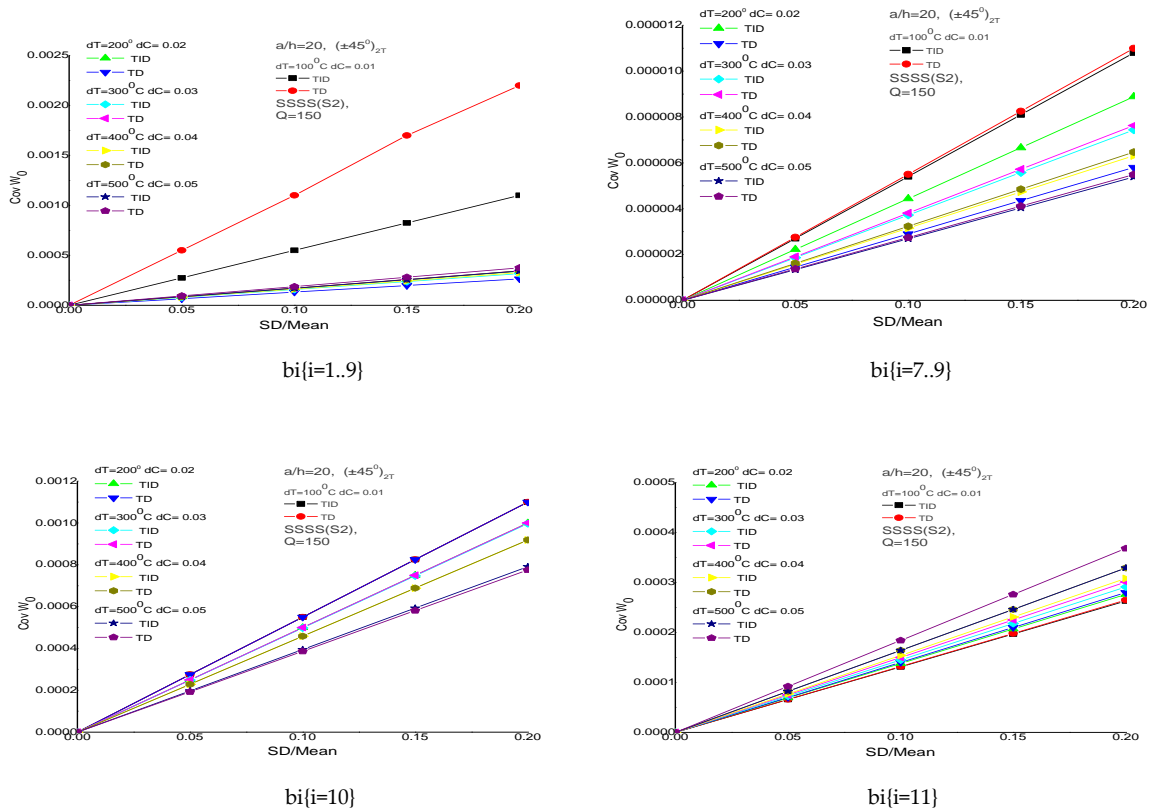


FIGURE 9. RANDOM COV RESULTS FOR FLEXURAL RESPONSE

**Validation Study for Mean Hygrothermal Free Vibration Load**

Table 10. Shows the comparison of dimensionless fundamental frequency ( $\omega_1$ ) for perfect (00/900)2T laminated square plates plate thickness ratio ( $a/h=20$ ), aspect ratio ( $a/b=1.0$ ), where  $a=0.1$ ,  $b=0.1$ , initial temperature ( $T_0=250C$ ), simple support S2 under environmental conditions with biaxial compression.. The results are compared with semi analytical method of Huang et al. [16] to show the performance of the present formulation. It is obvious from the result that present C0 FEM using HSDT approach yields an improved accuracy over semi analytical HSDT of Huang et al. [2004]. Also the convergence of present results is found to be excellent.

TABLE 10 COMPARISON OF DIMENSIONLESS FUNDAMENTAL FREQUENCY ( $\omega_1$ ) FOR PERFECT (00/900)2T LAMINATED SQUARE PLATES. PLATE THICKNESS RATIO ( $A/H=20$ ), ASPECT RATIO ( $A/B=1.0$ ), WHERE  $A=0.1$ ,  $B=0.1$ , INITIAL TEMPERATURE ( $T_0=250C$ ), SIMPLE SUPPORT S2 UNDER ENVIRONMENTAL CONDITIONS WITH BIAxIAL COMPRESSION.

Lay-up	Environmental Conditions	$(\omega_1) = \omega a^2 \sqrt{(Q_0/E_{22}/ h^2)}$ .					
		Hung et al. [2004]			Present [HSDT]		
		$V_f=0.5$	$V_f=0.6$	$V_f=0.7$	$V_f=0.5$	$V_f=0.6$	$V_f=0.7$
(0°/90°)2T	$\Delta T=0^\circ C, \Delta C=0\%$	9.865	10.587	11.331	9.475	10.369	11.319
	$\Delta T=100^\circ C, C=1\%$	8.978	9.704	10.399	9.076	9.970	10.885
	$\Delta T=200^\circ C, C=3\%$	7.813	8.502	9.074	7.707	8.169	8.406

**Validation Study for Random Hygrothermal Free Vibration Load**

Comparison for present [FOPT] with present [MCS] for material property ( $E_{11}$ ) plate thickness ratio ( $a/h=30$ ), aspect ratio ( $a/b=1$ ), dimensionless expected mean ( $W_0$ ) TID=8.6002, TD=8.3419,  $\Delta T=1000C$ ,  $\Delta C=1\%$ , simple support SSSS (S2), cross ply (0/900)2T, fiber volume fraction ( $V_f=0.6$ ), for geometric property ( $h$ ) plate thickness ratio ( $a/h=30$ ), dimensionless expected mean ( $W_0$ ) TID =18.4662, TD=17.5438  $\Delta T=2000C$ ,  $\Delta C=3\%$ , . Present [FOPT] results are in good agreement with present [MCS] results as shown in Figure 10.

Table 11(a) and (b). Show the effects of individual random variables  $b_i$ ,  $\{(i = 1 \text{ to } 10) = 0.10\}$  on the dimensionless expected mean ( $\omega_1$ ) and coefficient of variation ( $\omega_1^2$ ) of the fundamental frequency of perfect cross ply (00/900)2T laminated composite square plates, plate thickness ratio ( $a/h=10$ ), fiber volume fraction( $V_f=0.6$ ), initial temperature ( $T_0=250C$ ), simple support (S2) under environmental conditions . The dimensionless expected mean fundamental frequency ( $\omega_1$ ) is given in brackets. All edges simply supported boundary condition subjected to uniform moisture & temperature change with temperature & moisture independent and dependent material properties. It is observed that for the same fiber volume fraction the fundamental frequency is most affected by random change in  $E_{11}$  and  $v_{12}$ . Tight control of these parameters is therefore required if high reliability of the plate is desired.

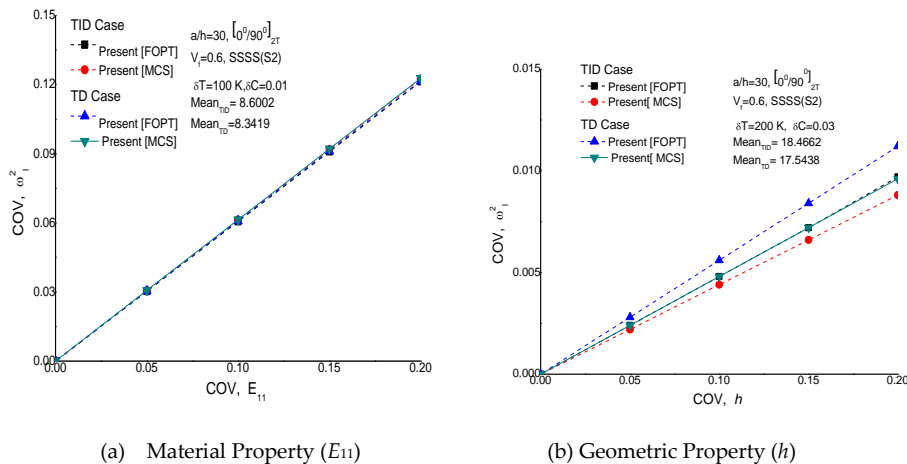


FIGURE 10. COMPARISON OF THE PRESENT [DISFEM] RESULT WITH INDEPENDENT MONTE CARLO SIMULATION RESULTS FREE VIBARTION RESPONSE

TABLE 11 (A) EFFECTS OF THE VARIATION OF INDIVIDUAL RANDOM SYSTEM PROPERTY  $b_i$ ,  $\{i=1 \text{ TO } 10\} = 0.10\}$  ON THE DIMENSIONLESS EXPECTED MEAN ( $\omega_1$ ) AND COEFFICIENT OF VARIATION ( $\omega_2$ ) OF THE FUNDAMENTAL FREQUENCY OF PERFECT CROSS PLY [00/900]2T LAMINATED COMPOSITE SQUARE PLATES, PLATE THICKNESS RATIO ( $A/H=10$ ), FIBER VOLUME FRACTION( $V_f=0.6$ ), INITIAL TEMPERATURE ( $T_0=250C$ ), SIMPLE SUPPORT (S2) UNDER ENVIRONMENTAL CONDITIONS.

$b_i$	(TID)			
	$COV, \omega^2$	$COV, \omega^2$	$COV, \omega^2$	$COV, \omega^2$
	$\Delta T=0^\circ C, \Delta C=0\%$	$\Delta T=100^\circ C, \Delta C=1\%$	$\Delta T=200^\circ C, \Delta C=3\%$	$\Delta T=300^\circ C, \Delta C=5\%$
$E_{11} (i=1)$	$(\omega_1=8.9741) 0.0545$	$(\omega_1=8.9533) 0.0553$	$(\omega_1=8.7437) 0.0584$	$(\omega_1=8.5511) 0.0615$
$E_{22} (i=2)$	0.0179	0.0011	1.5599e-04	4.5393e-05
$G_{12}(i=3)$	0.0038	0.0039	0.0041	0.0043
$G_{13} (i=4)$	0.0214	0.0218	0.0225	0.0237
$G_{23} (i=5)$	0.0107	0.0109	0.0113	0.0119
$V_{12} (i=6)$	0.8084	0.0577	0.0104	0.0040
$\alpha_{11} (i=7)$	4.1753e-05	2.9997e-04	7.3495e-04	0.0014
$\alpha_{22} (i=8)$	4.5590e-04	0.0021	0.0036	0.0049
$\beta_{22} (i=9)$	0.0015	0.0074	0.0127	0.0172
$h (i=10)$	0.0111	0.0115	0.0122	0.0133

TABLE 11 (B) EFFECTS OF THE VARIATION OF INDIVIDUAL RANDOM SYSTEM PROPERTY  $b_i$ ,  $\{i=1 \text{ TO } 10\} = 0.10\}$  ON THE DIMENSIONLESS EXPECTED MEAN ( $\omega_1$ ) AND COEFFICIENT OF VARIATION ( $\omega_2$ ) OF THE FUNDAMENTAL FREQUENCY OF PERFECT CROSS PLY [00/900]2T LAMINATED COMPOSITE SQUARE PLATES, PLATE THICKNESS RATIO ( $A/H=10$ ), FIBER VOLUME FRACTION( $V_f=0.6$ ), INITIAL TEMPERATURE ( $T_0=250C$ ), SIMPLE SUPPORT (S2) UNDER ENVIRONMENTAL CONDITIONS.

$b_i$	(TD)			
	$COV, \omega^2$	$COV, \omega^2$	$COV, \omega^2$	$COV, \omega^2$
	$\Delta T=0^\circ C, \Delta C=0\%$	$\Delta T=100^\circ C, \Delta C=1\%$	$\Delta T=200^\circ C, \Delta C=3\%$	$\Delta T=300^\circ C, \Delta C=5\%$
$E_{11} (i=1)$	$(\omega_1=8.9324)0.0546$	$(\omega_1=8.7409) 0.0555$	$(\omega_1=8.3600) 0.0590$	$(\omega_1=7.9892) 0.0625$
$E_{22} (i=2)$	0.0091	0.0058	5.2485e-04	1.4063e-04
$G_{12}(i=3)$	0.0039	0.0041	0.0045	0.0049
$G_{13} (i=4)$	0.0213	0.0214	0.0216	0.0219
$G_{23} (i=5)$	0.0107	0.0107	0.0108	0.0110
$V_{12} (i=6)$	0.0409	0.0302	0.0033	0.0011
$\alpha_{11} (i=7)$	4.2135e-05	3.1344e-04	7.9352e-04	0.0015
$\alpha_{22} (i=8)$	4.6285e-04	0.0023	0.0041	0.0059
$\beta_{22} (i=9)$	0.0016	0.0075	0.0130	0.0179
$h (i=10)$	0.0112	0.0119	0.0131	0.0145

Table 12(a) and (b). Present the effect of boundary conditions and input random variables  $b_i\{i=1\dots 9, 7-8, 9 \text{ and } 10=0.10\}$  on the dimensionless expected mean( $\omega_1$ ) and coefficient of variation ( $\omega_2$ ) of fundamental frequency of perfect cross ply (00/900)2T laminated composite square plates, plate thickness ratio ( $a/h=20$ ), fiber volume fraction ( $V_f=0.6$ ), initial temperature ( $T_0=250C$ ) under environmental conditions. It is observed that for temperature and moisture independent material properties without rise in moisture and temperature condition expected mean and coefficient of variation of fundamental frequency is significantly affected when the plate is clamped supported compared to other supports. On rising moisture and temperature there is decrease in expected mean and coefficient of variation of fundamental frequency. For temperature and moisture dependent material properties, there is further decrease in expected mean of fundamental frequency for both without and with rise in moisture and temperature conditions and different sets of random input variables as shown in Figure 11.

TABLE 12(A) EFFECT OF BOUNDARY CONDITIONS AND INPUT RANDOM VARIABLES  $bi$  ( $i=1\dots 9, 7-8, 9$  AND  $10=0.10$ ) ON THE DIMENSIONLESS EXPECTED MEAN ( $\omega_1$ ) AND COEFFICIENT OF VARIATION ( $\omega_1^2$ ) OF THE FUNDAMENTAL FREQUENCY OF PERFECT CROSS PLY  $[00/900]_{2T}$  LAMINATED COMPOSITE SQUARE PLATES, PLATE THICKNESS RATIO ( $A/H=20$ ), FIBER VOLUME FRACTION ( $V_f=0.6$ ), INITIAL TEMPERATURE ( $T_0=250C$ ), SIMPLE SUPPORT ( $S_2$ ) UNDER ENVIRONMENTAL CONDITIONS.

BCs	(TID)									
	$\Delta T=0^{\circ}C, \Delta C=0\%$					$\Delta T=200^{\circ}C, \Delta C=3\%$				
	Mean ( $\omega_1$ )	COV, $\omega_1^2$				Mean ( $\omega_1$ )	COV, $\omega_1^2$			
		bi					bi			
(i=1....9)		(i=7.-8)	(i=9)	(i=10)	(i=1... 9)		(i=7.-8)	(i=9)	(i=10)	
SSSS S1	10.9518	0.1075	0.0012	0.0040	0.0213	7.3899	0.1813	0.0207	0.0663	0.0442
SSSS S2	10.3699	0.1258	0.0014	0.0045	0.0276	8.1692	0.1313	0.0169	0.0540	0.0443
CCCC	19.5079	0.0913	4.37e-04	0.0014	0.0140	17.3812	0.0787	0.0043	0.0138	0.0178
CSCS	14.7273	0.1058	7.53e-04	0.0024	0.0097	12.8666	0.0923	0.0077	0.0246	0.0126

TABLE 12(B) EFFECT OF BOUNDARY CONDITIONS AND INPUT RANDOM VARIABLES  $bi$  ( $i=1\dots 9, 7-8, 9$  AND  $10=0.10$ ) ON THE DIMENSIONLESS EXPECTED MEAN ( $\omega_1$ ) AND COEFFICIENT OF VARIATION ( $\omega_1^2$ ) OF THE FUNDAMENTAL FREQUENCY OF PERFECT CROSS PLY  $[00/900]_{2T}$  LAMINATED COMPOSITE SQUARE PLATES, PLATE THICKNESS RATIO ( $A/H=20$ ), FIBER VOLUME FRACTION ( $V_f=0.6$ ), INITIAL TEMPERATURE ( $T_0=250C$ ), SIMPLE SUPPORT ( $S_2$ ) UNDER ENVIRONMENTAL CONDITIONS.

BCs	(TD)									
	$\Delta T=0^{\circ}C, \Delta C=0\%$					$\Delta T=200^{\circ}C, \Delta C=3\%$				
	Mean ( $\omega_1$ )	COV, $\omega_1^2$				Mean ( $\omega_1$ )	COV, $\omega_1^2$			
		bi					bi			
(i=1....9)		(i=7.-8)	(i=9)	(i=10)	(i=1.. 9)		(i=7.-8)	(i=9)	(i=10)	
SSSS S1	10.8924	0.0847	0.0013	0.0040	0.0213	6.6662	0.2032	0.0267	0.0768	0.0488
SSSS S2	10.3147	0.0893	0.0014	0.0045	0.0276	7.7014	0.1346	0.0199	0.0571	0.0455
CCCC	19.4194	0.0696	4.44e-04	0.0014	0.0141	16.5062	0.0805	0.0050	0.0145	0.0190
CSCS	14.6547	0.0779	7.65e-04	0.0025	0.0097	12.2297	0.0936	0.0089	0.0256	0.0136

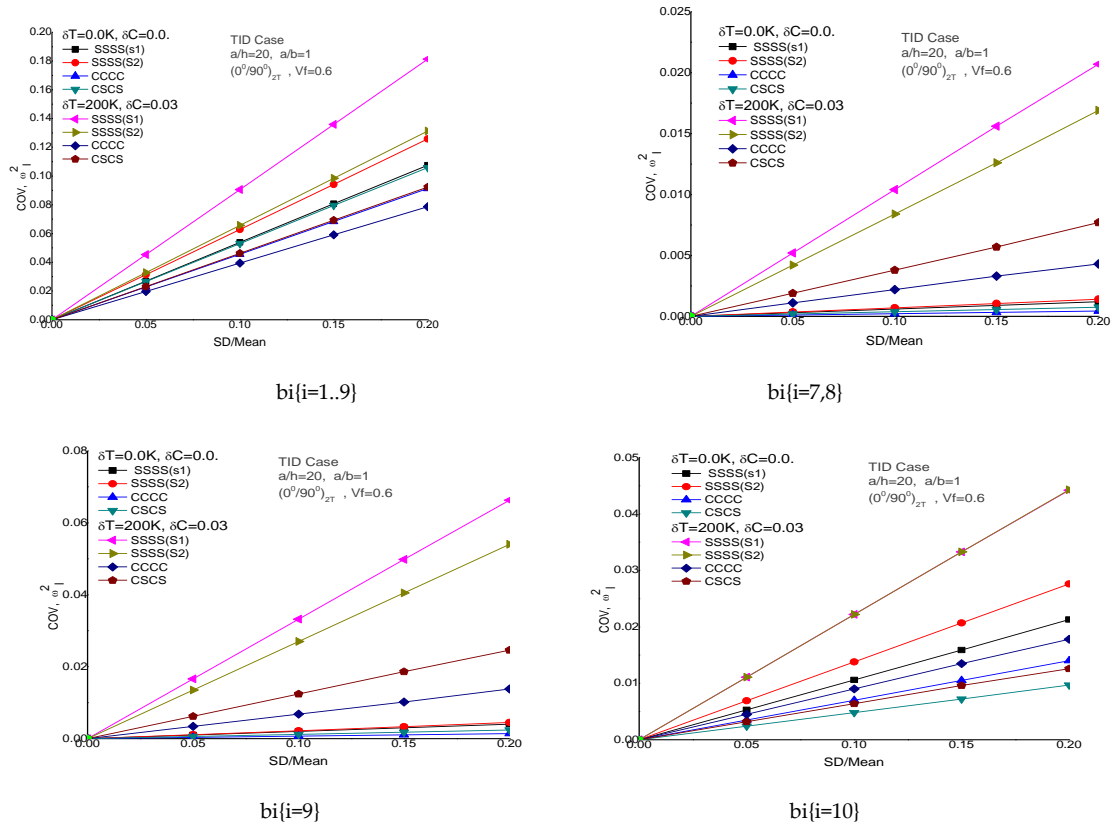


FIGURE 11. RANDOM COV RESULTS FOR FREE RESPONSE

Table 13 (a) and (b). show the effect of plate thickness ratio ( $a/h$ ) and input random variables  $bi$  ( $i=1\dots 9, 7-8, 9$  and  $10=0.10$ ) on the expected mean ( $\omega$ ) and coefficient of variation ( $\omega^2$ ) of fundamental frequency of perfect cross ply (00/900)2T laminated composite square plates, fiber volume fraction ( $V_f=0.6$ ), initial temperature ( $T_0=250C$ ) under environmental conditions. It is seen that for temperature and moisture independent material properties there is drastic change in expected mean and coefficient of variations of fundamental frequency when plate is exposed to moisture and temperature conditions. However for temperature and moisture dependent material properties there is decrease in expected mean and coefficient of variations of fundamental frequency with different combinations of random input variables as shown in Figure 12.

TABLE 13(A)EFFECT OF PLATE THICKNESS RATIO (A/H) AND INPUT RANDOM VARIABLES  $bi$  ( $i=1\dots 9, 7-8, 9$  AND  $10=0.10$ ) ON THE EXPECTED MEAN ( $\omega$ ) AND COEFFICIENT OF VARIATION ( $\omega^2$ ) OF THE FUNDAMENTAL FREQUENCY OF PERFECT CROSS PLY [00/900]2T LAMINATED COMPOSITE SQUARE PLATES, FIBER VOLUME FRACTION ( $V_f=0.6$ ), INITIAL TEMPERATURE ( $T_0=250C$ ) UNDER ENVIRONMENTAL CONDITIONS.

(a/h)	(TID)									
	Mean ( $\omega$ )	$\Delta T=0^\circ C, \Delta C=0\%$				$\Delta T=200^\circ C, \Delta C=3\%$				Mean ( $\omega$ )
		COV, $\omega^2$				COV, $\omega^2$				
		bi				bi				
(i=1-9)	(i=7-8)	(i=9)	(i=10)	(i=1-9)	(i=7-8)	(i=9)	(i=10)			
5	6.4020	0.0801	2.24e-04	7.29e-04	0.0049	6.3686	0.0561	0.0017	5.51e-04	0.0046
10	8.9741	0.1021	4.57e-04	0.0015	0.0111	8.7437	0.0638	0.0037	0.0012	0.0122
50	10.9618	0.1386	0.0077	0.0251	0.0346	8.5356	0.0468	0.04681	0.0150	0.0339
100	11.0246	0.1754	0.0306	0.0994	0.0369	51.9425	0.0539	0.0532	0.0161	0.0184

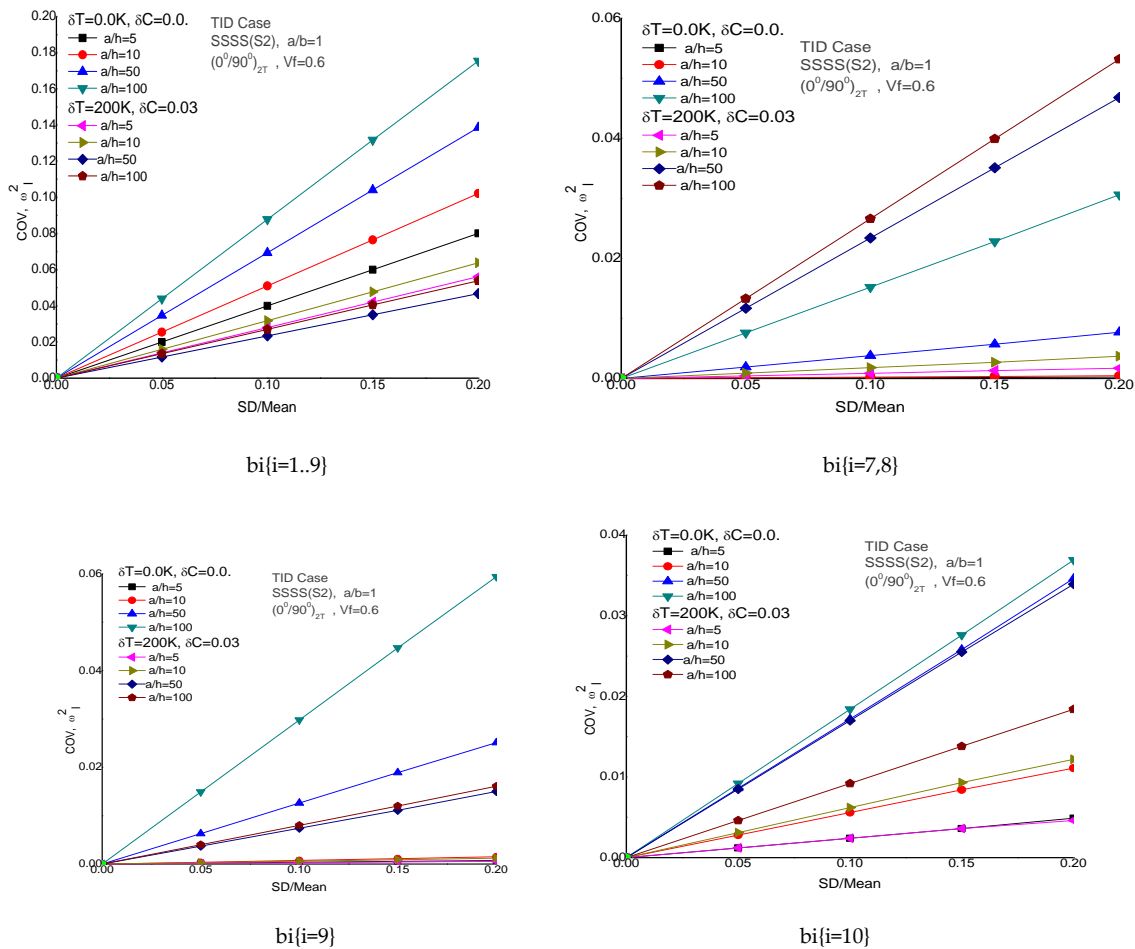


FIGURE 12. RANDOM COV RESULTS FOR FREE RESPONSE

TABLE 13(B) EFFECT OF PLATE THICKNESS RATIO (A/H) AND INPUT RANDOM VARIABLES  $b_i$  ( $i=1..9, 7-8, 9$  AND  $10=0.10$ ) ON THE EXPECTED MEAN ( $\omega_1$ ) AND COEFFICIENT OF VARIATION ( $\omega_1^2$ ) OF THE FUNDAMENTAL FREQUENCY OF PERFECT CROSS PLY  $[00/900]_2T$  LAMINATED COMPOSITE SQUARE PLATES, FIBER VOLUME FRACTION ( $V_f=0.6$ ), INITIAL TEMPERATURE ( $T_0=250C$ ) UNDER ENVIRONMENTAL CONDITIONS.

(a/h)	(TD)									
	$\Delta T=0^{\circ}C, \Delta C=0\%$					$\Delta T=200^{\circ}C, \Delta C=3\%$				
	Mean ( $\omega_1$ )	COV, $\omega_1^2$				Mean ( $\omega_1$ )	COV, $\omega_1^2$			
		$b_i$					$b_i$			
	(i=1-9)	(i=7-8)	(i=9)	(i=10)		(i=1-9)	(i=7-8)	(i=9)	(i=10)	
5	6.3787	0.0626	2.27e-04	7.29e-05	0.0049	6.1516	0.0557	0.0019	5.55e-04	0.0044
10	8.9324	0.0729	4.64e-04	1.49e-04	0.0112	8.3600	0.0641	0.0042	0.0012	0.0131
50	10.9005	0.0971	0.0079	0.0025	0.0346	8.0246	1.6119	0.2464	0.0699	0.5559
100	10.9601	0.1058	0.0312	0.0100	0.0369	49.3517	0.4925	0.0512	0.0137	0.2087

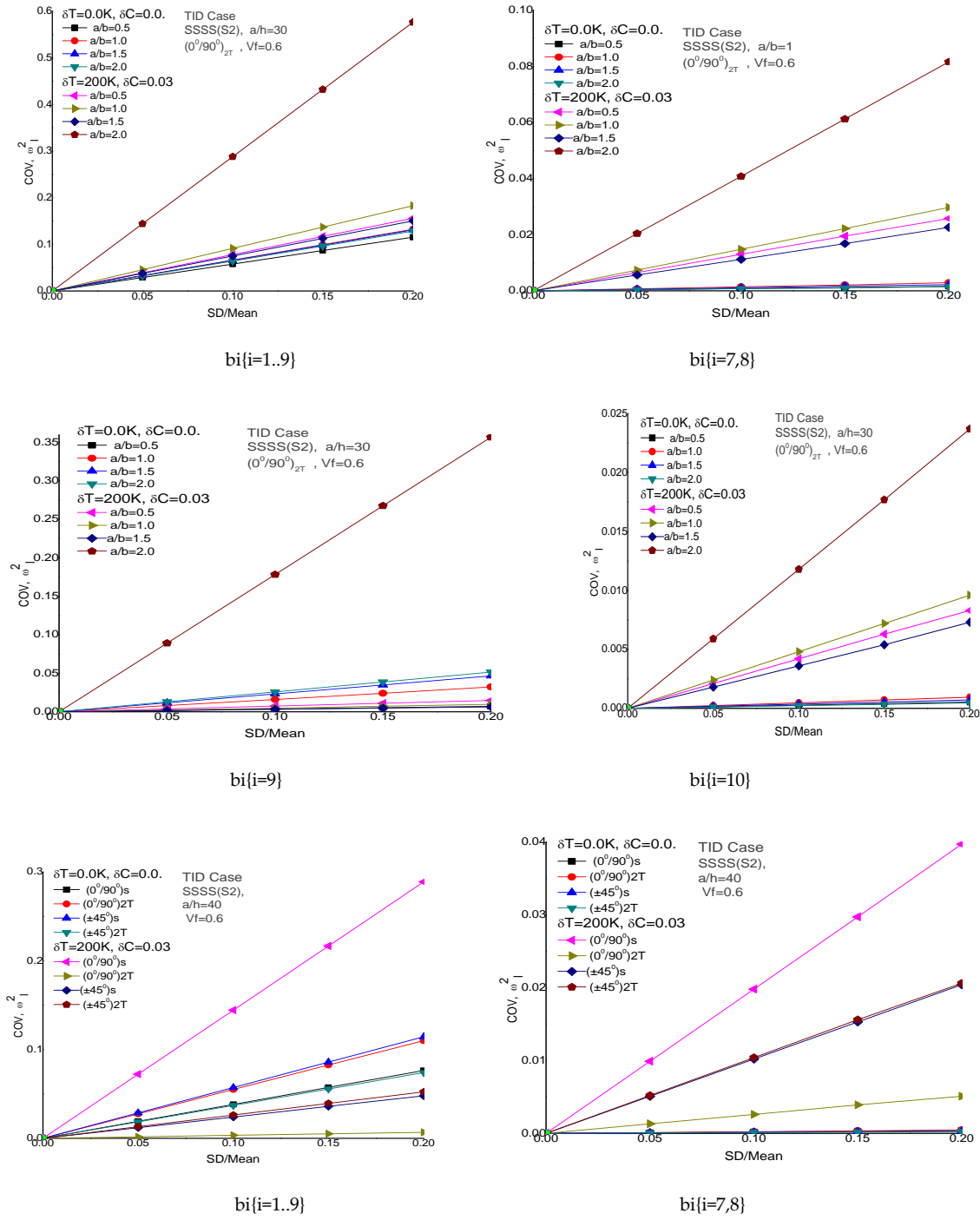


FIGURE 13. RANDOM COV RESULTS FOR FREE RESPONSE

Table 14(a) and (b). Effect of aspect ratio (a/b) and input random variables  $b_i$  ( $i=1\dots 9, 7-8, 9$  and  $10=0.10$ ) on the expected mean ( $\omega_1$ ) and coefficient of variation ( $\omega_2$ ) of fundamental frequency of perfect cross ply (00/900)2T laminated composite plates, plate thickness ratio ( $a/h=30$ ), fiber volume fraction ( $V_f=0.6$ ), initial temperature ( $T_0=250C$ ), simple support S2 under environmental conditions. It is seen that aspect ratio significantly affects the expected mean and coefficient of variation of fundamental frequency when plate is without moisture and temperature exposure. When the plate is exposed to moisture and temperature there is drastic change in expected mean fundamental frequency besides slight rise in coefficient of variation for aspect ratio (1.5). The plate with temperature and moisture dependent material properties there is slight change in expected mean and coefficient of variation of fundamental frequency with different combinations of random input variables as shown in Figure 13.

TABLE 14(A) EFFECT OF ASPECT RATIOS (A/B) AND INPUT RANDOM VARIABLES  $b_i$  ( $i=1\dots 9, 7-8, 9$  AND  $10=0.10$ ) ON THE EXPECTED MEAN ( $\omega_1$ ) AND COEFFICIENT OF VARIATION ( $\omega_2$ ) OF THE FUNDAMENTAL FREQUENCY OF PERFECT CROSS PLY [00/900]2T LAMINATED COMPOSITE SQUARE PLATES, PLATE THICKNESS RATIO (A/H=30), FIBER VOLUME FRACTION ( $V_f=0.6$ ), INITIAL TEMPERATURE ( $T_0=250C$ ), SIMPLE SUPPORT (S2) UNDER ENVIRONMENTAL CONDITIONS.

a/ b	(TID)									
	$\Delta T=0^\circ C, \Delta C=0\%$					$\Delta T=200^\circ C, \Delta C=3\%$				
	Mean ( $\omega_1$ )	COV, $\omega_2$				Mean ( $\omega_1$ )	COV, $\omega_2$			
		b <sub>i</sub>					b <sub>i</sub>			
(i=1-9)		(i=7-8)	(i=9)	(i=10)	(i=1-9)		(i=7-8)	(i=9)	(i=10)	
0.5	7.1611	0.1154	0.0016	5.28e-04	0.0071	4.9307	0.1561	0.0258	0.0083	0.0148
1.0	10.7297	0.1325	0.0029	9.42e-04	0.0322	18.4662	0.1829	0.0297	0.0096	0.0097
1.5	18.5549	0.1310	0.0022	7.09e-04	0.0465	48.3038	0.1504	0.0226	0.0073	0.0063
2.0	30.6824	0.1284	0.0015	4.61e-04	0.0515	11.7417	0.5765	0.0816	0.0237	0.3565

TABLE 14(B) EFFECT OF ASPECT RATIOS (A/B) AND INPUT RANDOM VARIABLES  $b_i$  ( $i=1\dots 9, 7-8, 9$  AND  $10=0.10$ ) ON THE EXPECTED MEAN ( $\omega_1$ ) AND COEFFICIENT OF VARIATION ( $\omega_2$ ) OF THE FUNDAMENTAL FREQUENCY OF PERFECT CROSS PLY [00/900]2T LAMINATED COMPOSITE SQUARE PLATES, PLATE THICKNESS RATIO (A/H=30), FIBER VOLUME FRACTION ( $V_f=0.6$ ), INITIAL TEMPERATURE ( $T_0=250C$ ), SIMPLE SUPPORT (S2) UNDER ENVIRONMENTAL CONDITIONS.

a/b	(TD)									
	$\Delta T=0^\circ C, \Delta C=0\%$					$\Delta T=200^\circ C, \Delta C=3\%$				
	Mean ( $\omega_1$ )	COV, $\omega_2$				Mean ( $\omega_1$ )	COV, $\omega_2$			
		b <sub>i</sub>					b <sub>i</sub>			
(i=1-9)		(i=7-8)	(i=9)	(i=10)	(i=1-9)		(i=7-8)	(i=9)	(i=10)	
0.5	7.1236	0.0850	0.0016	5.30e-004	0.0072	4.6075	0.1628	0.0309	0.0090	0.0165
1.0	10.6707	0.0940	0.0030	9.46e-004	0.0322	17.5438	0.1846	0.0344	0.0100	0.0112
1.5	18.4519	0.0948	0.0022	7.12e-004	0.0465	46.9859	0.1454	0.0250	0.0073	0.0075
2.0	30.5108	0.0950	0.0015	4.63e-004	0.0515	11.5511	0.5377	0.0876	0.0232	0.0330

Table 15(a) and (b). Effect of lay-up and input random variables  $b_i$  ( $i=1\dots 9, 7-8, 9$  and  $10=0.10$ ) on the expected mean ( $\omega_1$ ) and coefficient of variation ( $\omega_2$ ) of fundamental frequency of laminated composite square plates, plate thickness ratio ( $a/h=40$ ), fiber volume fraction ( $V_f=0.6$ ), initial temperature ( $T_0=250C$ ), simple support S2 under environmental conditions. It is noticed that for both cross ply & angle ply plates the effects of lay-up is less when moisture and temperature exposure is not present, but in moisture and temperature exposure there is significant change in expected mean and coefficient of variations of fundamental frequency. However for temperature and moisture dependent material properties the value of expected mean and coefficient of variations of fundamental frequency are quite increased as shown in Figure 14.

Table 16(a) and (b). Effect of fiber volume fraction ( $V_f$ ) and input random variables  $b_i$  ( $i=1\dots 9, 7-8, 9$  and  $10=0.10$ ) on the expected mean ( $\omega_1$ ) and coefficient of variation ( $\omega_2$ ) of fundamental frequency of perfect cross ply (00/900)2T laminated composite square plates plate, thickness ratio ( $a/h=40$ ), fiber volume fraction ( $V_f=0.6$ ), initial temperature ( $T_0=250C$ ), simple support S2 under environmental conditions. With the change of fiber volume fraction, there is no much appreciable change in expected mean and coefficient of variation of fundamental frequency when the plate is not exposed to moisture and temperature, but with when the plate is exposed to

moisture and temperature environment the effects of fiber volume fraction is quite significant. It is noticed that expected mean and coefficient of variation of fundamental frequency decreases on increase of fiber volume fraction beyond sixty five percent for both temperature and moisture independent & temperature and moisture dependent material properties with different combinations of moisture and temperature as shown in Figure 15.

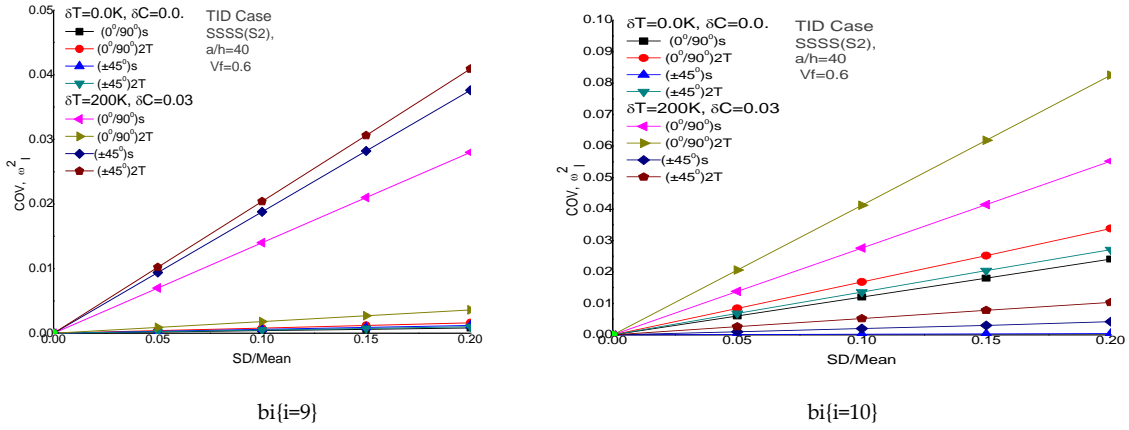


FIGURE 14. RANDOM COV RESULTS FOR FREE RESPONSE

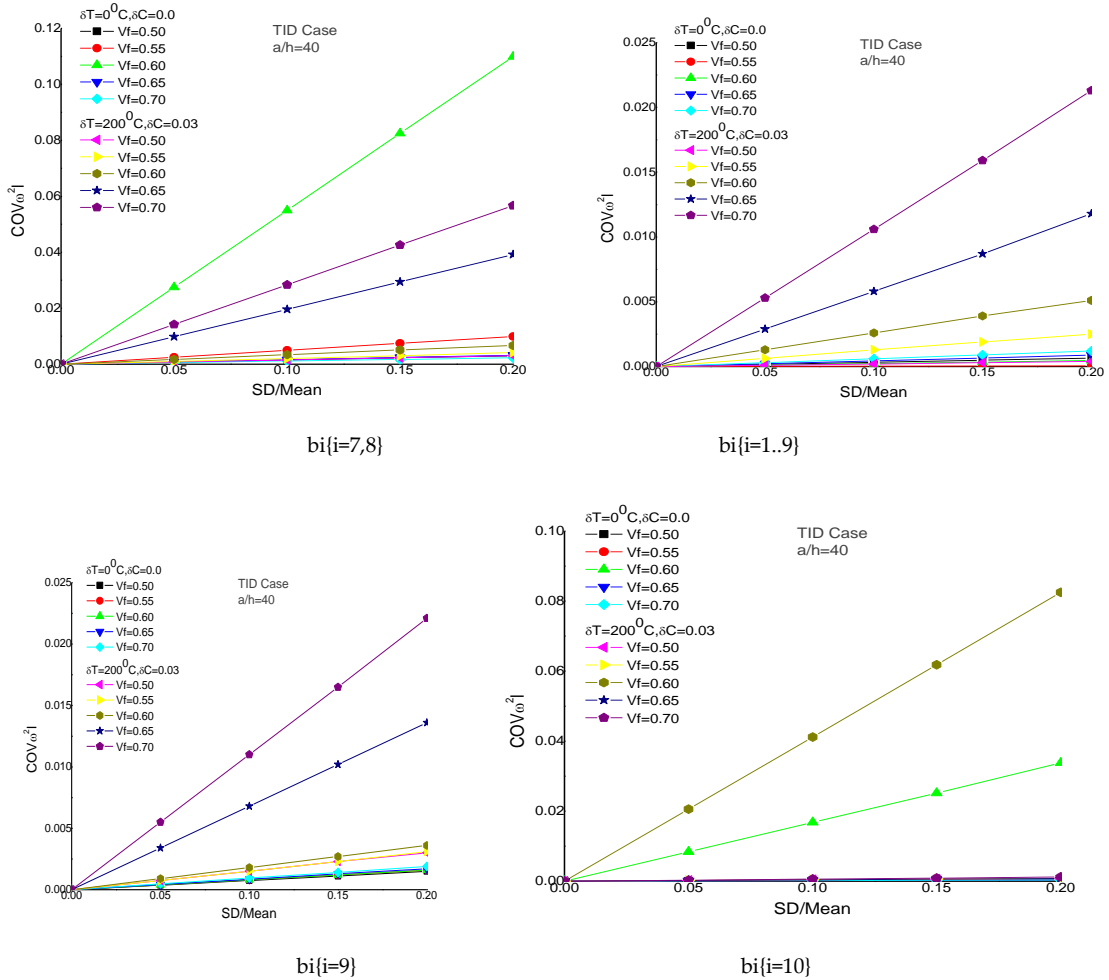


FIGURE 15. RANDOM COV RESULTS FOR FREE RESPONSE

TABLE 15(A)EFFECT OF LAY-UP AND INPUT RANDOM VARIABLES  $bi\{i=1...9, 7-8, 9 \text{ AND } 10=0.10\}$  ON THE EXPECTED MEAN ( $\omega_1$ ) AND COEFFICIENT OF VARIATION ( $\omega_2$ ) OF THE FUNDAMENTAL FREQUENCY OF PERFECT CROSS PLY  $[00/900]_2T$  LAMINATED COMPOSITE SQUARE PLATES, PLATE THICKNESS RATIO ( $A/H=40$ ), FIBER VOLUME FRACTION( $V_f=0.6$ ), INITIAL TEMPERATURE ( $T_0=250C$ ), SIMPLE SUPPORT ( $S_2$ ) UNDER ENVIRONMENTAL CONDITIONS.

Lay-up	(TID)									
	$\Delta T=0^{\circ}C, \Delta C=0\%$					$\Delta T=200^{\circ}C, \Delta C=3\%$				
	Mean ( $\omega_1$ )	COV, $\omega_2^2$				Mean ( $\omega_1$ )	COV, $\omega_2^2$			
		bi					bi			
(i=1- 9)		(i=7-.8)	(i=9)	(i=10)	(i=1- 9)		(i=7-.8)	(i=9)	(i=10)	
$(0^{\circ}/90^{\circ})_{S_2}$	11.7725	0.0763	3.91e-04	8.19e-04	0.0241	17.8690	0.2889	0.0397	0.0280	0.0552
$(0^{\circ}/90^{\circ})_{T_2}$	10.8800	0.1099	4.58e-04	0.0016	0.0338	21.3689	0.0067	0.0051	0.0036	0.0825
$(\pm 45^{\circ})_S$	13.9617	0.1144	2.87e-04	0.0012	4.36e-04	19.0274	0.0479	0.0204	0.0376	0.0042
$(\pm 45^{\circ})_{2T}$	14.9053	0.0741	2.44e-04	0.0010	0.0271	20.7776	0.0523	0.0206	0.0409	0.0103

TABLE 15(B)EFFECT OF LAY-UP AND INPUT RANDOM VARIABLES  $bi\{i=1...9, 7-8, 9 \text{ AND } 10=0.10\}$  ON THE EXPECTED MEAN ( $\omega_1$ ) AND COEFFICIENT OF VARIATION ( $\omega_2$ ) OF THE FUNDAMENTAL FREQUENCY OF PERFECT CROSS PLY  $[00/900]_2T$  LAMINATED COMPOSITE SQUARE PLATES, PLATE THICKNESS RATIO ( $A/H=40$ ), FIBER VOLUME FRACTION( $V_f=0.6$ ), INITIAL TEMPERATURE ( $T_0=250C$ ), SIMPLE SUPPORT ( $S_2$ ) UNDER ENVIRONMENTAL CONDITIONS.

Lay-up	(TD)									
	$\Delta T=0^{\circ}C, \Delta C=0\%$					$\Delta T=200^{\circ}C, \Delta C=3\%$				
	Mean ( $\omega_1$ )	COV, $\omega_2^2$				Mean ( $\omega_1$ )	COV, $\omega_2^2$			
		bi					bi			
(i=1- 9)		(i=7-.8)	(i=9)	(i=10)	(i=1- 9)		(i=7-.8)	(i=9)	(i=10)	
$(0^{\circ}/90^{\circ})_{S_2}$	11.7062	0.0386	3.95e-04	8.23e-04	0.0241	25.7712	0.0893	0.0196	0.0137	0.0157
$(0^{\circ}/90^{\circ})_{T_2}$	10.8196	0.0556	4.63e-04	0.0016	0.0338	19.9578	0.0105	0.0058	0.0038	0.0862
$(\pm 45^{\circ})_S$	13.8852	0.0577	2.90e-04	0.0012	4.35e-04	19.9021	0.2696	0.0720	0.1162	
$(\pm 45^{\circ})_{2T}$	14.8202	0.0375	2.46e-04	0.0010	2.71e-04	13.2935	0.1559	0.0414	0.0686	0.0130

TABLE 16(A)EFFECT OF FIBER VOLUME FRACTION ( $V_f$ ) AND INPUT RANDOM VARIABLES  $bi\{i=1...9, 7-8, 9 \text{ AND } 10=0.10\}$  ON THE EXPECTED MEAN ( $\omega_1$ ) AND COEFFICIENT OF VARIATION ( $\omega_2$ ) OF THE FUNDAMENTAL FREQUENCY OF PERFECT CROSS PLY  $[00/900]_2T$  LAMINATED COMPOSITE SQUARE PLATES, PLATE THICKNESS RATIO ( $A/H=40$ ), FIBER VOLUME FRACTION( $V_f=0.6$ ), INITIAL TEMPERATURE ( $T_0=250C$ ), SIMPLE SUPPORT ( $S_2$ ) UNDER ENVIRONMENTAL CONDITIONS.

$V_f$	(TID)									
	$\Delta T=0^{\circ}C, \Delta C=0\%$					$\Delta T=200^{\circ}C, \Delta C=3\%$				
	Mean ( $\omega_1$ )	COV, $\omega_2^2$				Mean ( $\omega_1$ )	COV, $\omega_2^2$			
		bi					bi			
(i=1- 9)		(i=7-8)	(i=9)	(i=10)	(i=1- 9)		(i=7-8)	(i=9)	(i=10)	
0.50	9.9403	0.0030	6.57e-04	0.0015	3.39e-04	19.9010	0.0031	3.92e-04	0.0030	8.38e-04
0.55	10.4098	0.0099	4.95e-05	0.0016	3.38e-04	20.6828	0.0042	0.0025	0.0031	8.39e-04
0.60	10.8800	0.1099	4.58e-04	0.0016	0.0338	21.3689	0.0067	0.0051	0.0036	0.0825
0.65	11.3586	0.0032	8.82e-04	0.0017	3.37e-04	21.3152	0.0392	0.0118	0.0136	7.74e-04
0.70	11.8557	0.0023	0.0012	0.0019	3.35e-04	18.9157	0.0567	0.0213	0.0221	0.0012

Table 17(a) and (b). Effects of environmental conditions and input random variables  $bi\{i=1...9, 7-8, 9 \text{ AND } 10=0.10\}$  on expected mean ( $\omega_1$ ) and coefficient of variation ( $\omega_2$ ) of fundamental frequency of perfect cross ply  $(00/900)_2T$  laminated composite square plates, plate thickness ratio ( $a/h=60$ ), fiber volume fraction ( $V_f=0.6$ ), initial

temperature ( $T_0=250C$ ), simple support  $S_2$  under environmental conditions. It is noticed that environmental conditions significantly affects the expected mean and coefficient of variation of fundamental frequency of plate with different sets for both temperature and moisture independent and temperature and moisture dependent material properties. Higher moisture and temperature play significant role for the analysis of plate as shown in Figure 16.

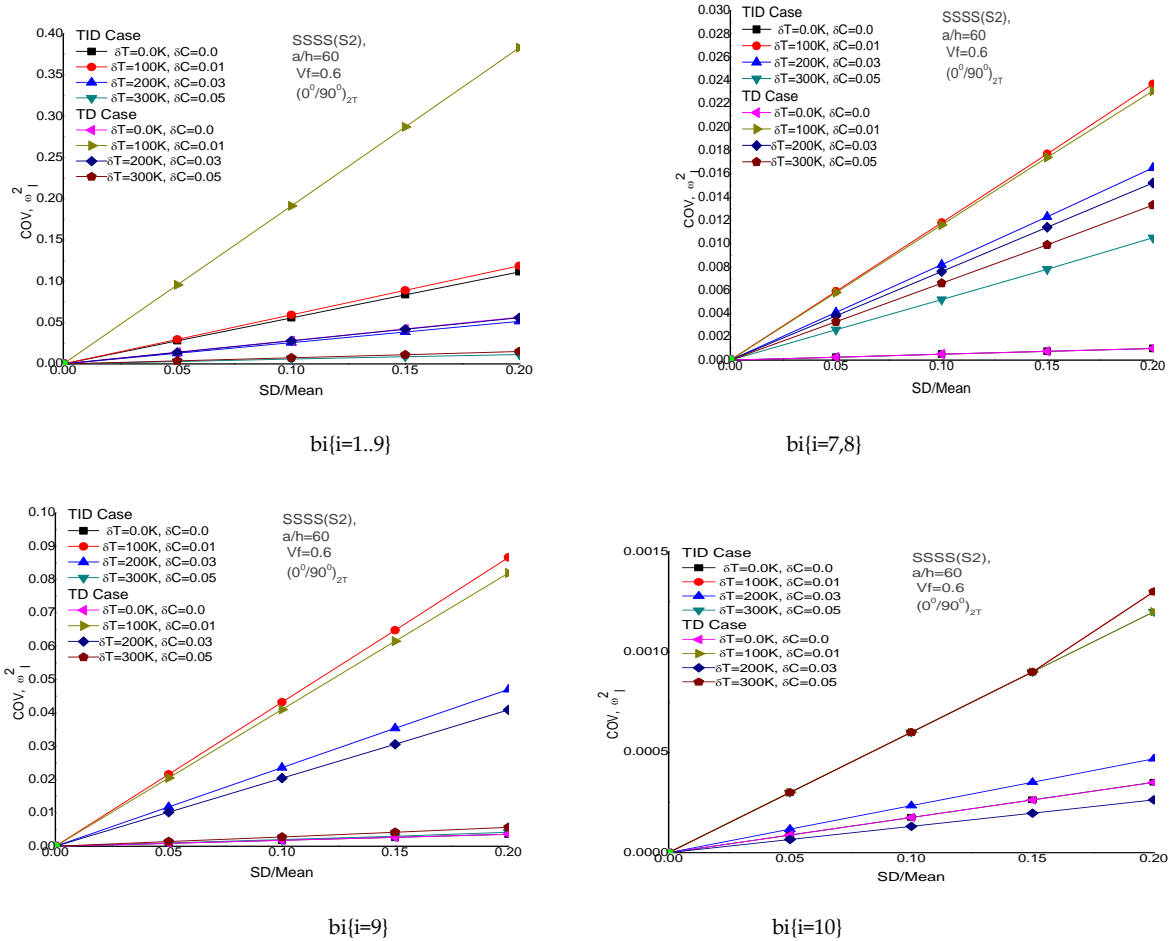


FIGURE 16. RANDOM COV RESULTS FOR FREE RESPONSE

TABLE 16(B)EFFECT OF FIBER VOLUME FRACTION (VF) AND INPUT RANDOM VARIABLES  $b_i$ ( $i=1..9, 7-8, 9$  AND  $10=0.10$ )ON THE EXPECTED MEAN ( $\Omega$ ) AND COEFFICIENT OF VARIATION ( $\Omega^2$ ) OF THE FUNDAMENTAL FREQUENCY OF PERFECT CROSS PLY  $[00/900]_{2T}$  LAMINATED COMPOSITE SQUARE PLATES, PLATE THICKNESS RATIO ( $A/H=40$ ), FIBER VOLUME FRACTION( $V_f=0.6$ ), INITIAL TEMPERATURE ( $T_0=250C$ ), SIMPLE SUPPORT ( $S_2$ ) UNDER ENVIRONMENTAL CONDITIONS.

$V_i$	(TD)									
	$\Delta T=0^\circ C, \Delta C=0\%$					$\Delta T=200^\circ C, \Delta C=3\%$				
	Mean ( $\omega$ )	COV, $\omega^2$				Mean ( $\omega$ )	COV, $\omega^2$			
		$b_i$					$b_i$			
	(i=1-9)	(i=7-8)	(i=9)	(i=10)		(i=1-9)	(i=7-8)	(i=9)	(i=10)	
0.50	9.8849	0.0033	6.64e-04	0.0015	3.39e-04	18.6212	0.0034	4.42e-04	0.0032	8.67e-04
0.55	10.3518	0.0127	5.01e-05	0.0016	3.38e-04	19.3362	0.0049	0.0028	0.0034	8.70e-04
0.60	10.8196	0.0556	4.63e-04	0.0016	0.0338	19.9578	0.0105	0.0058	0.0038	0.0862
0.65	11.2956	0.0030	8.92e-04	0.0017	3.36e-04	20.0044	1.5753	0.0129	0.0136	7.89e-04
0.70	11.7903	0.0023	0.0012	0.0019	3.35e-04	17.5988	0.0360	0.0242	0.0241	0.0013

TABLE 17(A) EFFECTS OF ENVIRONMENTAL CONDITIONS AND INPUT RANDOM VARIABLES  $b_i$  ( $i=1 \dots 9, 7-8, 9$  AND  $10=0.10$ ) ON EXPECTED MEAN ( $\Omega_1$ ) AND COEFFICIENT OF VARIATION ( $\Omega_2$ ) OF THE FUNDAMENTAL FREQUENCY OF PERFECT CROSS PLY [00/900]2T LAMINATED COMPOSITE SQUARE PLATES, PLATE THICKNESS RATIO ( $A/H=60$ ), FIBER VOLUME FRACTION ( $V_f=0.6$ ), INITIAL TEMPERATURE ( $T_0=250C$ ), SIMPLE SUPPORT (S2) UNDER ENVIRONMENTAL CONDITIONS.

Environmental Conditions.	Mean ( $\omega$ )	(TID)			
		COV, $\omega^2$			
		bi			
		(i=1-9)	(i=7-8)	(i=9)	(i=10)
$\Delta T=0^\circ C, \Delta C=0\%$	11.0115	0.1115	0.0010	0.0036	3.51e-04
$\Delta T=100^\circ C, \Delta C=1\%$	9.6617	0.1189	0.0237	0.0866	0.0013
$\Delta T=200^\circ C, \Delta C=3\%$	32.8633	0.0515	0.0165	0.0470	4.68e-04
$\Delta T=300^\circ C, \Delta C=5\%$	45.0589	0.0114	0.0105	0.0042	0.0012

TABLE 17(B) EFFECTS OF ENVIRONMENTAL CONDITIONS AND INPUT RANDOM VARIABLES  $b_i$  ( $i=1 \dots 9, 7-8, 9$  AND  $10=0.10$ ) ON EXPECTED MEAN ( $\Omega_1$ ) AND COEFFICIENT OF VARIATION ( $\Omega_2$ ) OF THE FUNDAMENTAL FREQUENCY OF PERFECT CROSS PLY [00/900]2T LAMINATED COMPOSITE SQUARE PLATES, PLATE THICKNESS RATIO ( $A/H=60$ ), FIBER VOLUME FRACTION ( $V_f=0.6$ ), INITIAL TEMPERATURE ( $T_0=250C$ ), SIMPLE SUPPORT (S2) UNDER ENVIRONMENTAL CONDITIONS.

Environmental Conditions.	Mean ( $\omega$ )	(TD)			
		COV, $\omega^2$			
		bi			
		(i=1-9)	(i=7-8)	(i=9)	(i=10)
$\Delta T=0^\circ C, \Delta C=0\%$	10.9496	0.0565	0.0010	0.0036	3.50e-04
$\Delta T=100^\circ C, \Delta C=1\%$	9.7744	0.3829	0.0231	0.0819	0.0012
$\Delta T=200^\circ C, \Delta C=3\%$	33.8795	0.0559	0.0152	0.0409	2.63e-04
$\Delta T=300^\circ C, \Delta C=5\%$	40.2525	0.0150	0.0133	0.0057	0.0013

## Conclusions

In the present study, the stochastic bending response of laminated composite plates in the presence of small random variation in the material properties TID and TD, geometric properties, coefficients of thermal expansion and coefficients of hygroscopic expansions using higher order shear deformation theory (HSDT) is investigated. The numerical results presented herein show that the plate deflections are reduced with increase in moisture and temperature. They also confirm that the characteristics of bending are significantly influenced by temperature rise, the degree of moisture concentration, fiber orientation, and fiber volume fraction. The dimensionless mean and coefficient of variation (COV) of fundamental frequency of the plate increases with increase in moisture and temperature.

It is also observed that hygrothermal dependent mechanical properties greatly affect the flexural behavior of the laminated composite plates. The dispersion in frequency of the plate is the higher with random change in  $E_{11}$ ,  $G_{12}$ ,  $V_{12}$  and  $h$  in both of the TID and TD material. Tight controls of these properties are therefore required for high reliability of the plate design. The flexural response of the laminated composite plate deteriorates considerably with the increase in temperature and moisture concentration and this hygrothermal environment becomes more detrimental as the working temperature reaches higher temperature.

The clamped support plate is more desirable from a dispersion point of view as compared to other support conditions of the plate subjected to all random system input variables. However, dimensionless mean fundamental frequency of the plate shows opposite effect. The effect of the randomness in the thermal expansion and hygroscopic coefficients and plate lamina thickness on the COV of the fundamental frequency subjected to hygrothermal loading is quite significant. It is therefore desirable to account for the uncertainty in these parameters for a reliable and safe design. The effects of various boundary conditions are also discussed, showing the applicability of the present solution methodology.

**NOTATIONS**

$A_{ij}, B_{ij}, etc$	: Laminate stiffnesses
$a, b$	: Plate length and breadth
$h$	: Thickness of the plate
$E_f, E_m$	: Elastic moduli of fiber and matrix, respectively.
$G_f, G_m$	: Shear moduli of fiber and matrix, respectively.
$\nu_f, \nu_m$	: Poisson's ratio of fiber and matrix, respectively.
$V_m, V_f$	: Volume fraction of fiber and matrix, respectively.
$\alpha_f, \alpha_m$	: Coefficient of thermal expansion of fiber and matrix, respectively.
$b_i$	: Basic random material properties
$E_{11}, E_{22}$	: Longitudinal and Transverse elastic moduli
$G_{12}, G_{13}, G_{23}$	: Shear moduli
$K_l$	: Linear bending stiffness matrix
$K_g$	: Thermal geometric stiffness matrix
$D$	Elastic stiffness matrices
$M_{\alpha\beta}, m_{\alpha\beta}$	: Mass and inertia matrices
$ne, n$	: Number of elements, number of layers in the laminated plate
$N_x, N_y, N_{xy}$	In-plane thermal buckling loads
$m$	: Number of nodes per element
$N_i$	: Shape function of $i$ th node
$\bar{C}_{ijkl}^p$	: Reduced elastic material constants
$f, \{f\}^{(e)}$	: Vector of unknown displacements, displacement vector of $e$ th element
$u, v, w$	: Displacements of a point on the mid plane of plate
$\bar{u}_1, \bar{u}_2, \bar{u}_3$	: Displacement of a point $(x, y, z)$
$\bar{\sigma}_{ij}, \bar{\epsilon}_{ij}$	: Stress vector, Strain vector
$\psi_y, \psi_x$	: Rotations of normal to mid plane about the $x$ and $y$ axis respectively
$\theta_x, \theta_y, \theta_k$	: Two slopes and angle of fiber orientation wrt $x$ -axis for $k$ th layer
$x, y, z$	: Cartesian coordinates
$\rho, \lambda, Var(.)$	: Mass density, eigenvalue, variance
$\omega, \bar{\omega}$	: Fundamental frequency and its dimensionless form
$RVs$	: Random variables
$\Delta T, \Delta C,$	: Difference in temperatures and moistures
$\alpha_1, \alpha_2, \beta_1, \beta_2$	: Thermal expansion and hygroscopic coefficients along $x$ and $y$ direction, respectively.

**APPENDIX**

$$(A_{ij}, B_{ij}, D_{ij}, E_{ij}, F_{ij}, H_{ij}) = \int_{-h/2}^{h/2} Q_{ij} (1, z, z^2, z^3, z^4, z^6) dz; \quad (i,j=1,2,6)$$

$$(A_{ij}, D_{ij}, F_{ij}) = \int_{-h/2}^{h/2} Q_{ij} (1, z^2, z^4) dz; \quad (i,j=4,5)$$

$$[K_b] = \sum_{i=1}^n \int_{A^{(e)}} [B_b]^T [D_b] [B_b] dA; [K_s] = \sum_{i=1}^n \int_{A^{(e)}} [B_s]^T [D_s] [B_s] dA, [K_g] = \sum_{i=1}^n \int_{A^{(e)}} [B_g]^T [N_0] [B_g] dA$$

$$\{q\} = \sum_{e=1}^{NE} \{\Lambda\}, [F^T] = \sum_{i=1}^n \int_{A^{(e)}} \left[ [B_{li}]^T [N^T] + [B_{bli}]^T [M^T] + [B_{b2i}]^T [P^T] \right] dA$$

where

$$[D_b] = \begin{bmatrix} \varphi_{i,x} & 0 & 0 & 0 & 0 & 0 & 0 & 0 \\ \varphi_{i,y} & 0 & 0 & 0 & 0 & 0 & 0 & 0 \\ 0 & \varphi_{i,x} & 0 & 0 & 0 & 0 & 0 & 0 \\ 0 & \varphi_{i,y} & 0 & 0 & 0 & 0 & 0 & 0 \\ 0 & 0 & \varphi_{i,x} & 0 & 0 & 0 & 0 & 0 \\ 0 & 0 & \varphi_{i,y} & 0 & 0 & 0 & 0 & 0 \\ 0 & 0 & 0 & C_1 \varphi_{i,x} & 0 & 0 & 0 & 0 \\ 0 & 0 & 0 & 0 & C_1 \varphi_{i,y} & 0 & 0 & 0 \\ 0 & 0 & 0 & C_1 \varphi_{i,y} & C_1 \varphi_{i,x} & 0 & 0 & 0 \\ 0 & 0 & 0 & -C_2 \varphi_{i,x} & 0 & -C_2 \varphi_{i,x} & 0 & 0 \\ 0 & 0 & 0 & 0 & -C_2 \varphi_{i,y} & 0 & -C_2 \varphi_{i,y} & 0 \\ 0 & 0 & 0 & -C_2 \varphi_{i,y} & -C_2 \varphi_{i,x} & -C_2 \varphi_{i,y} & -C_2 \varphi_{i,x} & 0 \end{bmatrix} \{q\}, [D_s] = \begin{bmatrix} 0 & 0 & \varphi_{i,x} & 1 & 0 & 0 & 0 \\ 0 & 0 & \varphi_{i,x} & 0 & 1 & 0 & 0 \\ 0 & 0 & 0 & -3 & 0 & -3 & 0 \\ 0 & 0 & 0 & 0 & -3 & 0 & -3 \end{bmatrix} \{q\}$$

$$[B_{ii}] = \begin{bmatrix} \varphi_{i,x} & 0 & 0 & 0 & 0 & 0 & 0 \\ 0 & \varphi_{i,y} & 0 & 0 & 0 & 0 & 0 \\ 0 & 0 & 0 & 0 & 0 & 0 & 0 \\ \varphi_{i,y} & \varphi_{i,x} & 0 & 0 & 0 & 0 & 0 \end{bmatrix}, [B_{bi}] = \begin{bmatrix} 0 & 0 & 0 & 0 & 0 & C_1 \varphi_{i,x} & 0 \\ 0 & 0 & 0 & 0 & 0 & 0 & C_1 \varphi_{i,y} \\ 0 & 0 & 0 & 0 & 0 & C_1 \varphi_{i,y} & C_1 \varphi_{i,x} \end{bmatrix}, [B_{si}] = \begin{bmatrix} 0 & 0 & \varphi_{i,x} & 0 & 0 & C_1 \varphi_i & 0 \\ 0 & 0 & \varphi_{i,y} & 0 & 0 & 0 & C_1 \varphi_i \end{bmatrix}$$

$$[B_{gi}] = \begin{bmatrix} 0 & 0 & \varphi_{i,x} & 0 & 0 & 0 & 0 \\ 0 & 0 & \varphi_{i,y} & 0 & 0 & 0 & 0 \end{bmatrix}, [N_0] = \begin{bmatrix} N_x & N_{xy} \\ N_{xy} & N_y \end{bmatrix}, [B_{li}] = [B_{ii}]; [B_{bii}] = [B_{bi}]; [B_{b2i}] = [B_{si}];$$

$$\bar{C}_{ijkl} = \begin{bmatrix} \bar{Q}_{11} & \bar{Q}_{12} & \bar{Q}_{16} & 0 & 0 \\ \bar{Q}_{12} & \bar{Q}_{22} & \bar{Q}_{26} & 0 & 0 \\ \bar{Q}_{16} & \bar{Q}_{26} & \bar{Q}_{66} & 0 & 0 \\ 0 & 0 & 0 & \bar{Q}_{44} & \bar{Q}_{45} \\ 0 & 0 & 0 & \bar{Q}_{45} & \bar{Q}_{55} \end{bmatrix}, \begin{aligned} \bar{Q}_{11} &= Q_{11} \cos^4 \alpha + 2(Q_{12} + 2Q_{66}) \cos^2 \alpha \sin^2 \alpha + Q_{22} \sin^4 \alpha \\ \bar{Q}_{12} &= \bar{Q}_{21} = (Q_{11} + Q_{22} - 4Q_{66}) \cos^2 \alpha \sin^2 \alpha + Q_{12} (\cos^4 \alpha + \sin^4 \alpha) \\ \bar{Q}_{16} &= (Q_{11} - Q_{12} - 2Q_{66}) \sin \alpha \cos^3 \alpha + (Q_{12} - Q_{22} + 2Q_{66}) \sin^3 \alpha \cos \alpha \\ \bar{Q}_{22} &= Q_{11} \sin^4 \alpha + 2(Q_{12} + 2Q_{66}) \cos^2 \alpha \sin^2 \alpha + Q_{22} \cos^4 \alpha \\ \bar{Q}_{26} &= (Q_{11} - Q_{12} - 2Q_{66}) \sin^3 \alpha \cos \alpha + (Q_{12} - Q_{22} + 2Q_{66}) \sin \alpha \cos^3 \alpha \\ \bar{Q}_{66} &= (Q_{11} + Q_{22} - 2Q_{12} - 2Q_{66}) \cos^2 \alpha \sin^2 \alpha + Q_{66} (\cos^4 \alpha + \sin^4 \alpha) \\ \bar{Q}_{44} &= Q_{44} \cos^2 \alpha + Q_{55} \sin^2 \alpha \\ \bar{Q}_{45} &= (Q_{55} - Q_{44}) \sin \alpha \cos \alpha - Q_{54} \\ \bar{Q}_{55} &= Q_{55} \cos^2 \alpha + Q_{44} \sin^2 \alpha \end{aligned}$$

$$\text{Where } Q_{11} = \frac{E_{11}}{(1-\nu_{12}\nu_{21})}, Q_{12} = \frac{\nu_{12}E_{22}}{(1-\nu_{12}\nu_{21})} = \frac{\nu_{21}E_{11}}{(1-\nu_{12}\nu_{21})} = Q_{21},$$

$$Q_{22} = \frac{E_{22}}{(1-\nu_{12}\nu_{21})}, Q_{66} = G_{12}, Q_{44} = G_{13}, Q_{55} = G_{12}, \nu_{21} = \frac{\nu_{12}E_{22}}{E_{11}}$$

**REFERENCES**

- [1] Whitney, J. M. and Ashton, J. E, "Effect of Environment on the Elastic Response of Layered Composite Plates, AIAA Journal vol. 9 pp 1708-13,1971.
- [2] Sai Ram, K. S., Sinha P. K, "Hygrothermal effects on the bending characteristics of laminated composite plates". Computers & Structures", vol. 40 (4) pp 1009-1015, 1991.
- [3] Shen H-S, "Non-linear bending of shear deformable laminated plates under lateral pressure and thermal loading and resting on elastic foundations". J Strain Anal Eng Des, vol. 35 pp 93-108, 2000.

- [4] Shen, Hui-Shen, "Hygrothermal Effects on the Nonlinear Bending of Shear Deformable Laminated Plates". *Journal of Engineering Mechanics Asce*, M, pp 493, 2002.
- [5] Lee, S. Y., Chou, C. J., Jang, J. L., J. S, "Hygrothermal effects on the linear and nonlinear analysis of symmetric angle-ply laminated plates". *Compos. Struc* vol. 21 (1), pp 41–48, 1992.
- [6] Patel,B.P, Ganapathi M., Makhecha,D.P, "Hygrothermal effects on the structural behavior of thick composite laminates using higher-order theory", *Composite Structures*, vol. 56 pp 25–34, 2002.
- [7] Onkar AK, Yadav D, "Non-linear response statistics of composite laminates with random material properties under random loading", *Composite Structures*, vol. 60pp 375–83, 2003.
- [8] Singh BN, Iyengar NGR, Yadav D, "A C0 finite element investigation for buckling analysis of composite plates with random material properties". *International Journal of Structural Engineering and Mechanics*, vol. 13 pp 53–74, 2000.
- [9] Upadhyay, AK, Pandey, Ramesh and Shukla, KK. "Nonlinear flexural response of laminated composite plates under hygro-thermo-mechanical loading", *Commun Nonlinear Sci Numer Simulat*, vol. 15 pp 2634–2650, 2010.
- [10] Rajesh, Kumar, Lal, A and Patil,H.S. " Hygrothermal effects on the flexural response of laminated composite plates with random material properties." , *Micromechanical Model. J. of Applied Engineering and Research*, Research India Publication, India 2011.
- [11] Rajesh, Kumar, Lal, A and Patil,HS. " Hygrothermal effects on the flexural response of laminated composite plates with random material properties." *Micromechanical Model. 2nd International conference on emerging trends in Engineering and Technology ,IETET*, 2011.
- [12] Rajesh, Kumar, Lal, A and Patil,H.S. " Nonlinear Flexural Response of Laminated Composite Plates on a Nonlinear Elastic Foundation with Uncertain System Properties under Lateral Pressure and Hygrothermal Loading." , *Micromechanical Model. J. of Aerospace Engineering* vol. 1 pp 168, 2012.
- [13] Lien-Wen Chen and Y. M. Chen, "Vibrations of Hygrothermal Elastic Composite Plates", *Engineering Fracture Mechanics* vol. 31(2) pp 209-220, 1988.
- [14] K. S. Sai Ram and P. K. Sinha, "Hygrothermal effects on the free vibration of laminated composite plates", *Journal of Sound and Vibration* vol. 158(l) pp 133-148, 1992.
- [15] X-L Huang, J-J Zheng, "Nonlinear vibration and dynamic response of simply supported shear deformable laminated plates on elastic foundations". *Eng Struct* vol. 25 pp. 1107–19, 2003.
- [16] Xiao-Lin Huang J.-J. Zheng , "Nonlinear vibration and dynamic response of shear deformable laminated plates in hygrothermal environments", *Composites Science and Technology*, vol. 64 pp 1419–1435, 2004.
- [17] Lal A., and Singh, B. N, "Stochastic Nonlinear free vibration response of laminated composite plates resting on elastic foundation in thermal environments", *Computational Mechanics.*, vol. 44(1)pp 15-25, 2009.
- [18] Rajesh, Kumar, Patil, H. S., and Lal, A, "Hygrothermoelastic free vibration response of laminated composite plates resting on elastic foundations with random system properties *Micromechanical model*". *Journal of Thermoplastic Composite Materials*, vol. 26(5)pp 573–604, 2011.
- [19] Rajesh, Kumar, Patil, H. S., and Lal, A, "Hygrothermally Induced Nonlinear Free Vibration Response of Nonlinear Elastically Supported Laminated Composite Plates with Random System Properties : *Micromechanical Stochastic Finite Element Model*". *Int. Journal of Frontiers in Aerospace Engg.*vol. 2(2) pp 143-156, 2013.
- [20] Zongeen Z, Suhaun C, "The standard deviation of the eigen solutions for random multi degree freedom systems". *Computers and Structures* vol. 39 (6) pp 603–7, 1990.
- [21] Zhang Y, Chen S, Lue Q, Liu T, "Stochastic perturbation finite elements", *Computers and Structures*, vol. 59(3)pp 425–9, 1996.
- [22] Liu WK, Ted B, Mani A, "A random field finite elements". *International Journal of Numerical Methods in Engineering* vol. 23 pp 1831–45, 1986.

- [23] Zhang J, Ellingwood B, "Effects of uncertain material properties on structural stability", ASCE Journal of Structural Engineering, vol. 121 pp 705–16, 1993.
- [24] Reddy, J.N, "Mechanics of laminated composite plates, theory and analysis", Florida: CRC Press 1996.
- [25] Reddy, J.N, "Mechanics of laminated composite plates: theory and analysis", Boca Raton, FL: CRC Press, 1997.
- [26] Kleiber, M, Hien T.D, "The stochastic finite element method", John Wiley & Sons, 1992.
- [27] Robert M Jones, "Mechanics of composite materials", International Student Edition, McGraw Hill Kogakusha, Ltd Texas. 1975.
- [28] Reddy, J.N, "A simple higher order theory for laminated composite plates", J Appld Mech Trans ASME, vol. 51 pp 745-752, 1984.

# Effects of Elastic Foundations on Thermomechanically Induced Postbuckling Response of Square Cutouts FGM Plates

Rajesh Kumar

School of Mechanical Engineering, JIT, Jimma University, ETHIOPIA  
rajeshtrpathi63@gmail.com

## Abstract

Effects of elastic foundations on thermomechanically induced postbuckling response of square cutouts FGM Plates are investigated. The basic formulation is based on higher order shear deformation theory [HSDT] using modified C0 continuity. A nonlinear finite element method [DIFEM] with first order regular perturbation technique [FORPT] for composite plates is extended for FGM plates to solve the random eigenvalue problem. Typical numerical results are presented to examine the effect of volume fractions index, plate length to thickness ratios, plate aspect ratios, types of loadings, amplitude ratios, support conditions and various sized holes with random thermomechanical properties. The results obtained by the present solution approach are validated with those available in the literatures and independent Monte Carlo Simulation (MCS).

## Keywords

*Functionally Graded Materials Plate; Postbuckling Response; Random Material Properties; Regular Perturbation Technique; Elastic Foundations*

## Introduction

FGMs consisting of metal and ceramic possess some outstanding mechanical properties such as high fracture toughness and high degree of temperature resistance by maintaining the desired structural integrity. Plates with circular, square and other openings are extensively used as structural members to further reduce the weight of structures, cutouts for hardware to pass through, or in the case of fuselage windows and doors. Although, the sizing of structural members with various shaped cutouts is often determined by stability (buckling) constraints. Buckling behaviour of geometrically nonlinear FGMs plates resting on elastic foundations, subjected to in-plane loadings with temperature dependent and independent properties is of utmost importance in the design and development of high performance structural components for stability point of view. In order to predict the structural response in terms of stability accurately and enable a better understanding of characterization of actual behaviour under thermomechanical loading with various shaped cutouts is an important problem to pay special attention for reliability of design.

Numerous studies on modelling and analysis of thermomechanical of FGMs plate based on deterministic analysis have been performed. For examples, Fuchiyama et al. [1], Feldman et al. [2], Noda [3], Reddy [4], Javaheri et al. [5], Javaheri et al. [6], Najafizadeh et al. [7], Vel et al. [8], Yang et al. [9], Ma et al. [10], Wu [11], Na et al. [12], Na et al. [13], Wu et al. [14], Saji et al. [15], Zhao et al. [16], Matsunga et al. [17] and Lee et al. [18].

Relatively little efforts have been made in the past by the researchers and investigators on the prediction of postbuckling response statistics of the structures made of laminated composites and FGMs having random system properties. In this direction, Yang et al. [20] evaluated the second-order statistics for elastic buckling of FGM plates with randomness in the material properties using stochastic FEM via first-order shear deformation theory in conjunction with FOPT. Onkar et al. [21] investigated the generalized buckling of laminated composite circular cut-out plate with random material properties using classical plate theory (CLT) combined with FOPT. Lal et al. [22] investigated the effect of random system properties on the postbuckling of laminated composite plates supported

with elastic foundation using HSDT based  $C^0$  nonlinear FEM combined with direct iterative procedure in conjunction with FOPT. Jagtap et al. [23] presented the stochastic nonlinear free vibration response of FGMs plates resting on two parameter Pasternak foundation having Winkler cubic non-linearity with random system properties subjected to uniform and non-uniform temperature changes with temperature independent (TID) and dependent (TD) material properties based on higher order shear deformation theory (HSDT) with von-Karman nonlinear strains using modified  $C^0$  continuity.

Alireza Hassanzadeh Taheri et al. [32] investigated the free vibration characteristics of functionally graded structures by an isogeometrical analysis approach. Yin S et al. [33] carried out a cut-out isogeometric analysis for thin laminated composite plates using level sets. Shuohui Yin et al. [34] investigated the in-plane material inhomogeneity of functionally graded plates using a higher-order shear deformation plate isogeometric theory. Tiantang Yu et al. [35] studied on the thermal buckling analysis of functionally graded plates with internal defects using extended isogeometric analysis.

It is evident from the available literatures mentioned above that the studies of stochastic postbuckling response of FGM plates resting on elastic foundations, subjected to thermomechanical loadings involving randomness in thermomechanical material properties of constituent materials with square cut-outs using computationally efficient direct iterative based  $C^0$  nonlinear FEM in combined with mean centred FORPT is not dealt by the researchers to the best of author’s knowledge.

The results are presented with new concept in the form of tables, which can suit as a bench mark for the future research.

**Mathematical Formulations**

Consider a rectangular FGM plate with holes consisting of metal and ceramic at the top and bottom layer of length  $a$ , width  $b$ , and total thickness  $h$ , defined in  $(x, y, z)$  system with  $x$ - and  $-y$  axes located in the middle plane and its origin placed at the corner of the plate. Let  $(\bar{u}, \bar{v}, \bar{w})$  be the displacements parallel to the  $(x, y, z)$  axes, respectively as shown in Fig. 1(a). In the present analysis, for plate with circular and square holes of various sizes one quarter plate is used due to symmetry of the FGM plate. The load – displacement relation between the plate and the supporting foundations is given as

$$P=K_1w -K_2\nabla^2w \tag{1}$$

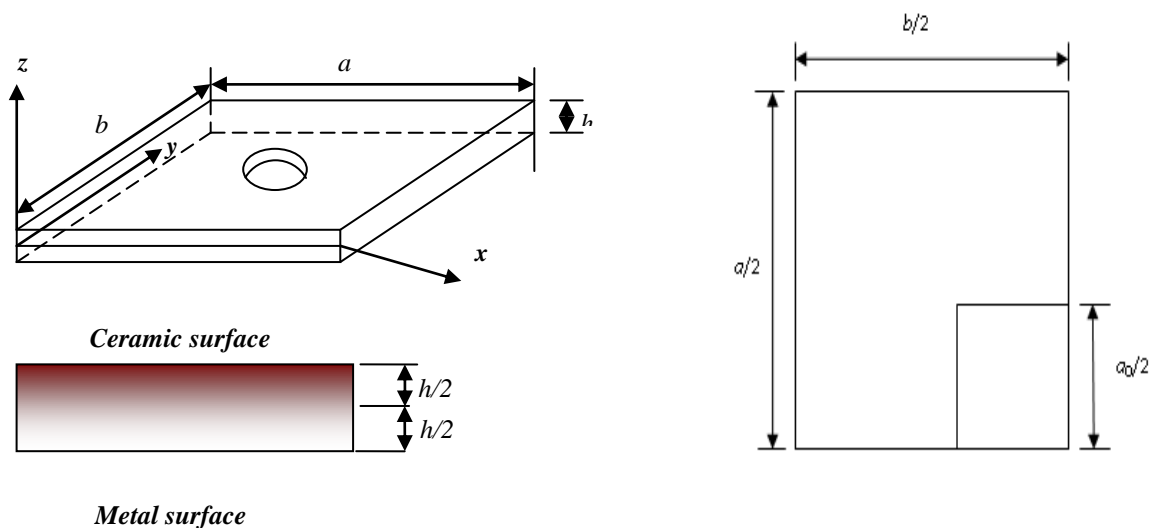


FIGURE.1 (a) GEOMETRY OF RECTANGULAR FGM PLATE WITH CIRCULAR CUTOUS(b)QUARTER OF FGM PLATES WITH SQUARE CUTOUT.

where  $P$  is the foundation reaction per unit area,  $\nabla^2 = \partial^2/\partial x^2 + \partial^2/\partial y^2$  and  $K_1$  and  $K_2$  are linear Winkler (normal) foundation, linear Pasternak (shear layer) foundation parameters, respectively and  $w$  is the transverse displacement of the plate. This model is simply known as Winkler type when  $K_2 = 0$ . The square cut-outs geometry for one quarter of the FGM plate is given in Fig. 1(a). The hole size for square holes are expressed,  $a_0/a$ , where  $a_0$  are length of square holes, respectively.

The properties of the FGM plate are assumed to be vary according to Power law through the thickness of the plate only, such that the top surface  $z = h/2$  is ceramic-rich and the bottom surface  $z = -h/2$  is metal rich. The effective mechanical and thermal properties of the FGMs plate of an arbitrary point within the plate domain are expressed as:

$$\begin{aligned} E(z, T) &= E_b(T) + [E_t(T) - E_b(T)]V_c(z) \\ \alpha(z, T) &= \alpha_b(T) + [\alpha_t(T) - \alpha_b(T)]V_c(z) \\ k(z, T) &= k_b(T) + [k_t(T) - k_b(T)]V_c(z) \end{aligned} \quad (1a)$$

where,  $t$  and  $b$  represent the ceramic and metal constituents, respectively. With  $E$ ,  $\alpha$  and  $k$  are the effective Young's modulus, thermal expansion coefficient and thermal conductivity, respectively. The ceramic metal volume fraction  $V_c$  is the function of coordinate in the thickness direction,  $z$  and is expressed as

$$V_c(z) = \left(0.5 + \frac{z}{h}\right)^n, \quad -h/2 \leq z \leq h/2, \quad 0 \leq n < \infty \quad (2)$$

where,  $n$  is the volume fraction index and is always positive. For  $n$  is taken as zero, the plate is fully ceramic and  $n$  is taken as one, the composition of ceramic and metal is linear. The Poisson's ratio  $\nu$  depends weakly on temperature change and is assumed to be constant [25].

### Displacement Field Model

In the present study, the assumed displacement field is based on the Reddy's higher order shear deformation plate theory [28] which requires  $C_1$  continuous element approximation. The slightly modified to make the suitability of  $C_0$  continuous element [29]. A  $C_0$  continuity permits easy isoparametric finite element formulation and consequently can be applied for non-rectangular geometries as well. In modified form, the derivatives of out-of-plane displacement two involved in the in-plane are themselves considered as separate degree of freedom (DOFs). Thus five DOFs with  $C_1$  continuity are transformed into seven DOFs with  $C_0$  continuity due to conformity with the HSDT. In this process the artificial constraints are imposed which can be enforced variationally through a penalty approach. However, the literature [29] demonstrates that without enforcing these constraints the accurate results using  $C_0$  can be obtained in order to satisfy the constraints. The modified displacement field along the  $x$ ,  $y$ , and  $z$  directions for an arbitrary FGMs plate is now written as

$$\begin{aligned} \bar{u} &= u + f_1(z)\psi_x + f_2(z)\phi_x; \\ \bar{v} &= v + f_1(z)\psi_y + f_2(z)\phi_y; \\ \bar{w} &= w; \end{aligned} \quad (3)$$

where  $\bar{u}$ ,  $\bar{v}$  and  $\bar{w}$  denote the displacements of a point along the  $(x, y, z)$  coordinates axes:  $u$ ,  $v$ , and  $w$  are corresponding displacements of a point on the mid plane. Here  $\phi_x = w_{,x}$  and  $\phi_y = w_{,y}$  are the slopes along  $x$  and  $y$  axes, respectively and  $\psi_x$ ,  $\psi_y$  are the rotations of normal to the mid plane about the  $y$ -axis and  $x$ -axis, respectively.

The function  $f_1(z)$  and  $f_2(z)$  given in Eq. (1) can be written as

$$f_1(z) = C_1 z - C_2 z^3; \quad f_2(z) = -C_4 z^3 \quad \text{with} \quad C_1 = 1, C_2 = C_4 = 4h^2/3.$$

The displacement vector for the modified  $C_0$  continuous model can be written as

$$\{q\} = [u \quad v \quad w \quad \phi_y \quad \phi_x \quad \psi_y \quad \psi_x]^T, \quad (4)$$

where, comma (,) denotes partial differential.

### Strain Displacement Relations

For the FGM plate considered here, the relevant strain vector consisting of linear strain (in term of mid plane deformation, rotation of normal and higher order terms), non-linear strain (von-Karman type) and thermal strains vectors associate with the displacement are expressed as

$$\{\bar{\varepsilon}_{ij}\} = \{\bar{\varepsilon}_{ij}^L\} + \{\bar{\varepsilon}_{ij}^{NL}\} - \{\bar{\varepsilon}_{ij}^T\} \quad (i, j = 1, 2, \dots, 6) \quad (5)$$

where  $\{\bar{\varepsilon}_{ij}^L\}$ ,  $\{\bar{\varepsilon}_{ij}^{NL}\}$  and  $\{\bar{\varepsilon}_{ij}^T\}$  are the linear, non-linear and thermal strain vectors, respectively.

From Eq. (5), the linear strain tensor using HSDT can be written as :

$$\bar{\varepsilon}_{ij}^L = H_{mn} \varepsilon_{kl}^L \quad (6)$$

where,  $H_{mn}$  is the function of  $z$  and unit step vector as defined in Appendix (A.1) and  $\varepsilon_{kl}^L$  is reference plain linear strain tensor defined as

$$\varepsilon_{kl}^L = \{\varepsilon_1^0 \quad \varepsilon_2^0 \quad \varepsilon_6^0 \quad k_1^0 \quad k_2^0 \quad k_6^0 \quad k_1^2 \quad k_2^2 \quad k_6^2 \quad \varepsilon_4^0 \quad \varepsilon_5^0 \quad k_4^2 \quad k_5^2\}^T \quad (7)$$

Assuming that the strains are much smaller than the rotations (in the von-Karman sense), one can rewrite nonlinear strain vector  $\{\bar{\varepsilon}_{ij}^{NL}\}$  given in Eq. (5) as [23]

$$\bar{\varepsilon}_{ij}^{NL} = \frac{1}{2} [A_{nij}] \{\phi_{ij}\} \quad (8)$$

$$\text{where, } A_{nij} = \frac{1}{2} \begin{bmatrix} w_{,x} & 0 \\ 0 & w_{,y} \\ w_{,y} & w_{,x} \\ 0 & 0 \\ 0 & 0 \end{bmatrix} \text{ and } \phi_{ij} = \begin{Bmatrix} w_{,x} \\ w_{,y} \end{Bmatrix}$$

The thermal strain vector  $\{\bar{\varepsilon}_{ij}^T\}$  given in Eq. (5) is represented as [23]

$$\{\bar{\varepsilon}_{ij}^T\} = \Delta T \begin{Bmatrix} \alpha_1 \\ \alpha_2 \\ 0 \\ 0 \\ 0 \end{Bmatrix}; \quad (i, j = 1, 2, \dots, 6) \quad (9)$$

Here,  $\alpha_1$  and  $\alpha_2$  are coefficients of thermal expansion along the  $x$  and  $y$  directions, respectively and  $\Delta T$  denotes the uniform and non uniform change in temperature.

The temperature field for non uniform temperature change is expressed as [25]

$$\Delta T = T(z) - T_0 \quad (10)$$

where,  $T_0$  is initial temperature and can be expressed as

$$T(z) = T_b + (T_t - T_b)\eta(z) \quad (10a)$$

where,  $T(z)$  is the temperature distribution along  $z$  direction,  $t$  and  $b$  are referred as top and bottom surface parameter  $\eta(z)$  can be written as

$$\eta(Z) = \frac{1}{c} \left[ \begin{aligned} & \left( 0.5 + \frac{z}{h} \right) - \frac{k_{tb}}{(n+1)k_b} \left( 0.5 + \frac{z}{h} \right)^{n+1} + \frac{k_{tb}^2}{(2n+1)k_b^2} \left( 0.5 + \frac{z}{h} \right)^{2n+1} - \frac{k_{tb}^3}{(3n+1)k_b^3} \left( 0.5 + \frac{z}{h} \right)^{3n+1} \\ & + \frac{k_{tb}^4}{(4n+1)k_b^4} \left( 0.5 + \frac{z}{h} \right)^{4n+1} - \frac{k_{tb}^5}{(5n+1)k_b^5} \left( 0.5 + \frac{z}{h} \right)^{5n+1} \end{aligned} \right] \quad (11)$$

where  $C = 1 - \frac{k_{tb}}{(n+1)k_b} + \frac{k_{tb}^2}{(2n+1)k_b^2} - \frac{k_{tb}^3}{(3n+1)k_b^3} + \frac{k_{tb}^4}{(4n+1)k_b^4} - \frac{k_{tb}^5}{(5n+1)k_b^5}$

Here  $k$ ,  $z$  and  $n$  indicate thermal conductivity, distance from central axis and volume fraction, respectively, with  $ktb = kt - kb$ .

For uniform temperature change Eq. (10) can be written as

$$T(z) = T_0 + (T_t - T_b) \quad (12)$$

For uniform and non-uniform temperature rise, the initial ( $T_0$ ) and bottom ( $T_b$ ) temperatures of the plate is assumed to be 300K and  $T_c$  as 600K, respectively throughout whole analysis, unless otherwise mentioned.

### Constitutive Relations

The constitutive law of thermo-elasticity for material under consideration relates the stresses with strains in a plane stress state for an isotropic layer of a of a laminate is expressed as

$$\bar{\sigma}_{ij} = \bar{C}_{ijkl} \bar{\varepsilon}_{ij} \quad (i, j = 1, 2, \dots, 6) \quad (13)$$

where,  $\bar{C}_{ijkl}$  is elastic material constant matrix as defined in Appendix of (A.2).

### Strain Energy

The strain energy of FGM plate consisting of linear and nonlinear strain energy undergoing large deformation can be expressed as,

$$\Pi_1 = \Pi_L + \Pi_{NL} \quad (14)$$

where  $\Pi_L$  and  $\Pi_{NL}$  are the linear and nonlinear strain energy of laminated plate, respectively.

From Eq. (14), the strain energy ( $\Pi_a$ ) of the FGM plate can be expressed as

$$\Pi_L = \int_{\Omega} \frac{1}{2} \bar{C}_{ijkl} \bar{\varepsilon}_{ij}^L \bar{\varepsilon}_{kl}^L d\Omega = \int_{\Delta} \frac{1}{2} \varepsilon_{ij} D_{mn} \varepsilon_{kl} d\Delta \quad (15)$$

where,  $D_{mn}$  is the laminate elastic stiffness matrix as defined in Appendix (A.3).

From Eq. (14) the nonlinear strain energy ( $\Pi_{NL}$ ) of the plate can be rewritten as

$$\begin{aligned} \Pi_{NL} = & \int_{\Omega} \frac{1}{2} \bar{\varepsilon}_{ij}^{-L} D_3^{-NL} \bar{\varepsilon}_{ij}^{-NL} d\Omega + \frac{1}{2} \int_{\Omega} \bar{\varepsilon}_{kl}^{-NL} D_4^{-L} \bar{\varepsilon}_{ij}^{-L} d\Omega \\ & + \frac{1}{2} \int_{\Omega} \bar{\varepsilon}_{kl}^{-NL} D_5^{-NL} \bar{\varepsilon}_{ij}^{-NL} d\Omega \quad (i, j, k, l = 1, 2, 3) \end{aligned} \quad (16)$$

where  $\Omega$ ,  $\bar{\varepsilon}_{ij}^L$  and  $\bar{\varepsilon}^{NL}$  denotes un-deformed configuration of plate and linear and nonlinear strain tensors, respectively.

Using Eq. (8) the Eq. (16) can be expressed as

$$\begin{aligned} \Pi_{NL} = & \frac{1}{2} \int_{\Omega} A_{nij} \phi_{nij} D_3 \bar{\varepsilon}_{ij}^L d\Omega + \frac{1}{2} \int_{\Omega} \bar{\varepsilon}_{ij}^L D_4 A_{nkl} \phi_{nkl} d\Omega \\ & + \frac{1}{2} \int_{\Omega} A_{nij} \phi_{nij} D_5 A_{nkl} \phi_{nkl} d\Omega, \quad (i, j, k, l = 1, 2, 3) \end{aligned} \quad (17)$$

where D3, D4 and D5 are the laminate stiffness matrices of the plate defined in Appendix (A.4).

The potential energy ( $\Pi_2$ ) storage by thermal load (non-uniform change in temperature across the thickness) due to change in temperature, pre buckling stresses, i.e., in plane thermal compressive stress resultants in the plate are generated. These stress resultants are the reason for the buckling. The potential energy due to the in plane thermal stress resultants is expressed as

$$\begin{aligned} \Pi_2 = & \frac{1}{2} \int_A \left[ N_{xym} (w_{,x})^2 + N_{ytm} (w_{,y})^2 + 2N_{xytm} (w_{,x})(w_{,y}) \right] dA \\ = & \frac{1}{2} \int_A \begin{Bmatrix} w_{,x} \\ w_{,y} \end{Bmatrix}^T \begin{bmatrix} N_{xym} & N_{xytm} \\ N_{xytm} & N_{ytm} \end{bmatrix} \begin{Bmatrix} w_{,x} \\ w_{,y} \end{Bmatrix} dA \end{aligned} \quad (18)$$

where,  $N_{xym}$ ,  $N_{ytm}$  and  $N_{xytm}$  are written as the  $N_{xm}$ - $N_{xt}$ ,  $N_{ym}$ - $N_{yt}$  and  $N_{xym}$ - $N_{xyt}$  respectively. Here  $N_{xm}$ ,  $N_{ym}$ ,  $N_{xym}$  and  $N_{xt}$ ,  $N_{yt}$ ,  $N_{xyt}$  are the in-plane compressive mechanical and thermal stresses per unit length along  $x$ ,  $y$  and  $x$ - $y$  directions, respectively. For mechanical loading, in the above expression  $N_{xt}$ ,  $N_{yt}$ ,  $N_{xyt}$  are assumed as zero.

Strain energy due to elastic foundations can be expressed as:

$$\begin{aligned} \Pi_3 = & \frac{1}{2} \int_A \left\{ K_1 w^2 + K_2 \left[ (w_{,x})^2 + (w_{,y})^2 \right] \right\} dA, \\ \Pi_3 = & \frac{1}{2} \int_A \begin{Bmatrix} w \\ w_{,x} \\ w_{,y} \end{Bmatrix}^T \begin{bmatrix} K_1 & 0 & 0 \\ 0 & K_2 & 0 \\ 0 & 0 & K_2 \end{bmatrix} \begin{Bmatrix} w \\ w_{,x} \\ w_{,y} \end{Bmatrix} dA \end{aligned} \quad (18a)$$

## Solution Procedure Using Finite Element Models

### Strain Energy of the Plate Element

the present study, a  $C^0$  nine-noded isoparametric finite element with 7 DOFs per node is employed. For this type of element, the displacement vector and the element geometry are expressed as

$$\{q\} = \sum_{i=1}^{NN} \varphi_i \{q\}_i; \quad x = \sum_{i=1}^{NN} \varphi_i x_i; \quad \text{and} \quad y = \sum_{i=1}^{NN} \varphi_i y_i \quad (19)$$

where  $\varphi_i$  is the interpolation function for the  $i^{th}$  node,  $\{q\}_i$  is the vector of unknown displacements for the  $i^{th}$  node,  $NN$  is the number of nodes per element and  $x_i$  and  $y_i$  are Cartesian coordinate of the  $i^{th}$  node.

The linear mid plane strain vector as given in Eq. (7) can be expressed in terms of mid plane displacement field and then the energy is computed for each element and then summed over all the elements to get the total strain energy [22].

Following this and using finite element model as given in Eq. (19), Eq. (14) after summed over all the elements can be written as

$$\Pi_1 = \sum_{e=1}^{NE} \Pi_1^{(e)} \quad (20)$$

Where,  $NE$  is the number of elements and  $\Pi_1^{(e)}$  is the elemental potential energy of the plate.

Using Eq. (15) and Eq. (17), Eq. (20) can be further expressed as,

$$\begin{aligned}\Pi_1 &= \frac{1}{2} \sum_{e=1}^{NE} \left[ \{q_i\}^{T(e)} [K_{ij}]^{(e)} \{q_j\}^{(e)} - \{q_i\}^{T(e)} [F_i^T]^{(e)} \right] \\ &= \frac{1}{2} \{q_i\}^T [K_{ij}] \{q_j\} - \{q_i\}^T [F_i^T]\end{aligned}\quad (21)$$

where  $[K_{ij}] = [K_{Lij} + K_{NLij}]$  with  $[K_{NLij}] = \frac{1}{2} [K_{NL1ij}] + [K_{NL2ij}] + \frac{1}{2} [K_{NL3ij}]$

where  $[K_{Lij}]$  and  $[K_{NLij}]$  are defined as global linear and nonlinear stiffness matrix of the plate and are defined in Appendix (A.5)

### Thermomechanical Buckling Analysis

Using finite element model of Eq. (19) the Eq. (18) can be written as

$$\begin{aligned}\Pi_2 &= \sum_{e=1}^{NE} \Pi_2^{(e)} = \frac{1}{2} \sum_{e=1}^{NE} \{q_i\}^{T(e)} \lambda [K_{(G)ij}]^{(e)} \{q_j\}^{(e)} dA \\ &= \frac{1}{2} \lambda \{q_i\}^T [K_{(G)ij}] \{q_j\}\end{aligned}\quad (22)$$

where,  $\lambda$  and  $[K_{(G)ij}]$  are defined as the thermal buckling load parameters and the global geometric stiffness matrix (arises due to thermal loadings), respectively.

### Governing Equations

The governing equation for postbuckling analysis of FGMs plates resting on elastic foundations, subjected to thermomechanical loadings can be derived using Variational principle, which is generalization of the principle of virtual displacement. For the displacement field of the buckling, the minimization of  $\Pi(\Pi_1 + \Pi_2 + \Pi_3)$  with respect to generalized displacement vector and after simplification, using this, Eq. (21) and Eq. (22) can be represented as [27]

$$[K_{ij}] \{q_i\} = [F_i^T] \quad (23)$$

For the critical buckling state corresponding to the neutral equilibrium condition, the second variation of total potential energy ( $\Pi$ ) must be zero. Following this conditions, once obtains as standard eigenvalue problem

$$\left\{ \left[ [K_{ij}] + \lambda_i [K_{(G)ij}] \right] \right\} \{q_i\} = 0 \quad (24)$$

Using this Eq. (23) can be rewritten as

$$[K_{ij}] \{q_i\} = \lambda_i [K_{(G)ij}] \{q_i\} \quad (25)$$

The plate stiffness matrix  $[K_{ij}]$  consisting of linear and nonlinear stiffness matrices and geometric stiffness matrix are random in nature, being dependent on the system properties of the structure. Consequently, the eigenvalue and eigenvectors obtained by Eq. (25) are random in nature. In deterministic environment, the solution of Eq. (25) can be obtained using standard solution procedure such as direct iterative method, Newton-raphson method or subspace iteration method etc. However, in random environment it is not possible to obtain the solution using above mentioned numerical methods. Further analysis is required to obtain the complete solution of Eq. (25) with random material properties. For this purpose, novel probabilistic/stochastic DISFEM procedure successfully applied by authors [23] for FGM plates, is extended for this problem in the present work.

### Solution Approach

#### A DISFEM for Postbuckling Problems

The novel probabilistic DISFEM approach is the combination of deterministic based on direct iterative based nonlinear FEM technique successfully combined with mean centred FORPT with reasonable accuracy to obtain the solution of random nonlinear governing equation of postbuckling response. Steps for the direct iterative technique are given in [31].

The detailed DISFEM solution procedure for postbuckling analysis is shown in flowchart of Fig. 4.

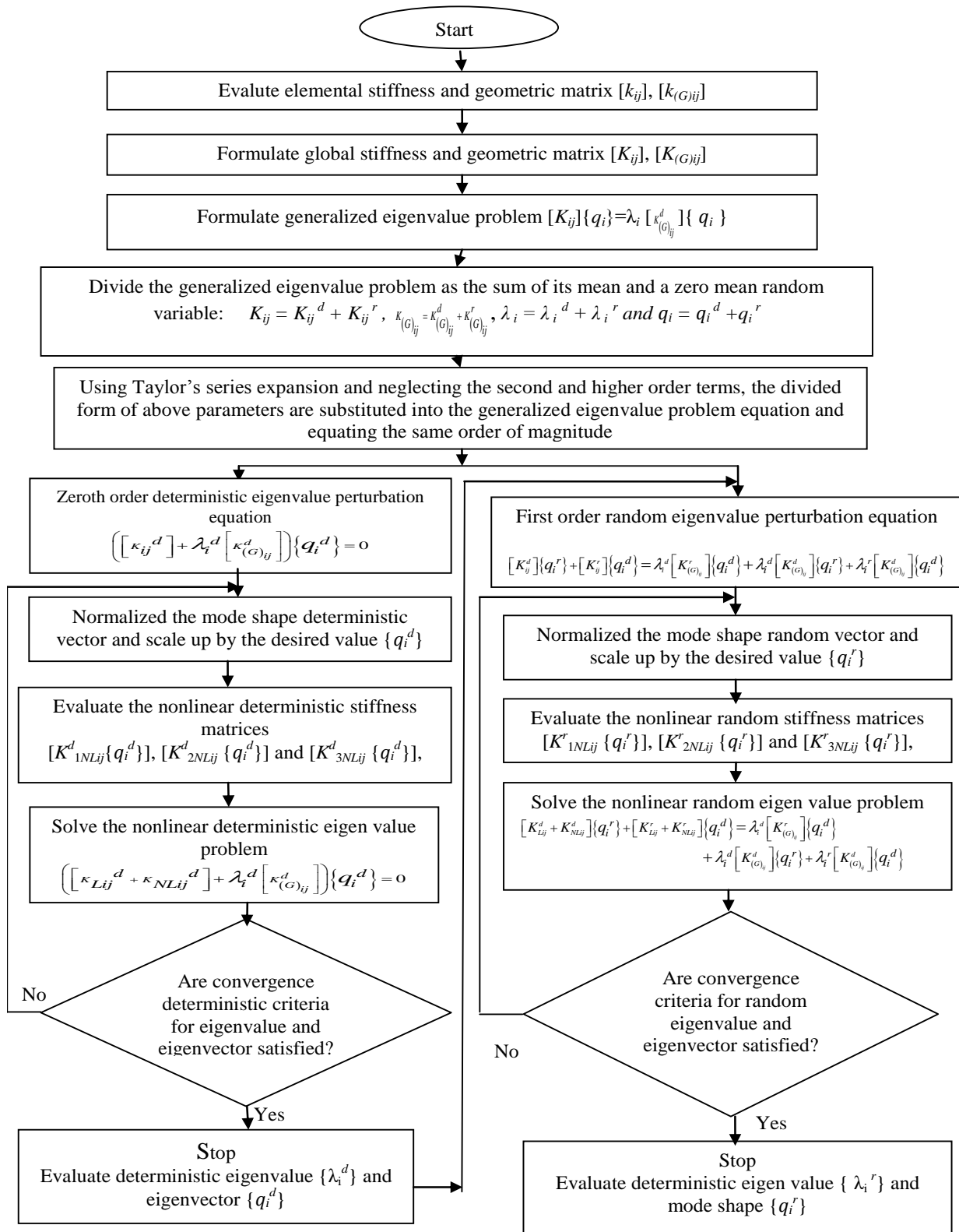


FIGURE.4 FLOW CHART OF SOLUTION PROCEDURE OF STOCHASTIC POSTBUCKLING PROBLEM

### A DISFEM for Postbuckling Problem

The novel probabilistic DISFEM approach is the combination of deterministic based on direct iterative based nonlinear FEM technique successfully combined with mean centered FOPT with reasonable accuracy to obtain the solution of random nonlinear governing equation of postbuckling response.

#### Steps for the Direct Iterative Technique

The nonlinear eigenvalue problem as given in Eq. (25) is solved by employing a DISFEM assuming that the random changes in eigenvector during iterations does not affect the nonlinear stiffness matrices with the following steps.

(i) By setting amplitude to zero, the random linear eigenvalue problem  $\left[ [K_{L_j}] \{q_{L_i}\} = \lambda_i [K_{(G)_j}] \{q_{L_i}\} \right]$  is obtained from Eq. (25) neglecting the nonlinear stiffness matrices. Then the random linear eigenvalue problem is broken up into zeroth and first order equations using perturbation technique. The zeroth order linear eigenvalue problem is solved by normal eigen solution procedure to obtain the linear critical load parameters  $\lambda$  and the linear eigenvector  $\{q_{L_i}\}$ .

The first order perturbation equation is used to obtain the standard deviation of the thermal post buckling load which is presented in next sub-section of perturbation technique. The computation of buckling load and eigenvector under initial thermal stress condition for the zeroth order deterministic eigenvalue problem requires as following.

A linear mechanical and thermal problem by assuming nonlinear stiffness matrix as zero is solved first for the reference mechanical and thermal load  $\{q_i\}$  for a given constraints of the plate. The linear solution is used for computing the initial thermal stress tensor  $\bar{\sigma}_{ij}$ . The thermal stress tensor  $\bar{\sigma}_{ij}$  at each integration point is used to compute the geometric stiffness matrix. After the geometric stiffness matrix is computed, the system stiffness matrix is modified by geometric stiffness matrix to solve the deterministic eigenvalue problem using proposed by Eq. (25). This is generalizes eigenvalue problem where  $[K_{ij}]$  and  $[K_{(G)_i}]$  are symmetric matrices and are generally found to be positive definite. In some cases  $[K_{(G)_i}]$  can be positive semi-definite which can overcome by shifting invert transformation. In such cases the right most eigenvalue gives the minimum value of the mean post buckling load parameter. The critical or minimum mean post buckling load of the structure is obtained by multiplying the load parameter  $\lambda_i$  with reference load (consists of mechanical and thermal).

(ii) For a specified maximum deflection C at a centre of the plate, the linear normalized eigenvector is scaled up by C times, so that resultant vector will have a displacement C at the maximum deflection point.

Using the scale-up eigenvector, the nonlinear terms in the stiffness matrix  $[K_{NL_j}]$  can be obtained. The problem may now be treated as a linear eigenvalue problem with new updated stiffness matrices. The random eigenvalue problem can again be broken up into zeroth and first order equation using perturbation technique. The deterministic zeroth order can be used to obtain critical post buckling load  $\lambda_{NL_i}$  and eigenvector  $\{q_{NL_i}\}$  and the random first order equations can be used to obtain the standard deviation (SD) of the eigen solutions using the first order perturbation technique as presented in the next section.

(iii) Steps (ii)-(iii) are repeated by replacing  $\{q_{L_i}\}$  by  $\{q_{NL_i}\}$  in the step (ii) to obtain the converged mean and standard deviation of the nonlinear critical buckling load  $\lambda_{NL_i}$  to a prescribed accuracy ( $\approx 10^{-3}$ )

(iv) Steps (i) to (iv) are repeated for various value of C.

The detailed DISFEM solution procedure for postbuckling analysis is shown in flowchart of Fig. 2.

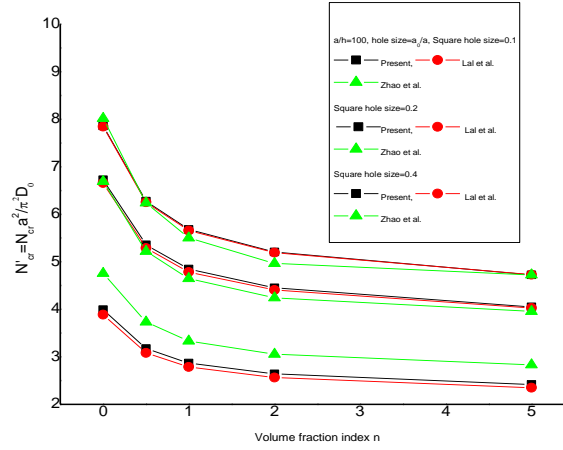


FIGURE.2 VALIDATION STUDY OF DIMENSIONLESS MEAN POSTBUCKING LOAD OF CLAMPED SQUARE FGMS PLATE SUBJECTD TO THERMOMECHANICAL LOADING BIAXIAL COMPRESSION

Consider a class of problems where the random variation is very small as compared to the mean part of random system properties. Further it is quite logical to assume that the dispersions in the derived quantities like  $[K_{ij}]$ ,  $\lambda_{NL}$ , etc. are also small with respect to their mean values. In the present analysis, the lamina material properties, thermal expansion coefficients and the foundation stiffness parameters are treated as independent random variables (RVs). However, the formulation can be easily extended for even dependent random variables.

In general, without any loss of generality any arbitrary random variable can be represented as the sum of its mean and zero mean random part, denoted by superscripts 'd' and 'r', respectively

$$[K_{ij}] = [K_{ij}^d] + [K_{ij}^r], [K_{(G)ij}] = [K_{(G)ij}^d] + [K_{(G)ij}^r], \lambda_i = \lambda_i^d + \lambda_i^r, \{q_i\} = \{q_i^d\} + \{q_i^r\} \quad (26)$$

where,  $[K_{ij}^d]$  and  $[K_{(G)ij}^d]$  are the mean elastic (linear and nonlinear) and geometric stiffness matrices of the structures, respectively. Correspondingly  $[K_{ij}^r]$  and  $[K_{(G)ij}^r]$  are the first order derivatives of elastic and geometric (arises due to plate thickness) matrices, respectively with respect to the  $r^{\text{th}}$  basic random variables (BRV) with "R" is the total number of random input variables chosen for the analysis.

By substituting Eq. (26) in Eq. (25), and expanding the random parts in Taylor's series keeping up to the first order terms and neglecting the second and higher order terms, since first order approximation is sufficient to yield results with the desired accuracy having low variability as in the sensitive applications. After comparing the zeroth and first order terms once obtained as

Zeroth order perturbation equation:

$$\left( [K_{ij}^d] + \lambda_i^d [K_{(G)ij}^d] \right) \{q_i^d\} = 0 \quad (i = 1, 2, 3, \dots, n : \text{no sum over } k) \quad (27)$$

First order perturbation equation:

$$[K_{ij}^d] \{q_i^r\} + [K_{ij}^r] \{q_i^d\} = \lambda_i^d [K_{(G)ij}^r] \{q_i^d\} + \lambda_i^d [K_{(G)ij}^d] \{q_i^r\} + \lambda_i^r [K_{(G)ij}^d] \{q_i^d\} \quad (i = 1, 2, 3, \dots, n : \text{no sum over } k) \quad (28)$$

Here Eq. (27) is the deterministic equation relating to the mean eigen values and corresponding mean eigenvectors, which can be determined by conventional eigen solution procedures Eq. (28) is the random equation, defining the

stochastic nature of the mechanical and thermal buckling which cannot be solved using conventional method. For this a further analysis is required.

**Variance of Postbuckling Load**

The first order equation is used to obtain the first order partial derivatives of eigenvalue with respect to the basic random variables which are then used to the post buckling load covariance.

To obtained the statistics of critical postbuckling load, multiply both sides of Eq. (28) by mean eigenvector  $\{q_i^d\}$  computed from Eq. (27) for minimum mean eigenvalue  $\{\lambda_{cr}^d\}$ . This gives

$$\{q_i^d\} \left( [K_{ij}^d] + \lambda_{cr}^d [K_{(G)ij}^d] \right) \{q_i^r\} = -\lambda_{cr}^r \left( \{q_i^d\} [K_{(G)ij}^d] \{q_j^d\} \right) - \{q_i^d\} \left( [K_{ij}^r] + \lambda_{cr}^d [K_{(G)ij}^r] \right) \{q_j^d\} \tag{29}$$

Since both  $[K_{ij}^d]$  and  $[K_{(G)ij}^d]$  are symmetric therefore the left hand side of Eq. (29) equals zero by definition of the zeroth order equation. By employing  $[K_{(G)ij}^d]$  orthonormal conditions (using orthogonal properties), the first term on the right hand side equation reduces to  $\lambda_{cr}^r$ .

The expression for the first order derivative of the eigenvalue is then written as

$$\lambda_{cr}^r = -\{q_i^d\} \left( [K_{ij}^r] + [K_{(G)ij}^r] \right) \{q_j^d\} \quad (i, j = 1, 2, \dots, n). \tag{30}$$

Using equation (21), the variances of the eigenvalue can now be expressed as [22]

$$Var(\lambda_{cr}) = \sum_{j=1}^p \sum_{k=1}^p \lambda_{i,j}^d \lambda_{i,k}^d Cov(b_j^r, b_k^r) \tag{31}$$

Where  $Cov(b_j^r, b_k^r)$  is the cross variance between  $b_j^r$  and  $b_k^r$ . The standard deviation (SD) is obtained by the square root of the variance. As revealed by the expression, the post buckling load dispersion of the plate exhibits linear variation with all random input variables. The systematic overview of present study is shown in Fig. 3.

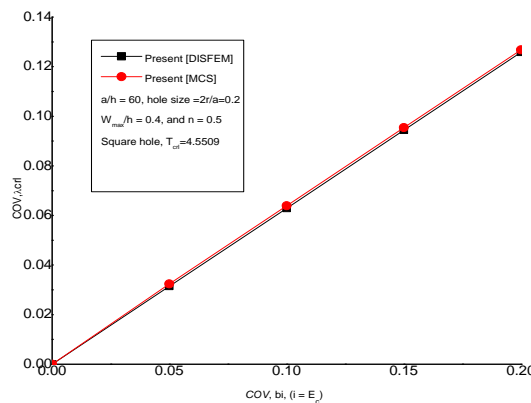


FIGURE.3 VALIDATION STUDY FOR THE COV OF THE INITIAL BUCKLING LOAD DUE TO RANDOMNESS IN MATERIAL PROPERTIES( $b_i, (i=1, \dots, 4)$ ) FOR CCCC BI-AXIALLY COMPRESSED SQUARE Al/ZrO2 PLATE WITH VOLUME FRACTION INDES ( $n = 0.2$  and  $0.8$ ) AND  $a/h = 10$

**Result and Discussions**

A computer programme has been developed in MATLAB [R2010a] environment to compute the second order statistics of postbuckling response of the FGM plate resting on Winkler and Pasternak elastic foundation, subjected

to thermomechanical loading with square cutouts using the proposed DISFEM probabilistic method. The validity and efficacy of the proposed algorithm is examined by comparing the results with those available in literatures and independent MCS. A nine noded Lagrangian isoparametric element with 7 degree of freedom per node for the present HSDT model has been used for discretizing the plate. For the computation of results non-uniform temperature with TID and TD material properties have been taken.

For the computation of results, full integration schemes (3x3) are used for thick plate and selective integration scheme (2x2) for thin plate. In the present analysis, foundation stiffness parameters, various support conditions, volume fraction index and hole sizes are used to check the efficacy of the present model. However, the formulation and code do not put any limitations.

The outlined proposed DISFEM technique for composite structure is extended for FGM structures with reasonable accuracy. Throughout the analysis, it is assumed that materials are perfectly elastic during the deformation.

In the present study, the following sets of boundary conditions are used. These can be written as

All edges simply supported (SSSS)

$$u = v = w = \theta_y = \psi_y = 0, \text{ at } x = 0, a; \quad u = v = w = \theta_x = \psi_x = 0 \text{ at } y = 0, b;$$

All edges clamped (CCCC):

$$u = v = w = \psi_x = \psi_y = \theta_x = \theta_y = 0, \text{ at } x = 0, a \quad \text{and } y = 0, b;$$

Two opposite edges clamped and other two simply supported (CSCS):

$$u = v = w = \psi_x = \psi_y = \theta_x = \theta_y = 0, \text{ at } x = 0 \quad \text{and } y = 0;$$

$$v = w = \theta_y = \psi_y = 0, \text{ at } x = a \quad u = w = \theta_x = \psi_x = 0, \text{ at } y = b;$$

The temperature dependent [TD] material properties of functionally graded materials (Ti-6Al-4V/ZrO<sub>2</sub>) are used throughout the analysis, unless otherwise mentioned. The COV is defined as coefficient of variation. The dimensional mean is represented as dimensional postbuckling thermomechanical critical load. Being the linear nature of variations of COV as mentioned earlier and passing through origin, the results are only presented by coefficient of correlation (COC) of system properties equal to 0.1. However, the presented results for standard deviation revealed that the DISFEM approach would be valid up to COV of 0.2 [24, 30], moreover the presented results would be sufficient to extrapolate the results of other COV keeping in mind the limitation of the FORPT.

The assumed basic random input variables (bi) are sequenced and written as

$$b_1 = E_c, \quad b_2 = E_m, \quad b_3 = \nu_c, \quad b_4 = \nu_m, \quad b_5 = n, \quad b_6 = \alpha_c, \quad b_7 = \alpha_m, \quad b_8 = k_1 \quad \text{and } b_9 = k_2 \quad b_{10} = k_c \quad \text{and } b_{11} = k_m$$

where  $E_c, E_m, \nu_c, \nu_m, \alpha_c, \alpha_m, k_1, k_2, k_c, k_m$  and  $n$  are Young's moduli, Poisson's ratios, coefficient of thermal expansion, Winkler and Pasternak elastic foundations, thermal conductivity of ceramic and metal, respectively and volume fraction index.

The results presented in tables using DISFEM are divided into two parts. In the given table, in first part one set of mean thermomechanical postbuckling load and temperature characteristic of compressive loaded plates with square holes are discussed. In the second part, the effect of randomness in the material properties on the postbuckling load and temperature with and without foundation parameters are presented. These two sets of problems are solved separately to determine the dimensionless mean and COV response of our interest. It is noted that for the present analysis uniaxial and/or biaxial in-plane thermomechanical loading acting separately with square and circular holes have been taken throughout the study. In the present analysis, mean centred first order perturbation technique has been used to compute the numerical results, keeping in mind the complicity and difficulty of using higher order perturbation at cost of very little improvement of results especially for nonlinear

problem. It is also noted that results are presented for lower amplitude ratios ( $W_{max}/h = 0.2$  to  $0.8$ ) due to convergence and computational time for various shaped holes. For the computation of results following dimensionless postbuckling parameters are used and expressed as:

$$\lambda_{cr} = \frac{N_{cr} a^2}{\pi^2 D_0}, \text{ where } D_0 = \frac{E_c h^3}{12(1-\nu_c^2)}, \text{ and } \lambda_{Tcr} = \alpha(\Delta T)_{cr} \times 10^3$$

where  $\lambda_{cr}$  and  $\lambda_{Tcr}$  are dimensionless mean postbuckling load and temperature parameters, respectively. In the above expression,  $N_{cr}$  and  $(\Delta T)_{cr}$  are the dimensional critical postbuckling load and temperature, respectively. In the above expression  $(\Delta T)_{cr}$  is expressed as  $\lambda_T \Delta T$  where  $\lambda_T$  is the critical thermal buckling load parameter and  $\Delta T$  is considered as  $T_c - T_m$ . For the mean dimensional postbuckling analysis of FGM plate, the dimensionless parameters  $\lambda_{cr}$  and  $\lambda_{Tc}$  are used. While for the calculation of coefficient of variance (COV), the dimensional mean  $N_{cr}$  and  $(\Delta T)_{cr}$  are used. It is noted that the values given in parenthesis in the tables are the dimensionless mean values of thermomechanical postbuckling load and temperature. Throughout the analysis both type of loadings, uniaxial and biaxial compression without considering shear effect has been used. For the numerical illustration, the following parameters are taken as plate thickness ratio ( $a/h = 10, 15, 40, 50, 60,$  and  $100$ ), plate aspect ratio ( $a/b = 1$  and  $1.5$ ), amplitude ratio ( $W_{max}/h = 0.2, 0.4, 0.6$  and  $0.8$ ) and volume fraction index ( $n = 0.5, 1, 5$  and  $10$ ). The temperature dependent material properties of functionally graded material are taken in computation as shown in Table 1.

TABLE. 1 THE FOLLOWING Ti-6Al-4V/ZrO2 AND SUS304/ Si3N4 TYPES OF FGMs PROPERTIES FOR TID AND TD MATERIAL PROPERTIES ARE USED FOR COMPUTATION:

Types of material	Properties	$P_0$	$P_{-1}$	$P_1$	$P_2$	$P_3$	$P(T = 300K)$
ZrO <sub>2</sub>	E(Pa)	244.27e+9	0	-1.371e-3	1.214e-6	-3.681e-10	168.06e9
	$\alpha$ (1/K)	12.766e-6	0	-1.491e-3	1.006e-5	-6.778e-11	18.591e-6
Ti-6Al-4V	E(Pa)	122.56e+9	0	-4.586e-4	0	0	105.698e9
	$\alpha$ (1/K)	7.5788e-6	0	6.638e-4	-3.147e-6	0	6.941e-6
SUS304	E(Pa)	201.04e+9	0	30.79e-4	-6.534e-7	0	207.7877e9
	$\alpha$ (1/K)	12.330e-6	0	8.086e-4	0	0	18.591e-6
	$\rho$ (Kg/m <sup>3</sup> )	8166	0	0	0	0	8166
	$\nu$	0.3262	0	0	0	0	0.31776
Si <sub>3</sub> N <sub>4</sub>	E(Pa)	348.43e+9	0	-3.070e-4	2.016e-7	-8.946e-7	322.27e9
	$\alpha$ (1/K)	5.8723e-6	0	9.095e-4	0	0	7.4745e-6
	$\rho$ (Kg/m <sup>3</sup> )	2370	0	0	0	0	2370
	$\nu$	0.2400	0	0	0	0	0.2400

### Validation Study for Mean Postbuckling Response

To make assure the accuracy and proficiency of the present outlined probabilistic formulation, three test examples have been analyzed for postbuckling analysis of FGM plates resting on elastic foundations. For validation purpose, all the plates considered here are subjected to uniaxial compression with uniform or nonuniform temperature distribution. The properties of constituents (metal and ceramic) are assumed at room temperature (300K).

We first consider the accuracy of present deterministic FEM by comparing the results with those available in the literatures. The results of initial buckling load and temperature with cut-out are validated through numerical examples.

Validation study of buckling load parameter ( $\lambda_{cr} = N_{cr} a^2 / \pi^2 D_0$ ) of the SSSS and CCCC supported square Al/ZrO<sub>2</sub> plate with square cut-out under uniaxial compression with  $a/h = 100$ , with those available in Zhao et al. [16] and Lal et al. [31] as shown in Table 2. From these tables, it can be seen that the present outlined approach using C0 nonlinear FEM based on HSDT with von-Karman nonlinearity are in very good agreement with the results of Zhao

et al. [16] and Lal et al. [31], based on first order shear deformation theory in conjunction with the element free kp-Ritz method and third order shear deformation theory respectively.

TABLE 2 VALIDATION STUDY OF BUCKLING LOAD PARAMETER  $\hat{N}_{cr} = N_{cr}a^2/\pi^2D_0$  OF THE CLAMPED SQUARE AL/ZRO2 PLATE WITH SQUARE HOLES UNDER UNIAXIAL COMPRESSION WITH  $A/H = 100$ ,  $MODE = 1$ ,  $HOLE\ SIZE = A_0/A$  FOR SQUARE HOLE.

Types of hole	Hole size		$\hat{N}_{cr} = N_{cr}a^2/\pi^2D_0$				
			$n = 0$	$n = 0.5$	$n = 1$	$n = 2$	$n = 5$
Square	0.1	Present	7.8584	6.2750	5.6788	5.2064	4.7252
		Lal et al.[31]	7.8437	6.2507	5.6570	5.1948	4.7285
		Zhao et al.[16]	8.0186	6.2410	5.5031	4.9665	4.7236
	0.2	Present	6.7232	5.3577	4.8489	4.4527	4.0530
		Lal et al.[31]	6.6566	5.2873	4.7848	4.4049	4.0284
		Zhao et al.[16]	6.6873	5.2212	4.6465	4.2415	3.9557
	0.4	Present	3.9939	3.1724	2.8709	2.6429	2.4171
		Lal et al.[31]	3.8853	3.0813	2.7862	2.5649	2.3490
		Zhao et al.[16]	4.7551	3.7341	3.3344	3.0533	2.8329

### Validation Study for Stochastic Postbuckling Response

The probabilistic results obtained by outlined probabilistic DISFEM approach is also validated with the standard result using independent MCS. In this study, the influence of dispersion in the material properties is examined by allowing the coefficient of correlation (COC) changing from 0 to 20%. It is noted that for the analysis of COV, dimensional mean value of postbuckling load and temperature are taken into consideration throughout the analysis. The COV of postbuckling load and temperature of square simply supported FGM plates resting on elastic foundations subjected to thermomechanical loading with square holes (hole size = 0.2) having TD material properties obtained from present DISFEM approach, when only one material property  $b_i$ , ( $i = E_c$ ) changing at a time keeping others as deterministic to their mean values are examined in Table 3 and compared with independent MCS. For the MCS approach the sample values are generated using MATLAB software to fit the desired mean and SD using Gaussian probabilistic distribution function (GPDF). The convergence of MCS results are studied by taking the different numbers of samples of material properties  $E_c$  which are given as input to the present deterministic Eq. (27) and statistic of the sample of postbuckling load and temperature are calculated. From convergence study, it is experience that 12,000 samples are sufficient to give the desired statistics of postbuckling load and temperature. It is observed that the present results using DISFEM are closed to independent MCS results. This indicates the accuracy of present formulation for the range of COV considered.

TABLE 3 VALIDATION STUDY OF BUCKLING LOAD PARAMETER  $\hat{N}_{cr} = N_{cr}a^2/\pi^2D_0$  OF THE SIMPLY SUPPORTED SQUARE AL/ZRO2 PLATE WITH SQUARE HOLES UNDER UNIAXIAL COMPRESSION WITH  $A/H = 100$ ,  $MODE = 1$ ,  $HOLE\ SIZE = A_0/A$  FOR SQUARE HOLE.

Types of hole	Hole size		$\hat{N}_{cr} = N_{cr}a^2/\pi^2D_0$				
			$n = 0$	$n = 0.5$	$n = 1$	$n = 2$	$n = 5$
Square	0.1	Present	16.8098	13.2298	11.8196	10.7733	9.8987
		Lal et al.[31]	16.6303	13.1110	11.7121	10.6586	9.7705
		Zhao et al.[16]	17.3798	13.1274	10.8931	4.1186	1.6860
	0.2	Present	15.7290	12.3428	11.0292	10.0792	9.3037
		Lal et al.[31]	16.2686	12.7849	11.4230	10.4252	9.6034
		Zhao et al.[16]	15.2566	11.8608	10.4858	9.5211	8.9606

**Parametric Study for Second Order Statistics (Dimensionless Mean and COV) of Postbuckling Response**

Table 4. Effect of thermomechanical loading, volume fraction index with random material properties  $\{b_i (i = 1, \dots, 7) = 0.1\}$  on the dimensionless mean and COV of postbuckling load and temperature of SSSS supported FGM square plate without and with Winkler ( $k_1=100, k_2=0$ ) and Pasternak ( $k_1=100, k_2=10$ ) elastic foundations, square hole (hole size = 0.1) having TID and TD material properties,  $a/h = 50$ , and  $W_{max}/h = 0.4$ . The dimensionless mean thermomechanical postbuckling load and temperature are given in bracket. Uniaxial and Biaxial Compression. It is observed that plate with TID and TD material properties and Pasternak elastic foundations increase the mean and COV compared to Winkler elastic foundations and plates without foundation. TD conditions have significant effects when volume fraction index is increased.

TABLE 4 EFFECT OF THERMOMECHANICAL LOADING, VOLUME FRACTION INDEX WITH RANDOM MATERIAL PROPERTIES  $\{b_i (i = 1, \dots, 7) = 0.1\}$  ON THE DIMENSIONLESS MEAN AND COV OF POSTBUCKLING LOAD AND TEMPERATURE OF SSSS SUPPORTED FGM SQUARE PLATE WITHOUT AND WITH WINKLER ( $k_1=100, k_2=0$ ) AND PASTERNAK ( $k_1=100, k_2=10$ ) ELASTIC FOUNDATIONS, SQUARE HOLE (HOLE SIZE = 0.1) HAVING TID AND TD MATERIAL PROPERTIES,  $A/H = 50$ , AND  $W_{MAX}/H = 0.4$ . THE DIMENSIONLESS MEAN THERMOMECHANICAL POSTBUCKLING LOAD AND TEMPERATURE ARE GIVEN IN BRACKET. UNIAXIAL AND BIAXIAL COMPRESSION.

Loading	Hole types	Uniaxial				Biaxial			
		TID		TD		TID		TD	
		$n = 1$	$n = 5$	$n = 1$	$n = 5$	$n = 1$	$n = 5$	$n = 1$	$n = 5$
Thermo Mechanical	Square hole ( $k_1=000, k_2=0$ ) Nonlinear	(6.5069) 0.0610	(5.2904) 0.0592	(4.7285) 0.0614	(4.0725) 0.0616	(3.3793) 0.0610	(2.7467) 0.0587	0.0612 (2.4561)	0.0610 (2.1149)
	Linear	4.9087	4.1089	3.6698	3.2388	2.5478	2.1313	1.9044	1.6800
	Square hole ( $k_1=100, k_2=0$ ) Nonlinear	(7.8139) 0.0658	(6.5960) 0.0618	(5.636) 0.0657	(4.9800) 0.0626	(4.0976) 0.0664	(3.4653) 0.0617	(2.9504) 0.0659	(2.6093) 0.0620
	Linear	6.2250	5.4219	4.5794	4.1474	3.2662	2.8501	2.3988	2.1746
	Square hole ( $k_1=100, k_2=10$ ) Nonlinear	(10.2880) 0.0720	(9.0244) 0.0670	(7.3707) 0.0718	(6.6970) 0.0670	(5.5361) 0.0741	0.0694 (4.9030)	( 3.9402) 0.0731	0.0679 (3.5987)
	Linear	8.7640	7.9085	6.3473	5.8961	4.7039	4.2870	3.3884	3.1638

Effect of thermo mechanical loading, fibre volume fraction index and various hole sizes with random material properties  $\{b_i (i = 1, \dots, 7) = 0.1\}$  on the dimensionless mean and COV of post buckling load and temperature of SSSS supported FGM square plate without and with Winkler ( $k_1=100, k_2=0$ ) and Pasternak ( $k_1=100, k_2=10$ ) elastic foundations, square holes having TD material properties,  $a/h = 10$ , and  $W_{max}/h = 0.4$  shown in Table 5 . The dimensionless mean thermomechanical post buckling load and temperature are given in bracket. The dimensionless mean thermomechanical post buckling load and temperature are given in bracket. It is noticed that there is significant effects of biaxial compression on the pates without foundations and resting on elastic foundations when there is increase in volume fraction index. The mean and COV values for uniaxial and Pasternak elastic foundations are more compared to biaxially compressed plates.

Table 6 shows the effect of thermo-mechanical loading and amplitude ratios with random material properties  $\{b_i (i = 1, \dots, 7) = 0.1\}$  on the dimensionless mean and COV of postbuckling load and temperature of SSSS supported FGM square plate without and with Winkler ( $k_1=100, k_2=0$ ) and Pasternak ( $k_1=100, k_2=10$ ) elastic foundations, square holes having TD material properties,  $a/h = 60$ , hole size = 0.2 and  $n = 5$ . The dimensionless mean thermomechanical postbuckling load and temperature are given in bracket. It is noticed that when amplitude ratios is increased the

mean values and COV decrease for uniaxially and biaxially compressed plates without elastic foundations. The plates resting on Pasternak elastic foundations have significant effects on mean and COV when there is increase in amplitude ratios, however these value decrease for biaxially compressed plates.

TABLE 5 EFFECT OF THERMOMECHANICAL LOADING, FIBER VOLUME FRACTION INDEX AND VARIOUS HOLE SIZES WITH RANDOM MATERIAL PROPERTIES {BI (I = 1,..., 7) = 0.1} ON THE DIMENSIONLESS MEAN AND COV OF POST BUCKLING LOAD AND TEMPERATURE OF SSSS SUPPORTED FGM SQUARE PLATE WITHOUT AND WITH WINKLER (K1=100, K2=0) AND PASTERNAK (K1=100, K2=10) ELASTIC FOUNDATIONS, SQUARE HOLES HAVING TD MATERIAL PROPERTIES, A/H = 10, AND WMAX/H = 0.4. THE DIMENSIONLESS MEAN THERMOMECHANICAL POST BUCKLING LOAD AND TEMPERATURE ARE GIVEN IN BRACKET.

Loading	Hole Types	Uniaxial				Biaxial			
		n = 0.5		n = 10		n = 0.5		n = 10	
		Hole size=0.1	Hole size=0.2						
Thermo Mechanical	Square hole (k1=000, k2=0) Nonlinear	(4.1306) 0.0666	(3.5789) 0.0670	(3.1167) 0.0649	(2.6957) 0.0661	(2.1406) 0.0659	(2.0679) 0.0659	(1.6158) 0.0639	(1.5589) 0.0639
	Linear	3.1356	2.6729	2.4383	2.0758	1.6198	1.5523	1.2602	1.2072
	Square hole (k1=100, k2=0) Nonlinear	(4.9779) 0.0746	(4.3169) 0.0737	(3.9400) 0.0658	(3.4047) 0.0666	(2.6400) 0.0716	(2.5718) 0.0715	(2.1147) 0.0619	(2.0620) 0.0618
	Linear	4.0494	3.4194	3.3317	2.7906	2.1208	2.0504	1.7607	1.7043
	Square hole (k1=100, k2=10) Nonlinear	(6.5754) 0.1727	(5.6083) 0.0786	(5.6032) 0.0698	(4.6085) 0.0689	(3.6313) 0.0788	(3.5446) 0.0785	(3.1039) 0.0679	(3.0311) 0.0675
	Linear	5.6909	4.6713	4.8195	3.9280	3.1128	3.0109	2.7502	2.6593

TABLE 6 EFFECT OF THERMOMECHANICAL LOADING AND AMPLITUDE RATIOS WITH RANDOM MATERIAL PROPERTIES {BI(I = 1,..., 7) = 0.1} ON THE DIMENSIONLESS MEAN AND COV OF POSTBUCKLING LOAD AND TEMPERATURE OF SSSS SUPPORTED FGM SQUARE PLATE WITHOUT AND WITH WINKLER (K1=100, K2=0) AND PASTERNAK (K1=100, K2=10) ELASTIC FOUNDATIONS, SQUARE HOLES HAVING TD MATERIAL PROPERTIES, A/H = 60, HOLE SIZE = 0.2 AND N = 5. THE DIMENSIONLESS MEAN THERMOMECHANICAL POSTBUCKLING LOAD AND TEMPERATURE ARE GIVEN IN BRACKET.

Loading	Hole types	Uniaxial				Biaxial			
		Wmax/h = 0.2	Wmax/h = 0.4	Wmax/h = 0.6	Wmax/h = 0.8	Wmax/h = 0.2	Wmax/h = 0.4	Wmax/h = 0.6	Wmax/h = 0.8
Thermo Mechanical	Square hole (k1=000, k2=0) Nonlinear	(3.4219) 0.0690	(3.9810) 0.0621	(4.7779) 0.0558	(4.8907) 0.0652	(1.8093) 0.0687	(2.1068) 0.0612	(2.5570) 0.0535	( 3.1591) 0.0469
	Linear	3.1471	3.1471	3.1471	3.1471	1.6652	1.6652	1.6652	1.6652
	Square hole (k1=100, k2=0) Nonlinear	(4.2814) 0.0708	(4.8151) 0.0654	(5.5737) 0.0610	(5.8109) 0.0690	(2.3011) 0.0711	(2.6004) 0.0647	(3.0530) 0.0577	(3.6563) 0.0512
	Linear	4.0183	4.0183	4.0183	4.0183	2.1560	2.1560	2.1560	2.1560
	Square hole (k1=100, k2=10) Nonlinear	(5.8566) 0.1566	( 6.3874) 0.1406	(7.2430) 0.1478	(8.1437) 0.0652	( 3.2620) 0.1838	(3.5641) 0.1920	(4.0204) 0.1939	(4.6281) 0.1911
	Linear	5.6054	5.6054	5.6054	5.6054	3.1155	3.1155	3.1155	3.1155

Effect of thermomechanical loading, volume fraction index, plate thickness ratios and various hole size with random material properties  $\{b_i(i = 1, \dots, 7) = 0.1\}$  on the dimensionless mean and COV of post buckling load and temperature of SSSS supported biaxially compressed FGM square plate without and with Winkler ( $k_1=100, k_2=0$ ) and Pasternak ( $k_1=100, k_2=10$ ) elastic foundations square holes having TD material properties,  $W_{max}/h = 0.4$  presented in Table 7. The dimensionless mean thermomechanical postbuckling load and temperature are given in bracket. It is seen that on varying plate thickness ratios and volume fraction index with increase in hole size the mean valued decrease while COV increases for plates without foundations. When plates are resting on Winkler and Pasternak elastic foundations, the mean values increases and decreases on increasing volume fraction index. COV is significant thin plates compared to thick plates.

Table 8 shows the effect of thermomechanical loading, volume fraction index, plate aspect ratios and various hole size with random material properties  $\{b_i(i = 1, \dots, 7) = 0.1\}$  on the dimensionless mean and COV of postbuckling load and temperature of SSSS supported uniaxially compressed FGM plate without and with Winkler ( $k_1=100, k_2=0$ ) and Pasternak ( $k_1=100, k_2=10$ ) elastic foundations ,square holes having TD material properties,  $a/h = 50, W_{max}/h = 0.4$ . The dimensionless mean thermomechanical postbuckling load and temperature are given in bracket. It is noticed that for aspect ratio 2 with volume fraction index 10 and hole size 0.3there is significant decrease in mean values without foundation conditions. However when plates are resting on elastic foundations the mean values increases drastically for lower volume fraction index. The COV significantly increases for Pasternak elastic foundations. Here hole size aspect ratio volume fraction index and elastic foundation matter much.

TANBLE 7 EFFECT OF THERMOMECHANICAL LOADING, VOLUME FRACTION INDEX, PLATE THICKNESS RATIOS AND VARIOUS HOLE SIZE WITH RANDOM MATERIAL PROPERTIES  $\{b_i(i = 1, \dots, 7) = 0.1\}$  ON THE DIMENSIONLESS MEAN AND COV OF POSTBUCKLING LOAD AND TEMPERATURE OF SSSS SUPPORTED BIAXIALY COMPRESSED FGM SQUARE PLATE WITHOUT AND WITH WINKLER ( $k_1=100, k_2=0$ ) AND PASTERNAK ( $k_1=100, k_2=10$ ) ELASTIC FOUNDATIONS SQUARE HOLES HAVING TD MATERIAL PROPERTIES,  $W_{MAX}/H = 0.4$ . THE DIMENSIONLESS MEAN THERMOMECHANICAL POSTBUCKLING LOAD AND TEMPERATURE ARE GIVEN IN BRACKET.

Loading	Hole types	$a/h = 40$				$a/h = 100$			
		$n = 0.5$		$n = 10$		$n = 0.5$		$n = 10$	
		Hole size=0.2	Hole size=0.3						
Thermo Mechanical	Square hole ( $k_1=000, k_2=0$ ) Nonlinear	(2.6777) 0.0670	(2.7209) 0.0670	(2.0308) 0.0658	(2.0625) 0.0663	(3.0601) 0.0679	(3.0002) 0.0679	(2.3189) 0.0677	(2.2785) 0.0679
	Linear	2.0790	2.1005	1.6238	1.6409	2.4319	2.3694	1.8931	1.8505
	Square hole ( $k_1=100, k_2=0$ ) Nonlinear	(3.2175) 0.0735	(3.2658) 0.0735	(2.5703) 0.0663	(2.6069) 0.0666	(3.5914) 0.0733	(3.5409) 0.0734	(2.8502) 0.0667	(2.8187) 0.0671
	Linear	2.6158	2.6421	2.1604	2.1821	2.9585	2.9028	2.4204	2.3841
	Square hole ( $k_1=100, k_2=10$ ) Nonlinear	(4.2689) 0.3252	(4.2854) 0.2967	(3.6197) 0.1621	(3.6230) 0.1444	(4.6352) 0.3075	(4.5641) 0.2912	(3.8931) 0.1511	(3.8374) 0.1374
	Linear	3.6624	3.6561	3.2052	3.1919	3.9972	3.9104	3.4585	3.3892

Effect of thermomechanical loading, volume fraction index, support conditions and various hole size with random material properties  $\{b_i(i = 1, \dots, 7) = 0.1\}$  on the dimensionless mean and COV of postbuckling load and temperature of uniaxially compressed FGM square plate without and with Winkler ( $k_1=100, k_2=0$ ) and Pasternak ( $k_1=100, k_2=10$ ) elastic foundations, square holes having TD material properties,  $a/h = 15, W_{max}/h = 0.4$  is shown in Table 9. The dimensionless mean thermomechanical postbuckling load and temperature are given in bracket. It is observed that Pasternak elastic foundation with clamp support with volume fraction index 0.5 and hole size 0.3 have significant effects on the plates compared to simple support. Mean and COV both increase for plates resting on elastic foundations.

TABLE 8 EFFECT OF THERMOMECHANICAL LOADING, VOLUME FRACTION INDEX, PLATE ASPECT RATIOS AND VARIOUS HOLE SIZE WITH RANDOM MATERIAL PROPERTIES  $\{b_i(i = 1, \dots, 7) = 0.1\}$  ON THE DIMENSIONLESS MEAN AND COV OF POSTBUCKLING LOAD AND TEMPERATURE OF SSSS SUPPORTED UNIAXIALLY COMPRESSED FGM PLATE WITHOUT AND WITH WINKLER ( $k_1=100, k_2=0$ ) AND PASTERNAK ( $k_1=100, k_2=10$ ) ELASTIC FOUNDATIONS, SQUARE HOLES HAVING TD MATERIAL PROPERTIES,  $a/h = 50, W_{max}/h = 0.4$ . THE DIMENSIONLESS MEAN THERMOMECHANICAL POSTBUCKLING LOAD AND TEMPERATURE ARE GIVEN IN BRACKET.

Loading	Hole types	$a/b = 1$				$a/b = 2.0$			
		$n = 0.5$		$n = 10$		$n = 0.5$		$n = 10$	
		Hole size=0.2	Hole size=0.3						
Thermo Mechanical	Square hole ( $k_1=000, k_2=0$ ) Nonlinear	(4.6826) 0.0675	(4.5740) 0.0684	(3.5565) 0.0671	(3.4729) 0.0693	(4.8495) 0.0764	(1.1946) 0.0793	(3.3311) 0.0943	(0.9059) 0.0954
	Linear	3.6516	3.5459	2.8526	2.7725	4.1891	0.5224	2.8352	0.3479
	Square hole ( $k_1=100, k_2=0$ ) Nonlinear	(5.5051) 0.0736	(5.2967) 0.0745	(4.3774) 0.0676	(4.1952) 0.0703	(1.1229) 0.2859	(1.2586) 0.0788	(3.3557) 0.0931	(1.1046) 0.0695
	Linear	4.5142	4.3275	3.7090	3.5412	4.2272	0.5808	2.8828	0.4122
	Square hole ( $k_1=100, k_2=10$ ) Nonlinear	(7.0754) 0.3095	(6.5918) 0.2020	(5.9100) 0.1283	(5.4214) 0.0775	(2.1345) 2.9312	(1.9358) 0.2017	(3.9444) 0.1231	(1.6055) 0.1239
	Linear	6.1123	5.6594	5.2500	4.8020	0.0695	1.0891	3.2920	0.9409

TABLE 9 EFFECT OF THERMOMECHANICAL LOADING, VOLUME FRACTION INDEX, SUPPORT CONDITIONS AND VARIOUS HOLE SIZE WITH RANDOM MATERIAL PROPERTIES  $\{b_i(i = 1, \dots, 7) = 0.1\}$  ON THE DIMENSIONLESS MEAN AND COV OF POSTBUCKLING LOAD AND TEMPERATURE OF UNIAXIALLY COMPRESSED FGM SQUARE PLATE WITHOUT AND WITH WINKLER ( $k_1=100, k_2=0$ ) AND PASTERNAK ( $k_1=100, k_2=10$ ) ELASTIC FOUNDATIONS, SQUARE HOLES HAVING TD MATERIAL PROPERTIES,  $a/h = 15, W_{max}/h = 0.4$ . THE DIMENSIONLESS MEAN THERMOMECHANICAL POSTBUCKLING LOAD AND TEMPERATURE ARE GIVEN IN BRACKET.

Loading	Hole types	SSSS				CCCC			
		$n = 0.5$		$n = 10$		$n = 0.5$		$n = 10$	
		Hole size=0.2	Hole size=0.3						
Thermo Mechanical	Square hole ( $k_1=000, k_2=0$ ) Nonlinear	(3.8201) 0.0668	(3.6290) 0.0681	(2.8855) 0.0658	(2.7360) 0.0682	(5.8418) 0.0974	(7.4320) 0.0954	(4.4943) 0.1135	(5.6934) 0.0912
	Linear	2.8872	2.7393	2.2481	2.1269	5.5351	7.3038	4.2621	5.6013
	Square hole ( $k_1=100, k_2=0$ ) Nonlinear	(4.5783) 0.0742	(4.2725) 0.0753	(3.6356) 0.0679	(3.3567) 0.0704	(6.2918) 0.1315	(7.5269) 0.0983	(4.6210) 0.0881	(5.7849) 0.0911
	Linear	3.6742	3.4336	3.0171	2.7952	5.8486	7.3927	4.5534	5.6892
	Square hole ( $k_1=100, k_2=10$ ) Nonlinear	(5.9608) 0.2952	(5.3478) 0.1608	(4.9264) 0.1275	(5.4049) 0.0800	(7.1997) 0.1412	(8.5721) 0.0850	(5.8531) 0.1097	(6.9278) 0.1343
	Linear	5.0488	4.5924	4.2926	4.7920	7.1054	8.5494	5.7912	6.8291

## Conclusions

The DISFEM procedure outlined in the present study is applied to compute the second order statistics (mean and COV) of postbuckling load and temperature of uniaxially or biaxially compressed FGM plates resting on Winkler and Pasternak elastic foundations with square holes of various sizes subjected to thermomechanical loading. The following conclusions are drawn based on observation from present study.

The mean dimensionless thermomechanical postbuckling load and temperature and corresponding COV of FGM plate subjected to uniaxial and biaxial compression decreases with increase in cutout size. The dimensionless mean postbuckling load and temperature and corresponding COV is higher for solid plate as compared to cutout plates. Plate is most sensitive with random change in  $E_c$  and  $E_m$  of FGM plate with Pasternak elastic foundation square cutout.

In general, as amplitude ratio increases the dimensionless mean postbuckling load increases while COV decreases. But increase in volume fraction index results in decrease in dimensionless mean postbuckling load. The dimensionless mean and COV of postbuckling load and temperature of FGM plate changes with the volume fraction index, thickness ratio, plate aspect ratio, types of loading, support conditions and types of material where stability at the cost of load is utmost important.

Thin plate with square cut-out is more sensitive than thick plate with respect to dimensionless mean and COV of postbuckling load and temperature subjected to uniaxial and biaxial compression. Therefore, for stability and reliability point of view rectangular plate with square cut-out having low volume fraction and Pasternak elastic foundation should be considered. For stability and reliability point of view, clamped supported plates with various shaped and cut-out would be desirable.

## Appendix A:

$$[H_{mm}] = \begin{bmatrix} 1 & 0 & 0 & z & 0 & 0 & z^3 & 0 & 0 & 0 & 0 & 0 & 0 \\ 0 & 1 & 0 & 0 & z & 0 & 0 & z^3 & 0 & 0 & 0 & 0 & 0 \\ 0 & 0 & 1 & 0 & 0 & z & 0 & 0 & z^3 & 0 & 0 & 0 & 0 \\ 0 & 0 & 0 & 0 & 0 & 0 & 0 & 0 & 0 & 1 & 0 & z^2 & 0 \\ 0 & 0 & 0 & 0 & 0 & 0 & 0 & 0 & 0 & 0 & 1 & 0 & z^2 \end{bmatrix}, \quad (\text{A.1})$$

$$\bar{C}_{ijkl} = \begin{bmatrix} \bar{Q}_{11} & \bar{Q}_{12} & \bar{Q}_{16} & 0 & 0 \\ \bar{Q}_{12} & \bar{Q}_{22} & \bar{Q}_{26} & 0 & 0 \\ \bar{Q}_{16} & \bar{Q}_{26} & \bar{Q}_{66} & 0 & 0 \\ 0 & 0 & 0 & \bar{Q}_{44} & \bar{Q}_{45} \\ 0 & 0 & 0 & \bar{Q}_{45} & \bar{Q}_{55} \end{bmatrix} \quad (\text{A.2})$$

where,

$$\bar{Q}_{11} = \bar{Q}_{22} = \frac{E(z,T)}{1-\nu^2}, \quad \bar{Q}_{12} = \frac{\nu E(z,T)}{1-\nu^2}, \quad \bar{Q}_{44} = \bar{Q}_{55} = \bar{Q}_{66} = \frac{E(z,T)}{2(1+\nu)},$$

$$\bar{Q}_{16} = \bar{Q}_{26} = \bar{Q}_{45} = \bar{Q}_{54} = 0$$

$$D_{mn} = \begin{bmatrix} A_{1ij} & B_{ij} & E_{ij} & 0 & 0 \\ B_{ij} & D_{1ij} & F_{1ij} & 0 & 0 \\ E_{ij} & F_{1ij} & H_{ij} & 0 & 0 \\ 0 & 0 & 0 & A_{2ij} & D_{2ij} \\ 0 & 0 & 0 & D_{2ij} & F_{2ij} \end{bmatrix} \quad (\text{A.3})$$

where,

$$\left( A_{1ij}, B_{ij}, D_{1ij}, E_{ij}, F_{1ij}, H_{ij} \right) = \int_{-h/2}^{h/2} \bar{Q}_{ij} \left( 1, z, z^2, z^3, z^4, z^6 \right) dz \quad (i, j = 1, 2, 6)$$

$$\left( A_{2ij}, D_{2ij}, F_{2ij} \right) = \int_{-h/2}^{h/2} \bar{Q}_{ij} \left( 1, z^2, z^4 \right) dz \quad (i, j = 4, 5)$$

With

$$\begin{aligned} A_{ij} &= \int_{-h/2}^{h/2} \left\{ Q_{ij}^m + (Q_{ij}^c - Q_{ij}^m) \left[ \frac{z}{h} + \frac{1}{2} \right]^n \right\} dz \\ &= Q_{ij}^m h + (Q_{ij}^c - Q_{ij}^m) h \left[ \frac{1}{n+1} \right] \end{aligned}$$

$$\begin{aligned} B_{ij} &= \int_{-h/2}^{h/2} \left\{ Q_{ij}^m + (Q_{ij}^c - Q_{ij}^m) \left[ \frac{z}{h} + \frac{1}{2} \right]^n \right\} z dz \\ &= Q_{ij}^m h^2 + (Q_{ij}^c - Q_{ij}^m) h^2 \left[ \frac{1}{n+2} - \frac{1}{2(n+1)} \right] \end{aligned}$$

$$\begin{aligned} D_{1ij} &= \int_{-h/2}^{h/2} \left\{ Q_{ij}^m + (Q_{ij}^c - Q_{ij}^m) \left[ \frac{z}{h} + \frac{1}{2} \right]^n \right\} z^2 dz \\ &= Q_{ij}^m h^3 + (Q_{ij}^c - Q_{ij}^m) h^3 \left[ \frac{1}{n+3} - \frac{1}{n+2} + \frac{1}{4(n+1)} \right] \end{aligned}$$

$$\begin{aligned} E_{ij} &= \int_{-h/2}^{h/2} \left\{ Q_{ij}^m + (Q_{ij}^c - Q_{ij}^m) \left[ \frac{z}{h} + \frac{1}{2} \right]^n \right\} z^3 dz \\ &= Q_{ij}^m h^4 + (Q_{ij}^c - Q_{ij}^m) h^4 \left[ \frac{1}{n+4} - \frac{3}{2(n+3)} + \frac{3}{4(n+2)} - \frac{1}{8(n+1)} \right] \end{aligned}$$

$$\begin{aligned} F_{1ij} &= \int_{-h/2}^{h/2} \left\{ Q_{ij}^m + (Q_{ij}^c - Q_{ij}^m) \left[ \frac{z}{h} + \frac{1}{2} \right]^n \right\} z^4 dz \\ &= Q_{ij}^m h^5 + (Q_{ij}^c - Q_{ij}^m) h^5 \left[ \frac{1}{n+5} - \frac{2}{(n+4)} + \frac{3}{2(n+3)} - \frac{1}{2(n+2)} + \frac{1}{16(n+1)} \right] \end{aligned}$$

$$\begin{aligned} H_{ij} &= \int_{-h/2}^{h/2} \left\{ Q_{ij}^m + (Q_{ij}^c - Q_{ij}^m) \left[ \frac{z}{h} + \frac{1}{2} \right]^n \right\} z^6 dz \\ &= Q_{ij}^m h^7 + (Q_{ij}^c - Q_{ij}^m) h^7 \left[ \frac{1}{n+7} - \frac{3}{n+6} + \frac{15}{4(n+5)} - \frac{5}{2(n+4)} + \frac{15}{16(n+3)} - \frac{3}{16(n+2)} + \frac{1}{64(n+1)} \right] \end{aligned}$$

$$[D_3] = \begin{bmatrix} [A_1] & 0 \\ [B] & 0 \\ [E] & 0 \\ 0 & [A_2] \\ 0 & [C_2] \end{bmatrix}, \quad [D_4] = [D_3]^T \quad \text{and} \quad [D_5] = \begin{bmatrix} [A_1] & 0 \\ 0 & [A_2] \end{bmatrix} \quad (\text{A.4})$$

$$[K_L] = \int_A \{B_L\}^T [D_{mm}] \{B_L\} dA \quad (\text{A.5a})$$

$$[K_{NL_1}] = \int_A \{B_{NL}\}^T [D_3] \{B_L\} dA \quad (\text{A.5b})$$

$$[K_{NL_2}] = \frac{1}{2} \int_A \{B_L\}^T [D_4] \{B_{NL}\} dA \quad (\text{A.5c})$$

$$[K_{NL_3}] = \frac{1}{2} \int_A \{B_{NL}\}^T [D_5] \{B_{NL}\} dA \quad (\text{A.5d})$$

$$[K_g] = \frac{1}{2} \int_A \{B_g\}^T [N_0] \{B_g\} dA \quad (\text{A.5e})$$

where,

$$[N_0] = \begin{bmatrix} N_{xym} & N_{xytm} \\ N_{xytm} & N_{ytm} \end{bmatrix}$$

$$[B_L] = \begin{bmatrix} \varphi_{i,x} & 0 & 0 & 0 & 0 & 0 & 0 \\ 0 & \varphi_{i,y} & 0 & 0 & 0 & 0 & 0 \\ \varphi_{i,y} & \varphi_{i,x} & 0 & 0 & 0 & 0 & 0 \\ 0 & 0 & 0 & 0 & 0 & 0 & C_1\varphi_{i,x} \\ 0 & 0 & 0 & 0 & 0 & C_1\varphi_{i,y} & 0 \\ 0 & 0 & 0 & 0 & 0 & C_1\varphi_{i,y} & C_1\varphi_{i,x} \\ 0 & 0 & 0 & 0 & -C_4\varphi_{i,x} & 0 & -C_2\varphi_{i,x} \\ 0 & 0 & 0 & -C_4\varphi_{i,y} & 0 & -C_4\varphi_{i,y} & 0 \\ 0 & 0 & 0 & -C_4\varphi_{i,x} & -C_4\varphi_{i,y} & -C_2\varphi_{i,y} & -C_2\varphi_{i,y} \\ 0 & 0 & 0 & 0 & 0 & -C_1 & 0 \\ 0 & 0 & \varphi_{i,y} & 0 & 0 & 0 & -C_1 \\ 0 & 0 & \varphi_{i,x} & -3C_4 & 0 & -3C_2 & 0 \\ 0 & 0 & 0 & 0 & -3C_4 & 0 & -3C_2 \end{bmatrix}$$

$$[B_{NL}] = \begin{bmatrix} 0 & 0 & \varphi_{,x^2} & 0 & 0 & 0 & 0 \\ 0 & 0 & \varphi_{,y^2} & 0 & 0 & 0 & 0 \\ 0 & 0 & 2\varphi_{,x}\varphi_{,y} & 0 & 0 & 0 & 0 \\ 0 & 0 & 0 & 0 & 0 & 0 & 0 \\ 0 & 0 & 0 & 0 & 0 & 0 & 0 \end{bmatrix}$$

$$[B_g] = \begin{bmatrix} 0 & 0 & \varphi_i & 0 & 0 & 0 & 0 \\ 0 & 0 & \varphi_{i,x} & 0 & 0 & 0 & 0 \\ 0 & 0 & \varphi_{i,x} & 0 & 0 & 0 & 0 \end{bmatrix}$$

## REFERENCES

- [1] Fuchiyama T, Noda N. Analysis of thermal stresses in a plate of functionally gradient material. Japanese Society of Automotive Engineers 1995;16(3):263–268.
- [2] Feldman E, Aboudi J. Buckling analysis of functionally graded plates subjected to uniaxial loading. Composite Structures 1997;38:29–36.
- [3] Noda N. Thermal stresses in functionally graded materials. Proceedings of the Third International Congress on Thermal Stresses, Cracow, Poland 1999;33–38.
- [4] Reddy JN. Analysis of functionally graded plates. International Journal of Numerical Methods in Engineering 2000;47:663–684.
- [5] Javaheri R, Eslami MR. Buckling of functionally graded plates under in-plane compressive loading. Z Angew Math Mech 2002;82(4):277–283.
- [6] Javaheri R, Eslami MR. Thermal buckling of functionally graded plates. AIAA Journal 2002;40(1):162–169.
- [7] Najafzadeh MM, Eslami MR. Buckling analysis of circular plates of functionally graded materials under uniform radial compression. International Journal of Mechanical Sciences 2002;44:2474–2493.
- [8] Vel SS, Batra RC. Exact solution for thermo-elastic deformations of functionally graded thick rectangular plates. AIAA Journal 2002;40:1421–1433.
- [9] Yang J, Shen HS. Non-linear analysis of functionally graded plates under transverse and in-plane loads. International Journal of Non-linear Mechanics 2003;38:467–482.

- [10] Ma LS, Wang TJ. Non linear bending and post-buckling of a functionally graded circular plate under mechanical and thermal loadings. *International Journal of Solids and Structures* 2003;40:3311–3330.
- [11] Wu L. Thermal buckling of a simply supported moderately thick rectangular FGM plate. *Composite Structures* 2004;64:211–218.
- [12] Na KS, Kim JH. Three-dimensional thermal buckling analysis of functionally graded materials. *Composites: Part B* 2004;35:429–437.
- [13] Na KS, Kim JH. Three-dimensional thermomechanical buckling analysis for functionally graded composite plates. *Composite Structures* 2006;73(4):413–422.
- [14] Wu TL, Shukla KK, Huang JH. Postbuckling analysis of functionally graded rectangular plates. *Composite Structures* 2007;81:1–10.
- [15] Saji D, Byji V, Pradhan SC. Finite element analysis for thermal buckling behaviour in functionally graded plates with cut-outs. *Proceedings of the International Conference on Aerospace Science and Technology, Bangalore, India (26-28 June 2008)*.
- [16] Zhao X, Lee YY, Liew KM. Mechanical and thermal buckling analysis of functionally graded plates. *Composite Structures* 2009;90:161–171.
- [17] Matsunaga H. Thermal buckling of functionally graded plates according to a 2D higher-order deformation theory. *Composite Structures* 2009;90:76–86.
- [18] Lee YY, Zhao X, Reddy JN. Postbuckling analysis of functionally graded plates subject to compressive and thermal loads. *Computer Methods in Applied Mechanics and Engineering* 2010;199:1645–1653.
- [19] Singh BN, Iyengar NGR, Yadav D. A C0 finite element investigation for buckling of shear deformable laminated composite plates with random material properties. *International Journal of Structural Engineering and Mechanics* 2002; 113(1):53–74.
- [20] Yang J, Kitipornchai S, Liew KM. Second order statistic of the elastic buckling of functionally graded rectangular plates. *Composite Science and Technology* 2005;65:1165–1175.
- [21] Onkar AK, Upadhyay CS, Yadav D. Stochastic finite element analysis buckling analysis of laminated with circular cut-outs under uniaxial compression. *Trans ASME Journal of Applied Mechanics* 2007;74:789–809.
- [22] Singh BN, Lal A, Rajesh Kumar. Postbuckling response of laminated composite plate on elastic foundation with random system properties. *Communications in Nonlinear Science and Numerical Simulation* 2009;14:284–300.
- [23] Jagtap KR, Lal A, Singh BN. Stochastic nonlinear free vibration analysis of elastically supported functionally graded materials plate with system randomness in thermal environment. *Composite Structures* 2011;93:3185–3199.
- [24] Kleiber M, Hien TD. *The stochastic finite element method*. Wiley, New York 1992.
- [25] Shen HS. *Functionally graded materials: Nonlinear Analysis of plate and shells*. CRC Press, Taylor and Frances Group, 2009.
- [26] Zhang Y, Chen S, Lue Q, Liu T. Stochastic perturbation finite elements. *Computers and Structures* 1996;23: 1831-45.
- [27] Reddy JN. *Energy and Variational Methods in Applied Mechanics*, John Wiley and Sons, 1984.
- [28] Reddy JN. A simple higher order theory for laminated composite plates. *Journal of Applied Mechanic Trans ASME* 1984;51:745–52.
- [29] Shankar CA, Iyengar NGR. A C0 element for the free vibration analysis of laminated composite plates. *Journal of Sound and Vibration* 1996;191(5): 721-738.
- [30] Zhang Y, Chen S, Lue Q, Lui T. Stochastic perturbation finite elements. *Computers and Structures* 1996;23: 1831-1845.
- [31] Lal A, Jagtap KR and Singh B.N. Postbuckling response of functionally graded plate subjected to mechanical and thermal loadings with random material properties. *Applied Mathematical Modelling*. Elsevier. 2012. DOI.org/10.1016.
- [32] Alireza Hassanzadeh Taheri, Mohammad Hossein Abolbashari and Behrooz Hassani. Free vibration characteristics of functionally graded structures by an isogeometrical analysis approach. *Compos. Struct.* 2013; 99: 309-326.

- [33] Yin S, Yu T, Bui T.Q, Xia S and Hirose S. A cut-out isogeometric analysis for thin laminated composite plates using level sets. *Compos. Struct.* 2015, 127, 152–164.
- [34] Shuohui Yin, Tiantang Yu, Tinh Quoc Bui, Xuejun Zheng and Satoyuki Tanaka. In-plane material inhomogeneity of functionally graded plates: A higher-order shear deformation plate isogeometric analysis. *Composites Part B: Engineering* ; 2016,106: 273-284.
- [35] Tiantang Yu, Tinh Quoc Bui, Shuohui Yin, Duc Hong Doan, C.T. Wu, Thom Van Do and Satoyuki Tanaka. On the thermal buckling analysis of functionally graded plates with internal defects using extended isogeometric analysis. *Composite Structures*; 2016,136:684-695.

### Nomenclature

$A_{ij}, B_{ij}, etc$	: Laminate stiffnesses
$a, b$	: Plate length and breadth
$h$	: Thickness of the plate
$E_f, E_m$	: Elastic moduli of fiber and matrix, respectively.
$G_f, G_m$	: Shear moduli of fiber and matrix, respectively.
$\nu_f, \nu_m$	: Poisson's ratio of fiber and matrix, respectively.
$V_m, V_f$	: Volume fraction of fiber and matrix, respectively.
$\alpha_f, \alpha_m$	: Coefficient of thermal expansion of fiber and matrix, respectively.
$b_i$	: Basic random material properties
$E_{11}, E_{22}$	: Longitudinal and Transverse elastic moduli
$G_{12}, G_{13}, G_{23}$	: Shear moduli
$K_l$	: Linear bending stiffness matrix
$K_g$	: Thermal geometric stiffness matrix
$D$	Elastic stiffness matrices
$M_{\alpha\beta}, m_{\alpha\beta}$	: Mass and inertia matrices
$n_e, n$	: Number of elements, number of layers in the laminated plate
$N_x, N_y, N_{xy}$	In-plane thermal buckling loads
$nm$	: Number of nodes per element
$N_i$	: Shape function of $i$ th node
$\bar{C}_{ijkl}^p$	: Reduced elastic material constants
$f, \{f\}^{(e)}$	: Vector of unknown displacements, displacement vector of $e$ th element
$u, v, w$	: Displacements of a point on the mid plane of plate
$\bar{u}_1, \bar{u}_2, \bar{u}_3$	: Displacement of a point $(x, y, z)$
$\bar{\sigma}_{ij}, \bar{\epsilon}_{ij}$	: Stress vector, Strain vector
$\psi_y, \psi_x$	: Rotations of normal to mid plane about the $x$ and $y$ axis respectively
$\theta_x, \theta_y, \theta_k$	: Two slopes and angle of fiber orientation wrt $x$ -axis for $k$ th layer
$x, y, z$	: Cartesian coordinates
$\rho, \lambda, Var(.)$	: Mass density, eigenvalue, variance
$\omega, \bar{\omega}$	: Fundamental frequency and its dimensionless form
$RVs$	: Random variables
$\Delta T, \Delta C,$	: Difference in temperatures and moistures
$\alpha_1, \alpha_2, \beta_1, \beta_2$	: Thermal expansion and hygroscopic coefficients along $x$ and $y$ direction,